Prepared for submission to JHEP

UCLA/14/TEP/109 CALT-TH-2014-172

Logarithmic singularities and maximally supersymmetric amplitudes

Zvi Bern[1], **Enrico Herrmann**[2], **Sean Litsey**[1], **James Stankowicz**[1], **Jaroslav Trnka**[2]

[1] *Department of Physics and Astronomy, UCLA, Los Angeles, CA 90095, USA*

[2] *Walter Burke Institute for Theoretical Physics,*
California Institute of Technology, Pasadena, CA 91125, USA

E-mail: bern@physics.ucla.edu, eherrmann@caltech.edu, slitsey@ucla.edu, jjstankowicz@ucla.edu, trnka@caltech.edu

Abstract: The dual formulation of planar $\mathcal{N} = 4$ super-Yang-Mills scattering amplitudes makes manifest that the integrand has only logarithmic singularities and no poles at infinity. Recently, Arkani-Hamed, Bourjaily, Cachazo and Trnka conjectured the same singularity properties hold to all loop orders in the nonplanar sector as well. Here we conjecture that to all loop orders these constraints give us the key analytic information contained in dual conformal symmetry. We also conjecture that to all loop orders, while $\mathcal{N} = 8$ supergravity has poles at infinity, at least at four points it has only logarithmic singularities at finite locations. We provide nontrivial evidence for these conjectures. For the three-loop four-point $\mathcal{N} = 4$ super-Yang-Mills amplitude, we explicitly construct a complete basis of diagram integrands that has only logarithmic singularities and no poles at infinity. We then express the complete amplitude in terms of the basis diagrams, with the coefficients determined by unitarity. We also give examples at three loops showing how to make the logarithmic singularity properties manifest via $d\log$ forms. We give additional evidence at four and five loops supporting the nonplanar logarithmic singularity conjecture. Furthermore, we present a variety of examples illustrating that these constraints are more restrictive than dual conformal symmetry. Our investigations show that the singularity structures of planar and nonplanar amplitudes in $\mathcal{N} = 4$ super-Yang-Mills are strikingly similar. While it is not clear how to extend either dual conformal symmetry or a dual formulation to the nonplanar sector, these results suggest that related concepts might exist and await discovery. Finally, we describe the singularity structure of $\mathcal{N} = 8$ supergravity at three loops and beyond.

Contents

1 Introduction

Recent years have seen remarkable progress in our understanding of the structure of scattering amplitudes in planar $\mathcal{N} = 4$ super-Yang-Mills (sYM) theory [1, 2]. (See reviews e.g. Refs. [3–8].) Along with the conceptual progress have come significant computational advances, including new explicit results for amplitudes after integration up to high loop orders (see e.g. Refs. [9–12]), as well as some all-loop order predictions [13]. Among the theoretical advances are connections to twistor string theory [14, 15], on-shell recursion relations [16–18], unveiling of hidden dual conformal symmetry [19–21], momentum twistors [22], a dual interpretation of scattering amplitudes as supersymmetric Wilson loops [23–25] and a duality to correlation functions [26, 27]. More recently, scattering amplitudes were reformulated using on-shell diagrams and the positive Grassmannian [28–33] (see related work in Ref. [34–38]). This reformulation fits nicely into the concept of the amplituhedron [39–43], and makes an extremely interesting connection to active areas of research in algebraic geometry and combinatorics (see e.g. [44–49]). This picture also makes certain properties of amplitudes completely manifest, including properties like Yangian invariance [50] that are obscure in standard field-theory descriptions.

A special feature of $\mathcal{N} = 4$ sYM scattering amplitudes that appears after integration is uniform transcendentality [51–53], a property closely related to the $d$log-structure of the integrand in the dual formulation [28] (for recent discussion on integrating $d$log forms see Ref. [54]). The dual formulation can perhaps also be extended to integrated results via special functions that are motivated by the positive Grassmannian [55–58]. Such an extension might naturally incorporate the integrability of $\mathcal{N} = 4$ sYM theory [59]. So far this has not played a major role in the dual formulation, but is very useful in the flux tube S-matrix approach [60–64], leading to some predictions at finite coupling. Integrability should be present in the dual formulation of the planar theory through Yangian symmetry. Therefore, it is natural to search for either a Yangian-preserving regulator of infrared divergences of amplitudes [65–68], or directly for Yangian-preserving deformations of the Grassmannian integral [69, 70].

In this paper we are interested in understanding how to carry these many advances and promising directions over to the nonplanar sector of $\mathcal{N} = 4$ sYM theory. Unfortunately much less is known about nonplanar $\mathcal{N} = 4$, in part because of the difficulty of carrying out loop integrations. In addition, lore suggests that we lose integrability and thereby many nice features of planar amplitudes believed to be associated with it. (We do not use a $1/N$ expansion.) Even at the integrand level, the absence of a unique integrand makes it difficult to study nonplanar amplitudes globally, rather than in some particular expansion. One approach to extending planar properties to

the nonplanar sector is to search for the dual formulation of the theory using on-shell diagrams. Despite the fact that these are well-defined objects beyond the planar limit with many interesting properties [71], yet it is still not known how to expand scattering amplitudes in terms of these objects.

Nevertheless, there are strong hints that at least some of the properties of the planar theory survive the extension to the nonplanar sector. In particular, the Bern–Carrasco–Johansson (BCJ) duality between color and kinematics [72, 73] shows that the nonplanar sector of $\mathcal{N} = 4$ sYM theory is intimately linked to the planar one, so we should expect that some of the properties carry over. BCJ duality can be used to derive $\mathcal{N} = 8$ supergravity integrands starting from $\mathcal{N} = 4$ sYM ones, suggesting that some properties of the gauge theory should extend to $\mathcal{N} = 8$ supergravity as well. An encouraging observation is that the two-loop four-point amplitude of both $\mathcal{N} = 4$ sYM theory and $\mathcal{N} = 8$ supergravity have a uniform transcendental weight [51, 74–76]. Related to the leading transcendentality properties is the recent conjecture by Arkani-Hamed, Bourjaily, Cachazo and one of the authors [76] that, to all loop orders, the full $\mathcal{N} = 4$ sYM amplitudes, including the nonplanar sector, have only logarithmic singularities and no poles at infinity. This is motivated by the possibility of dual formulation that would make these properties manifest [28]. As evidence for their conjecture, they rewrote the two-loop four-point amplitude [77] in a format that makes these properties hold term by term.

In this paper we follow this line of reasoning, showing that key features of planar $\mathcal{N} = 4$ sYM amplitudes carry over to the nonplanar sector. In particular, we demonstrate that the three-loop four-point amplitude of $\mathcal{N} = 4$ sYM theory has only logarithmic singularities and no poles at infinity. We find a diagrammatic representation of the amplitude, using standard Feynman propagators, where these properties hold diagram by diagram. While we do not expect that these properties can be made manifest in each diagram to all loop orders, for the amplitudes studied in this paper this strategy works well. We proceed here by analyzing all singularities of the integrand; this includes singularities both from propagators and from Jacobians of cuts. We then construct numerators to cancel unwanted singularities, where we take "unwanted singularities" to mean double or higher poles and poles at infinity. As a shorthand, we call numerators with the desired properties "$d$log numerators" (and analogously for "$d$log integrands" and "$d$log forms"). Once we have found all such objects, we use unitarity constraints to determine the coefficients in front of each contribution. To verify that the amplitude so deduced is complete and correct we evaluate a complete set of unitarity cuts. The representation of the three-loop four-point amplitude that we find in this way differs from the previously found ones [73, 78] by contact terms that have been nontrivially rearranged via the color Jacobi identity. While all forms of this amplitude

have only logarithmic singularities, it is not at all obvious in earlier representations that this is true, because of nontrivial cancellations between different diagrams.

After constructing the three-loop basis of $d$log integrands, we address some interesting questions. One is whether there is a simple pattern dictating the coefficients with which the basis integrands appear in the amplitude. Indeed, we show that many of the coefficients follow the rung rule [77], suggesting that a new structure remains to be uncovered. Another question is whether it is possible to explicitly write the integrands we construct as $d$log forms. In general, this requires a nontrivial change of variables, but we have succeeded in writing all but one type of basis integrand form as $d$log forms. We present three explicit examples at three loops showing how this is done. These $d$log forms make manifest that the integrand basis elements have only logarithmic singularities, although the singularity structure at infinity is not manifest.

The requirement of only logarithmic singularities and no poles at infinity strongly restricts the integrands. In fact, we conjecture that in the planar sector logarithmic singularities and absence of poles at infinity imply dual conformal invariance in the integrand. We check this for all contributions at four loops and give a five-loop example illustrating that these singularity conditions are even stronger than dual conformal symmetry.

Related to the $d$log forms, the results presented in this paper offer a useful bridge between integrands and integrated results. The objects we construct here are a subset of the uniform transcendental integrals needed in the Henn and Smirnov procedure [79–81] to find a relatively simple set of differential equations for them. Here we focus mainly on the subset with no poles at infinity, since they are the ones relevant for $\mathcal{N} = 4$ sYM theory. In any case, the methods described here offer an efficient means for identifying integrals of uniform transcendental weight.

Ref. [76] noted a simple relation between the singularity structure of the two-loop four-point amplitude of $\mathcal{N} = 8$ supergravity and the one of $\mathcal{N} = 4$ sYM. How much of this continues at higher loops? Starting at three loops, the situation is more complicated because the integrals appearing in the two theories are different. Nevertheless, by making use of the BCJ construction [72, 73], we can obtain the corresponding $\mathcal{N} = 8$ amplitude in a way that makes its analytic properties relatively transparent. In particular, it allows us to immediately demonstrate that away from infinity, $\mathcal{N} = 8$ supergravity has only logarithmic singularities. We also find that starting at three loops, $\mathcal{N} = 8$ supergravity amplitudes have poles at infinity whose degree grow with the number of loops.

This paper is organized as follows: In Sect. 2 we will briefly discuss logarithmic singularities and poles at infinity in loop integrands. In Sect. 3 we outline our strategy for studying nonplanar amplitudes and illustrate it using the two-loop four-point am-

plitude. In Sect. 4 we construct a basis of three-loop four-point integrands that have only logarithmic singularities and no poles at infinity. We then express the three-loop four-point amplitude in this basis and show that the rung rule determines a large subset of the coefficients. Then in Sect. 5 we discuss $d\log$ forms in some detail. In Sect. 6, we give a variety of multiloop examples corroborating that only logarithmic singularities are present in $\mathcal{N} = 4$ sYM theory. In Sect. 7, we present evidence that the constraints of only logarithmic singularities and no poles at infinity incorporate the constraints from dual conformal symmetry. In Sect. 8, we comment on the singularity structure of the $\mathcal{N} = 8$ supergravity four-point amplitude. In Sect. 9, we present our conclusions and future directions.

2 Singularities of the integrand

Integrands offer enormous insight into the structure of scattering amplitudes. This includes the discovery of dual conformal symmetry [19], the Grassmannian structure [28–31], the geometric structures [39], and ultraviolet properties [82–84]. The singularity structure of integrands, along with the integration contours, determine the properties of integrated expressions. In particular, the uniform transcendentality property is determined by the singularity structure of the integrand. The nonplanar sector of $\mathcal{N} = 4$ sYM theory is much less developed than the planar one. Studying integrands offers a means of making progress in this direction, especially at high loop orders where it is difficult to obtain integrated expressions.

It would be ideal to study the amplitude as a single object and not to rely on an expansion using diagrams as building blocks which carry their own labels. In the planar sector, we can avoid such an expansion by using globally defined dual variables to obtain a unique rational function called the *integrand* of the amplitude. Unfortunately, it is unclear how to define such a unique object in the nonplanar case. In this paper we sidestep the lack of global variables by focusing on smaller pieces of the amplitude, organized through covariant, local diagrams with only three-point vertices and Feynman propagators. Such diagrams have also proved useful in the generalized unitarity method. Diagrams with only cubic vertices are sufficient in gauge and gravity theories, because it is possible to express diagrams containing higher point vertices in terms of ones with only cubic vertices by multiplying and dividing by appropriate Feynman propagators. For future reference, when not stated otherwise, this is what we mean by a "diagrammatic representation" or an "expansion in terms of diagrams".

For a given diagram, there is no difficulty in having a well-defined notion of an integrand, at least for a given set of momentum labels. For this to be useful, we need to be able to expose the desired singularity properties one diagram at a time, or at worst

for a collection of a small subset of diagrams at a time. In general, there is no guarantee that this can be done, but in cases where it can be, it offers a useful guiding principle for making progress in the nonplanar sector. A similar strategy proved successful for BCJ duality. In that case, at most three diagrams at a time need to share common labels in order to define the duality, bypassing the need for global labels.

At three loops we will explicitly construct a basis of integrands that have only logarithmic singularities and no poles at infinity. We also discuss some higher-loop examples. Before doing so, we summarize the dual formulation of planar amplitudes, in order to point out the properties that we wish to carry over to the nonplanar case.

2.1 Dual formulation of planar theory

Here we summarize the dual formulation of planar $\mathcal{N} = 4$ sYM theory, with a focus on our approach to extending this formulation to the nonplanar sector. For details beyond what appear here, we refer the reader to Refs. [28–30].

As mentioned in the previous subsection, for planar amplitudes we can define an *integrand* based on a global set of variables valid for all terms in the amplitude [18]. Up to terms that vanish under integration, the integrand of a planar amplitude is a unique rational function constrained by the requirement that all unitarity cuts of the function are correct. Methods based on unitary and factorization construct the integrand using only on-shell input information. On-shell diagrams capitalize on this efficiency by representing integrands as graphs where all internal lines are implicitly on shell, and all vertices are three-point amplitudes.

An important further step is to promote on-shell diagrams from being only reference data to being actual building blocks for the amplitude. This idea was exploited in Ref. [29] where loop-level [18] recursion relations for integrands were interpreted directly in terms of higher-loop on-shell diagrams. A preliminary version of this notion is already visible in the early version of the BCFW recursion relations [16], where the tree-level amplitudes are expressed in terms of leading singularities of one-loop amplitudes.

More recently, the construction of amplitudes from on-shell diagrams has been connected [28] to modern developments in algebraic geometry and combinatorics [44–49] where the same type of diagrams appeared in a very different context. Each on-shell diagram can be labeled using variables associated with edges e_i or faces f_j, from which one can build a $k \times n$ matrix C, where n is the number of external particles, and k is related to the number of negative helicity particles. This matrix has a $\mathrm{GL}(k)$ symmetry and therefore belongs to a Grassmannian $C \in G(k, n)$. If the edge and face variables are taken to be real and to have fixed sign based on certain rules, all the maximal minors of the matrix C are positive and produce cells in the positive Grassmannian $G_+(k, n)$. This is more than just a mathematical curiosity, as this viewpoint can be

used to evaluate on-shell diagrams independently of the notion of the notion of gluing together three-point on-shell amplitudes.

After parametrizing the on-shell diagram as described, the diagram takes the value [29]

$$\Omega = \frac{df_1}{f_1} \wedge \frac{df_2}{f_2} \wedge \cdots \wedge \frac{df_m}{f_m}\, \delta(C(f_j) \cdot \mathcal{W})\,, \tag{2.1}$$

where we collectively encode all external data, both bosonic and fermionic, in $\mathcal{W}$. The delta function implies a set of equations that can be solved for the f_j in terms of external data. Any on-shell diagrams that have an interpretation as building blocks for tree-level amplitudes exactly determine all variables f_j so that Ω becomes a function of external data only, and Ω gives exactly the tree amplitude. Likewise, any on-shell diagrams that have an interpretation as building blocks of an L-loop integrand leave $4L$ variables f_j unfixed, and Ω is the $4L$-form giving exactly the unique L-loop integrand. Even on-shell diagrams that do not directly correspond to tree amplitudes or loop integrands have some meaning as cuts or factorizations of the amplitude. This construction is often referred to as the *dual formulation* of planar amplitudes. One of our motivations is to look for possible extensions of this formulation to the nonplanar sector.

A crucial feature of Ω is that it has only logarithmic singularities in f_j, inherited from the structure of Eq. (2.1). As written there, these singularities are in the abstract Grassmannian space, or equivalently in the extended bosonic variables within the amplituhedron construction of the integrand. When translated back to momentum (or twistor or momentum twistor) space, the logarithmic property is lost due to the supersymmetric-part of the delta function in Eq. (2.1). However, for both MHV ($k = 2$) and NMHV ($k = 3$) on-shell diagrams, the supersymmetric-part of delta functions can be separated from the bosonic parts, resulting in a logarithmic form in momentum space [39, 40]. The other property that is completely manifest when forms are written in momentum twistor space is the absence of poles at infinity. Both these properties are preserved for all on-shell diagrams and so are true for all tree-level amplitudes and integrands for planar loop amplitudes.

We can also compute nonplanar on-shell diagrams, either by gluing together three-point on-shell amplitudes or by using the relation to the Grassmannian. The relation to the positive part of the Grassmannian is naively lost, but reappears under more careful scrutiny [71]. We can still associate a logarithmic form to diagrams as in Eq. (2.1). Using the same arguments as in the planar sector, all MHV and NMHV on-shell diagrams have logarithmic singularities in momentum space. However, it is not known at present how to construct complete $\mathcal{N} = 4$ sYM amplitudes, including the nonplanar parts, using recursion relations of these nonplanar on-shell diagrams. Unlike in the planar sector, a major obstacle in the nonplanar sector is the absence of a unique in-

tegrand. If this problem can be solved so that the amplitude is expressible in terms of on-shell diagrams, then the same arguments as used in the planar sector would prove that the full nonplanar $\mathcal{N}=4$ sYM amplitudes have logarithmic singularities. In any case, even if the existence of a dual formulation for the nonplanar sector cannot be straightforwardly established, we can still test the key consequences: only logarithmic singularities and no poles at infinity. This is what we turn to now.

2.2 Logarithmic singularities

Before discussing the basis of integrands for $\mathcal{N}=4$ sYM amplitudes, we consider some simple toy cases that display the properties relevant for subsequent sections. It is natural to define an integrand form $\Omega(x_1,\ldots,x_m)$ of the integral F by stripping off the integration symbol

$$F=\int \Omega(x_1,\ldots,x_m)\,, \tag{2.2}$$

and to study its singularity structure. There is a special class of forms that we are interested in here: those that have only *logarithmic singularities*. A form has only logarithmic singularities if near any pole $x_i\to a$ it behaves as

$$\Omega(x_1,\ldots,x_m)\to \frac{dx_i}{x_i-a}\wedge\hat{\Omega}(x_1,\ldots,\hat{x}_i,\ldots,x_m)\,, \tag{2.3}$$

where $\hat{\Omega}(x_1,\ldots,\hat{x}_i,\ldots x_m)$ is an $(m-1)$-form[1] in all variables except $\hat{x}_i$. An equivalent terminology is that there are only simple poles. That is, we are interested in integrands where we can change variables $x_i\to g_i(x_j)$ such that the form becomes

$$\Omega=d\log g_1\wedge d\log g_2\wedge\cdots\wedge d\log g_m\,, \tag{2.4}$$

where we denote

$$d\log x\equiv\frac{dx}{x}\,. \tag{2.5}$$

We refer to this representation as a "$d$log form".

A simple example of such a form is $\Omega(x)=dx/x\equiv d\log x$, while $\Omega(x)=dx$ or $\Omega(x)=dx/x^2$ are examples of forms which do not have this property. A trivial two-form with logarithmic singularities is $\Omega(x,y)=dx\wedge dy/(xy)=d\log x\wedge d\log y$. A less trivial example of a $d$log form is

$$\Omega(x,y)=\frac{dx\wedge dy}{xy(x+y+1)}=d\log\frac{x}{x+y+1}\wedge d\log\frac{y}{x+y+1}\,. \tag{2.6}$$

[1]The signs from the wedge products will not play a role because at the end we will construct basis elements whose normalization in the amplitude is fixed from unitarity cuts.

In this case, the property of only logarithmic singularities is not obvious from the first expression, but a change of variables resulting in the second expression makes the fact that Ω is a $d\log$ form manifest. This may be contrasted with the form

$$\Omega(x,y) = \frac{dx \wedge dy}{xy(x+y)}\,, \tag{2.7}$$

which is not logarithmic because near the pole $x = 0$ it behaves as dy/y^2; this form cannot be written as a $d\log$ form. In general, the nontrivial changes of variables required can make it difficult to find the explicit $d\log$ forms even where they exist.

In a bit more detail, consider the behavior of a form near $x = 0$. If the integrand scales as dx/x^m for integer m, we consider two different regimes where integrands can fail to have logarithmic singularities. The first is when $m \geq 2$, which results in double or higher poles at $x = 0$. The second is when $m \leq 0$, which results in a pole at infinity. Avoiding unwanted singularities, either at finite or infinite values of x, leads to tight constraints on the integrand of each diagram. Since we take the denominators to be the standard Feynman propagators associated to a given diagram, in our expansion of the amplitude the only available freedom is to adjust the kinematic numerators. As a simple toy example, consider the form

$$\Omega(x,y) = \frac{dx \wedge dy\ N(x,y)}{xy(x+y)}\,. \tag{2.8}$$

As noted above, for a constant numerator $N(x,y) = 1$ the form develops a double pole at $x = 0$. Similarly, for $N(x,y) = x^2 + y^2$ the form behaves like dy for $x = 0$ and again it is not logarithmic. There is only one class of numerators that make the form logarithmic near $x = 0$ and $y = 0$: $N(x,y) = a_1 x + a_2 y$ for arbitrary a_1 and a_2.

Our discussion of loop integrands will be similar: constant numerators (i.e. those independent of loop momenta) are dangerous for they may allow double or higher poles located at finite values of loop momenta, while a numerator with too many powers of loop momentum can develop higher poles at infinity. It turns out that the first case is generally the problem in gauge theory, whereas the second case usually arises for gravity amplitudes, because the power counting of numerators is boosted relative to the gauge-theory case. For sYM integrands, we will carefully tune numerators so that only logarithmic singularities are present. The desired numerators live exactly on the boundary between too many and too few powers of loop momenta.

2.3 Loop integrands and poles at infinity

Now consider the special class of four-forms that correspond to one-loop integrands. Standard integral reduction methods [85, 86] reduce any massless one-loop amplitude

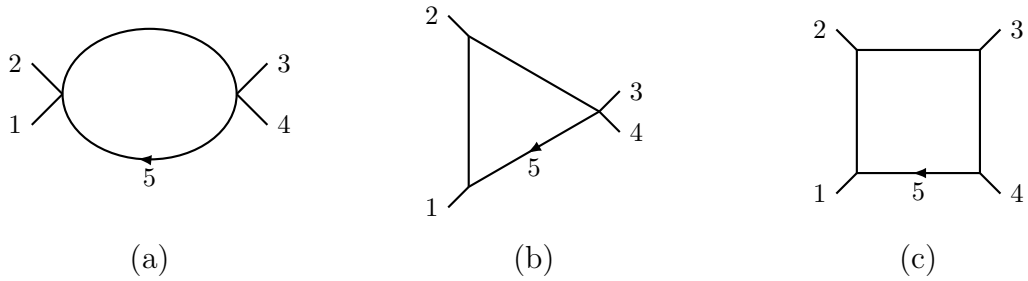

Figure 1. The (a) bubble, (b) triangle and (c) box one-loop diagrams.

to a linear combination of box, triangle and bubble integrals. In nonsupersymmetric theories there are additional rational terms arising from loop momenta outside of $D = 4$; these are not relevant for our discussion of $\mathcal{N} = 4$ sYM theory. While it will eventually be necessary to include the (-2ϵ) dimensional components of loop momenta, since these are in general required by dimensional regularization, for the purposes of studying the singularities of the integrand we simply put this matter aside. In any case, direct checks reveal that these (-2ϵ) dimensional pieces do not lead to extra contributions through at least six loops in $\mathcal{N} = 4$ sYM four-point amplitudes [87]. We focus here on the four-point case, but a similar analysis can be performed for larger numbers of external legs as well.

Consider the bubble, triangle and box integrals in Fig. 1. In these and all following diagrams, we take all external legs as outgoing. The explicit forms in $D = 4$ are

$$\begin{aligned} d\mathcal{I}_2 &= d^4\ell_5 \frac{1}{\ell_5^2(\ell_5 - k_1 - k_2)^2}\,, \\ d\mathcal{I}_3 &= d^4\ell_5 \frac{s}{\ell_5^2(\ell_5 - k_1)^2(\ell_5 - k_1 - k_2)^2}\,, \\ d\mathcal{I}_4 &= d^4\ell_5 \frac{st}{\ell_5^2(\ell_5 - k_1)^2(\ell_5 - k_1 - k_2)^2(\ell_5 + k_4)^2}\,, \end{aligned} \tag{2.9}$$

where we have chosen a convenient normalization. The variables $s = (k_1 + k_2)^2$ and $t = (k_2 + k_3)^2$ are the usual Mandelstam invariants, depending only on external momenta. Under integration, these forms are infrared or ultraviolet divergent and need to be regularized, but as mentioned about we set this aside and work directly in four dimensions.

In $D = 4$, we can parametrize the loop momentum in terms of four independent vectors constructed from the spinor-helicity variables associated with the external momenta $k_1 = \lambda_1\tilde{\lambda}_1$ and $k_2 = \lambda_2\tilde{\lambda}_2$. A clean choice for the four degrees of freedom of the

loop momentum is

$$\ell_5 = \alpha_1\lambda_1\widetilde{\lambda}_1 + \alpha_2\lambda_2\widetilde{\lambda}_2 + \alpha_3\lambda_1\widetilde{\lambda}_2 + \alpha_4\lambda_2\widetilde{\lambda}_1\,, \tag{2.10}$$

where the α_i are now the independent variables. Writing $d\mathcal{I}_2$ in this parametrization we obtain

$$d\mathcal{I}_2 = \frac{d\alpha_1 \wedge d\alpha_2 \wedge d\alpha_3 \wedge d\alpha_4}{(\alpha_1\alpha_2 - \alpha_3\alpha_4)(\alpha_1\alpha_2 - \alpha_3\alpha_4 - \alpha_1 - \alpha_2 + 1)}\,. \tag{2.11}$$

In general, since we are not integrating the expressions, we ignore Feynman's $i\epsilon$ prescription and any factors of i from Wick rotation.

To study the singularity structure, we can focus on subregions of the integrand by imposing on-shell or cut conditions. As an example, the cut condition $\ell_5^2 = 0$ can be computed in these variables by setting

$$0 = \ell_5^2 = (\alpha_1\alpha_2 - \alpha_3\alpha_4)s\,. \tag{2.12}$$

We can then eliminate one of the α_i, say α_4, by computing the residue on the pole located at $\alpha_4 = \alpha_1\alpha_2/\alpha_3$. This results in a residue,

$$\operatorname*{Res}_{\ell_5^2=0} d\mathcal{I}_2 = \frac{d\alpha_3}{\alpha_3} \wedge \frac{d\alpha_2}{(\alpha_2 + \alpha_1 - 1)} \wedge d\alpha_1\,. \tag{2.13}$$

Changing variables to $\alpha_\pm = \alpha_1 \pm \alpha_2$, this becomes

$$\operatorname*{Res}_{\ell_5^2=0} d\mathcal{I}_2 = \frac{d\alpha_3}{\alpha_3} \wedge \frac{d\alpha_+}{(\alpha_+ - 1)} \wedge d\alpha_-\,. \tag{2.14}$$

We can immediately see that the form $d\mathcal{I}_2$ is non-logarithmic in α_-, and thus the bubble integrand has a nonlogarithmic singularity in this region.

Carrying out a similar exercise for the triangle $d\mathcal{I}_3$ using the parametrization in Eq. (2.10), we obtain

$$d\mathcal{I}_3 = \frac{d\alpha_1 \wedge d\alpha_2 \wedge d\alpha_3 \wedge d\alpha_4}{(\alpha_1\alpha_2 - \alpha_3\alpha_4)(\alpha_1\alpha_2 - \alpha_3\alpha_4 - \alpha_2)(\alpha_1\alpha_2 - \alpha_3\alpha_4 - \alpha_1 - \alpha_2 + 1)}\,. \tag{2.15}$$

We can make a change of variables and rewrite it in the manifest $d\log$ form,

$$d\mathcal{I}_3 = d\log(\alpha_1\alpha_2 - \alpha_3\alpha_4) \wedge d\log(\alpha_1\alpha_2 - \alpha_3\alpha_4 - \alpha_2) \wedge d\log(\alpha_1\alpha_2 - \alpha_3\alpha_4 - \alpha_1 - \alpha_2 + 1) \wedge d\log\alpha_3\,. \tag{2.16}$$

Translating this back into momentum space:

$$d\mathcal{I}_3 = d\log\ell_5^2 \wedge d\log(\ell_5 - k_1)^2 \wedge d\log(\ell_5 - k_1 - k_2)^2 \wedge d\log(\ell_5 - k_1)\cdot(\ell_5^* - k_1)\,, \tag{2.17}$$

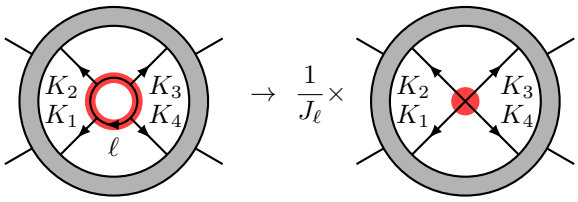

Figure 2. The left diagram is a generic L-loop contribution to the four-point $\mathcal{N}=4$ sYM amplitude. The thick (red) highlighting indicates propagators replaced by on-shell conditions. After this replacement, the highlighted propagators leave behind the simplified diagram on the right multiplied by an inverse Jacobian, Eq. (2.21). The four momenta $K_1, \ldots, K_4$ can correspond either to external legs or propagators of the higher-loop diagram.

where $\ell_5^* \equiv \beta\lambda_2\widetilde{\lambda}_1 + \lambda_1\widetilde{\lambda}_1$ is one of the two solutions to the triple cut. The parameter β is arbitrary in the triple cut solution, and the $d\log$ form is independent of it. For the box integral, a similar process followed in Ref. [28] results in

$$d\mathcal{I}_4 = d\log\frac{\ell_5^2}{(\ell_5-\ell_5^*)^2} \wedge d\log\frac{(\ell_5-k_1)^2}{(\ell_5-\ell_5^*)^2} \wedge d\log\frac{(\ell_5-k_1-k_2)^2}{(\ell_5-\ell_5^*)^2} \wedge d\log\frac{(\ell_5+k_4)^2}{(\ell_5-\ell_5^*)^2}\,, \quad (2.18)$$

where $\ell_5^* \equiv -\frac{\langle 14\rangle}{\langle 24\rangle}\lambda_2\widetilde{\lambda}_1 + \lambda_1\widetilde{\lambda}_1$; see also our discussion in subsection 5.1.

While both triangle and box integrands can be written in $d\log$ form, there is an important distinction between the triangle form $d\mathcal{I}_3$ and the box form $d\mathcal{I}_4$. On the cut $\alpha_4 = \alpha_1\alpha_2/\alpha_3$, only one $d\log$-factor in $d\mathcal{I}_3$ depends on α_3 and develops a singularity in the limit $\alpha_3 \to \infty$ (which implies $\ell_5 \to \infty$), while $d\mathcal{I}_4$ does not. We refer to any singularity that develops as a loop momentum approaches infinity (in our example, $\ell_5 \to \infty$) at any step in the cut structure as a *pole at infinity*. To be more specific, even if a $d\log$ form has no pole at infinity before imposing any cut conditions, it is possible to generate such poles upon taking residues, as we saw in the example of the triangle integrand above. In this sense, the pole at infinity property is more refined than simple power counting, which only considers the overall scaling of an integrand before taking any cuts.

The issue of poles at infinity will be important for our discussion of $\mathcal{N}=4$ sYM theory as well as $\mathcal{N}=8$ supergravity amplitudes. While a lack of poles at infinity implies ultraviolet finiteness, having poles at infinity does not necessarily mean that there are divergences. For example, the triangle integral contains such a pole in the cut structure but is ultraviolet finite. In principle, there can also be nontrivial cancellations between different contributions.

To find numerators that do not allow these poles at infinity and also ensure only logarithmic singularities, it is not necessary to compute every residue of the integrand.

This is because cutting box subdiagrams from a higher loop diagram, as on the left in Fig. 2, can only increase the order of remaining poles in the integrand. To see this, consider computing the four residues that correspond to cutting the four highlighted propagators in Fig. 2,

$$\ell^2 = (\ell - K_1)^2 = (\ell - K_1 - K_2)^2 = (\ell + K_4)^2 = 0\,. \tag{2.19}$$

This residue is equivalent to computing the Jacobian obtained by replacing the box propagator with on-shell delta functions. This Jacobian is then

$$J_\ell = |\partial P_i / \partial \ell^\mu|\,, \tag{2.20}$$

where the P_i correspond to the four inverse propagators placed on shell in Eq. (2.19). See, for example, Ref. [88] for more details. Another way to obtain this Jacobian by reading off the rational factors appearing in front of the box integrals—see appendix I of Ref. [89].

For the generic case J_ℓ contains square roots making, it difficult to work with. In special cases it simplifies. For example for $K_1 = k_1$ massless, the three-mass normalization is

$$J_\ell = (k_1 + K_2)^2 (K_4 + k_1)^2 - K_2^2 K_4^2\,. \tag{2.21}$$

If in addition $K_3 = k_3$ is massless, the so called "two-mass-easy" case, the numerator factorizes into a product of two factors, a feature that is important in many calculations. This gives,

$$J_\ell = (K_2 + k_1)^2 (K_4 + k_1)^2 - K_2^2 K_4^2 = (K_2 \cdot q)(K_2 \cdot \overline{q})\,, \tag{2.22}$$

where $q = \lambda_1 \widetilde{\lambda}_3$ and $\overline{q} = \lambda_3 \widetilde{\lambda}_1$. If instead both $K_1 = k_1$ and $K_2 = k_2$ are massless we get so called two-mass-hard normalization

$$J_\ell = (k_1 + k_2)^2 (K_3 + k_2)^2\,. \tag{2.23}$$

These formula are useful at higher loops, where the K_j depend on other loop momenta.

These Jacobians go into the denominator of the integrand after a box-cut is applied. It therefore can only raise the order of the remaining poles in the integrand. Our basic approach utilizes this fact: we cut embedded box subdiagrams from diagrams of interest and update the integrand by dividing by the obtained Jacobian (2.20). Then we identify all kinematic regions that can result in a double pole in the integrand.

It would be cumbersome to write out all cut equations for every such sequence of cuts, so we introduce a compact notation:

$$\text{cut} = \{\ldots,\, (\ell - K_i)^2\,, \ldots, B(\ell)\,, \ldots,\, B(\ell', (\ell' - Q))\,, \ldots\}\,. \tag{2.24}$$

Here:

- Cuts are applied in the order listed.
- A propagator listed by itself, as $(\ell - K_i)^2$ is, means: "Cut just this propagator."
- $B(\ell)$ means: "Cut the four propagators that depend on ℓ." This exactly corresponds to cutting the box propagators as in Eq. (2.19) and Fig. 2.
- $B(\ell', (\ell' - Q))$ means: "Cut the three standard propagators depending on ℓ', as well as a fourth $1/(\ell' - Q)^2$ resulting from a previously obtained Jacobian." The momentum Q depends on other momenta besides ℓ'. The four cut propagators form a box.

We use this notation in subsequent sections.

2.4 Singularities and maximum transcendental weight

There is an important link between the singularity structure of the integrand and the transcendental weight of an integral, as straightforwardly seen at one loop. If we evaluate the bubble, triangle and box integrals displayed in Fig. 1 in dimensional regularization [90], through $\mathcal{O}(\epsilon^0)$ in the dimensional regularization parameter ϵ, we have [91, 92]

$$\begin{aligned} I_2 &= \frac{1}{\epsilon} + \log(-s/\mu^2) + 2\,, \\ I_3 &= \frac{1}{\epsilon^2} - \frac{\log(-s/\mu^2)}{\epsilon} + \frac{\log^2(-s/\mu^2) - \zeta_2}{2}\,, \\ I_4 &= \frac{4}{\epsilon^2} - 2\,\frac{\log(-s/\mu^2) + \log(-t/\mu^2)}{\epsilon} + \log^2(-s/\mu^2) + \log^2(-t/\mu^2) - \log^2(s/t) - 8\zeta_2\,. \end{aligned} \tag{2.25}$$

Here μ is the dimensional regularization scale parameter, and the integrals are normalized by an overall multiplicative factor of

$$-i\frac{e^{\gamma\epsilon}(4\pi)^{2-\epsilon}}{(2\pi)^{4-2\epsilon}}\,, \tag{2.26}$$

where $s, t < 0$. In the bubble integral the $1/\epsilon$ singularity originates from the ultraviolet, while in the triangle and box integrals all $1/\epsilon$ singularities originate from the infrared.

Following the usual rules for counting transcendental weight in the normalized expressions of Eq. (2.25), we count logarithms and factors of $1/\epsilon$ to have weight 1 and $\zeta_2 = \pi^2/6$ to have weight 2. Integers have weight 0. With this counting we see that the bubble integral, which has nonlogarithmic singularities as explained in the previous subsection 2.3, is not of uniform transcendental weight, and has maximum weight 1.

On the other hand the triangle and box, which both have only logarithmic singularities, are of uniform weight 2.

Building on the one-loop examples, a natural conjecture is that the uniform transcendentality property of integrated expressions noted by Kotikov and Lipatov [51] is directly linked to the appearance of only logarithmic singularities. In fact, experience shows that after integration the L-loop planar $\mathcal{N} = 4$ sYM amplitudes have transcendental weight $2L$. Various examples are found in Refs. [10, 11, 13, 93]. One of our motivations is to make the connection between logarithmic forms and transcendental functions more precise. It is clearly an important connection that deserves further study.

Recently, Henn et al. observed [79–81] that integrals with uniform transcendental weight lead to simple differential equations. An interesting connection is that the integrands we construct do appear to correspond to integrals of uniform transcendental weight.[2] Here we mainly focus on the particular subset with no poles at infinity, since they are the ones relevant for $\mathcal{N} = 4$ sYM theory.

3 Strategy for nonplanar amplitudes

As introduced in Sect. 2, instead of trying to define a nonplanar global integrand, we subdivide the amplitude into diagrams with their own momentum labels and analyze them one by one. In Ref. [76], the $\mathcal{N} = 4$ sYM four-point two-loop amplitude was rewritten in a form with no logarithmic singularities and no poles at infinity. In this section, we develop a strategy for doing the same at higher loop orders. We emphasize that we are working at the level of the amplitude integrand prior to integration. In particular we do not allow for any manipulations that involve the integration symbol (e.g. integration-by-parts identities) to shuffle singularities between contributions.

Our general procedure has four steps:

1. Define a set of parent diagrams whose propagators are the standard Feynman ones. The parent diagrams are defined to have only cubic vertices and loop momentum flowing through all propagators.

2. Construct *d*log *numerators*. These are a basis set of numerators constructed so that each diagram has only logarithmic singularities and no poles at infinity. These numerators also respect diagram symmetries, including color signs. Each *d*log numerator, together with the diagram propagators, forms a basis diagram.

[2] We thank Johannes Henn for comparisons with his available results showing that after integration our integrands are of uniform transcendental weight.

3. Use simple unitarity cuts to determine the linear combination of basis diagrams that gives the amplitude.

4. Confirm that the amplitude so constructed is correct and complete. We use the method of maximal cuts [94] for this task.

There is no a priori guarantee that this will succeed. In principle, requiring $d$log numerators could make it impossible to expand the amplitude in terms of independent diagrams with Feynman propagators. Indeed, at a sufficiently high loop order we expect that even in the planar sector it may not be possible to find a covariant diagrammatic representation manifesting the desired properties; in such circumstances we would expect that unwanted singularities cancel between diagrams. This may happen even earlier in the nonplanar sector. As in many amplitude calculations, we simply assume that we can construct a basis with the desired properties, and then, once we have an ansatz, we check that it is correct by computing a complete set of cuts.

In this section, we illustrate the process of finding diagram integrands with the desired properties and explain the steps in some detail. For simplicity, we focus on the four-point amplitude, but we expect that a similar strategy is applicable for higher-point amplitudes in the MHV and NMHV sectors as well.

We use the one- and two-loop contributions to the four-point amplitudes to illustrate the procedure, before turning to three loops in Sect. 4. We find that the canonical one-loop numerator is already a $d$log numerator, while the two-loop result illustrates the issues that we face at higher loops. The two-loop amplitude was first obtained in [77], but in a form that does not make clear the singularity structure. In Ref. [76], the two-loop amplitude was rewritten in a form that makes these properties manifest by rearranging contact terms in the amplitude by using the color-Jacobi identity. In this section we replicate this result by following our strategy of systematically constructing a basis of integrands with the desired properties. In subsequent sections we apply our strategy to higher loops.

3.1 Constructing a basis

The construction of a basis of integrands starts from a set of parent diagrams. As mentioned in the introduction to Sect. 2, we focus on graphs with only cubic vertices. Furthermore we restrict to diagrams that do not have triangle or bubble subdiagrams, since these are not necessary for $\mathcal{N} = 4$ amplitudes that we study. We also exclude any diagrams in which a propagator does not carry loop momentum, because such contributions can be absorbed into diagrams in which all propagators contain loop momenta. At the end, we confirm this basis of diagrams is sufficient by verifying a set of unitarity cuts that fully determine the amplitude.

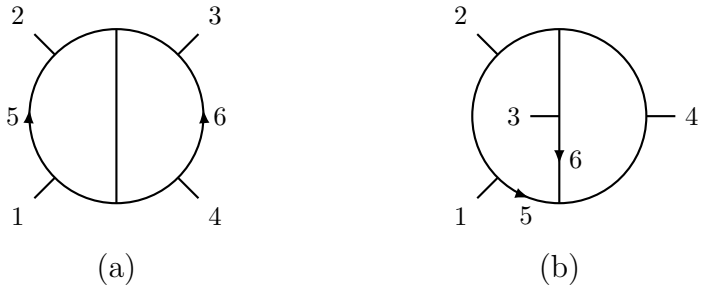

Figure 3. Two-loop four-point parent diagrams for $\mathcal{N}=4$ sYM theory.

At one loop the parent diagrams are the three independent box integrals, one of which is displayed in Fig. 1(c), and the other two of which are cyclic permutations of the external legs k_2, k_3 and k_4 of this one. At two loops the four-point amplitude of $\mathcal{N}=4$ sYM theory has twelve parent diagrams, two of which are displayed in Fig. 3; the others are again just given by relabelings of external legs.

Unlike the planar case, there is no global, canonical way to label loop momenta in all diagrams. In each parent diagram, we label L independent loop momenta as $\ell_5, \ldots, \ell_{4+L}$. By conserving momentum at each vertex, all other propagators have sums of the loop and external momenta flowing in them. We define the L-loop *integrand*, $\mathcal{I}^{(x)}$, of a diagram labeled by (x) by combining the kinematic part of the numerator with the Feynman propagators of the diagram as

$$\mathcal{I}^{(x)} \equiv \frac{N^{(x)}}{\prod_{\alpha_{(x)}} p^2_{\alpha_{(x)}}} \,. \tag{3.1}$$

The product in the denominator in Eq. (3.1) runs over all propagators $p^2_{\alpha_{(x)}}$ of diagram (x), and the kinematic numerator $N^{(x)}$ generally depends on loop momenta. From this we define an *integrand form*

$$d\mathcal{I}^{(x)} \equiv \prod_{l=5}^{4+L} d^4\ell_l \, \mathcal{I}^{(x)} \,. \tag{3.2}$$

This integrand form is a $4L$ form in the L independent loop momenta $\ell_5, \ldots, \ell_{4+L}$. We have passed factors of i, 2π, and coupling constants into the definition of the amplitude, Eq. (3.21). As mentioned previously, we focus on $D=4$.

We define an expansion of the numerator

$$N^{(x)} = \sum_i a_i^{(x)} N_i^{(x)} \,, \tag{3.3}$$

where the $N_i^{(x)}$ are the $d\log$ numerators we aim to construct, and the $a_i^{(x)}$ are coefficients. We put off a detailed discussion of how to fix these coefficients until subsection 3.2, and

here just mention that the coefficients can be obtained by matching an expansion of the amplitude in $d\log$ numerators to unitarity cuts or other physical constraints, such as leading singularities.

Starting from a generic numerator $N_i^{(x)}$, we impose the following constraints:

- *Overall dimensionality.* $N_i^{(x)}$ must be a local polynomial of momentum invariants (i.e. $k_a{\cdot}k_b$, $k_a{\cdot}\ell_b$, or $\ell_a{\cdot}\ell_b$) with dimensionality $N_i^{(x)} \sim (p^2)^K$, where $K = P{-}2L{-}2$, and P is the number of propagators in the integrand. We forbid numerators with $K < 0$.

- *Asymptotic scaling.* For each loop momentum ℓ_l, the integrand $\mathcal{I}^{(x)}$ must not scale less than $1/(\ell_l^2)^4$ for $\ell_l \to \infty$ in all possible labellings.

- *No double/higher poles.* The integrand $\mathcal{I}^{(x)}$ must be free of poles of order two or more in all kinematic regions.

- *No poles at infinity.* The integrand $\mathcal{I}^{(x)}$ must be free of poles of any order at infinity in all kinematic regions.

The overall dimensionality and asymptotic scaling give us power counting constraints on the subdiagrams. In practice, these two constraints dictate the initial form of an ansatz for the numerator, while the last two conditions of no higher degree poles and no poles at infinity constrain that ansatz to select "$d\log$ numerators". The constraint on overall dimensionality is the requirement that the overall mass dimension of the integrand is $-4L-4$;[3] in $D = 4$ this matches the dimensionality of gauge-theory integrands. The asymptotic scaling constraint includes a generalization of the absence of bubble and triangle integrals at one-loop order in $\mathcal{N} = 4$ sYM theory and $\mathcal{N} = 8$ supergravity [95, 96]. This constraint is a necessary, but not a sufficient, condition for having only logarithmic singularities and no poles at infinity.

At one loop, the asymptotic scaling constraint implies that only the box diagram, Fig. 1(c), appears; coupling that with the overall dimensionality constraint implies that the numerator is independent of loop momentum. The box numerator must then be a single basis element which we can normalize to be unity:

$$N_1^{(\mathrm{B})} = 1\,. \tag{3.4}$$

In the one-loop integrand, neither higher degree poles nor poles at infinity arise. Thus everything at one loop is consistent and manifestly exhibits only logarithmic singularities. A more thorough treatment of the one-loop box, including the sense in which

[3] The -4 in the mass dimension originates from factoring out a dimensionful quantity from the final amplitude in Eq. (3.21).

logarithmic singularities are manifest in a box, is found in the context of $d\log$ forms in subsection 5.1

Next consider two loops. Here the asymptotic scaling constraint implies that only the planar and nonplanar double box diagrams in Fig. 3 appear, since the constraint forbids triangle or bubble subdiagrams. We now wish to construct the numerators $N^{(\mathrm{P})}$ and $N^{(\mathrm{NP})}$ for the planar (Fig. 3(a)) and nonplanar (Fig. 3(b)) diagrams respectively. There are different ways of labeling the two graphs. As already mentioned, we prefer labels in Fig. 3, where the individual loop momenta appear in the fewest possible number of propagators. This leads to the tightest power counting constraints in the sense of our general strategy outlined above. We consider the planar and nonplanar diagrams separately.

For the planar diagram in Fig. 3, only four propagators contain either loop momentum ℓ_5 or ℓ_6. By the asymptotic scaling constraint, the numerator must be independent of both loop momenta: $N^{(\mathrm{P})} \sim \mathcal{O}((\ell_5)^0, (\ell_6)^0)$. Since overall dimensionality restricts $N^{(\mathrm{P})}$ to be quadratic in momentum, we can write down two independent numerator basis elements:

$$N_1^{(\mathrm{P})} = s\,, \qquad\qquad N_2^{(\mathrm{P})} = t\,. \tag{3.5}$$

The resulting numerator is then a linear combination of these two basis elements:

$$N^{(\mathrm{P})} = a_1^{(\mathrm{P})} s + a_2^{(\mathrm{P})} t\,, \tag{3.6}$$

where the $a_j^{(\mathrm{P})}$ are constants, labeled as discussed after Eq. (3.3). Again, as in the one-loop case, there are no hidden double poles or poles at infinity from which nontrivial constraints could arise.

The nonplanar two-loop integrand $\mathcal{I}^{(\mathrm{NP})}$ is the first instance where nontrivial constraints result from requiring logarithmic singularities and the absence of poles at infinity, so we discuss this example in more detail. The choice of labels in Fig. 3(b) results in five propagators with momentum ℓ_5 but only four with momentum ℓ_6, so $N^{(\mathrm{NP})}$ is at most quadratic in ℓ_5 and independent of ℓ_6: $N^{(\mathrm{NP})} \sim \mathcal{O}((\ell_5)^2, (\ell_6)^0)$. Overall dimensionality again restricts $N^{(\mathrm{NP})}$ to be quadratic in momentum. This dictates the form of the numerator to be

$$N^{(\mathrm{NP})} = c_1 \ell_5^2 + c_2(\ell_5 \cdot Q) + c_3 s + c_4 t\,, \tag{3.7}$$

where Q is some vector and the c_i are coefficients independent of loop momenta.

Now we search the integrand

$$\mathcal{I}^{(\mathrm{NP})} = \frac{c_1 \ell_5^2 + c_2(\ell_5 \cdot Q) + c_3 s + c_4 t}{\ell_5^2(\ell_5 + k_1)^2(\ell_5 - k_3 - k_4)^2 \ell_6^2(\ell_5 + \ell_6)^2(\ell_5 + \ell_6 - k_4)^2(\ell_6 + k_3)^2} \tag{3.8}$$

for double poles as well as poles at infinity, and impose conditions on the c_i and Q such that any such poles vanish. For the nonplanar double box, we apply this cut on the four propagators carrying momentum ℓ_6,

$$\ell_6^2 = (\ell_5 + \ell_6)^2 = (\ell_5 + \ell_6 - k_4)^2 = (\ell_6 + k_3)^2 = 0\,. \tag{3.9}$$

The Jacobian for this cut is

$$J_6 = (\ell_5 - k_3)^2(\ell_5 - k_4)^2 - (\ell_5 - k_3 - k_4)^2\ell_5^2 = (\ell_5 \cdot q)(\ell_5 \cdot \overline{q})\,, \tag{3.10}$$

where $q = \lambda_3\widetilde{\lambda}_4$, $\overline{q} = \lambda_4\widetilde{\lambda}_3$.

After imposing the quadruple cut conditions in Eq. (3.9) the remaining integrand, including the Jacobian (3.10), is

$$\operatorname*{Res}_{\ell_6\text{-cut}}\left[\mathcal{I}^{(\mathrm{NP})}\right] \equiv \widetilde{\mathcal{I}}^{(\mathrm{NP})} = \frac{c_1\ell_5^2 + c_2(\ell_5 \cdot Q) + c_3 s + c_4 t}{\ell_5^2(\ell_5 + k_1)^2(\ell_5 - k_3 - k_4)^2(\ell_5 \cdot q)(\ell_5 \cdot \overline{q})}\,, \tag{3.11}$$

where the integrand evaluated on the cut is denoted by a new symbol $\widetilde{\mathcal{I}}^{(NP)}$ for brevity.

To make the potentially problematic singularities visible, we parametrize the four-dimensional part of the remaining loop momentum as

$$\ell_5 = \alpha\lambda_3\widetilde{\lambda}_3 + \beta\lambda_4\widetilde{\lambda}_4 + \gamma\lambda_3\widetilde{\lambda}_4 + \delta\lambda_4\widetilde{\lambda}_3\,. \tag{3.12}$$

This gives us

$$\begin{aligned}\widetilde{\mathcal{I}}^{(\mathrm{NP})} =& \Big(c_1(\alpha\beta - \gamma\delta)s + c_2\left[\alpha(Q \cdot k_3) + \beta(Q \cdot k_4) + \gamma\langle 3|Q|4] + \delta\langle 4|Q|3]\right] + c_3 s + c_4 t\Big) \\ &\times \Big[s^2(\alpha\beta - \gamma\delta)(\alpha\beta - \gamma\delta - \alpha - \beta + 1) \\ &\qquad \times \Big((\alpha\beta - \gamma\delta)s + \alpha u + \beta t - \gamma\langle 13\rangle[14] - \delta\langle 14\rangle[13]\Big)\gamma\delta\Big]^{-1}\,,\end{aligned} \tag{3.13}$$

where we use the convention $2k_i \cdot k_j = \langle ij\rangle[ij]$ and $\langle i|k_m|j] \equiv \langle im\rangle[mj]$. Our goal is to identify double- or higher-order poles. To expose these, we take residues in a certain order. For example, taking consecutive residues at $\gamma = 0$ and $\delta = 0$ followed by $\beta = 0$ gives

$$\operatorname*{Res}_{\substack{\gamma=\delta=0\\ \beta=0}}\left[\widetilde{\mathcal{I}}^{(\mathrm{NP})}\right] = \frac{c_2\alpha(Q \cdot k_3) + c_3 s + c_4 t}{s^2 u\alpha^2(1-\alpha)}\,. \tag{3.14}$$

Similarly taking consecutive residues first at $\gamma = \delta = 0$ followed by $\beta = 1$, we get

$$\operatorname*{Res}_{\substack{\gamma=\delta=0\\ \beta=1}}\left[\widetilde{\mathcal{I}}^{(\mathrm{NP})}\right] = -\frac{c_1\alpha s + c_2\left[\alpha(Q \cdot k_3) + (Q \cdot k_4)\right] + c_3 s + c_4 t}{s^2 t\alpha(1-\alpha)^2}\,. \tag{3.15}$$

In both cases we see that there are unwanted double poles in α. The absence of double poles forces us to choose the c_i in the numerator such that the integrand reduces to at most a single pole in α. Canceling the double pole at $\alpha = 0$ in Eq. (3.14) requires $c_3 = c_4 = 0$. Similarly, the second residue in Eq. (3.15) enforces $c_1 s + c_2(Q\cdot(k_3+k_4)) = 0$ to cancel the double pole at $\alpha = 1$. The solution that ensures $N^{(\mathrm{NP})}$ is a $d\log$ numerator is

$$N^{(\mathrm{NP})} = \frac{c_1}{s}[\ell_5^2(Q\cdot(k_3+k_4)) - (k_3+k_4)^2(\ell_5\cdot Q)]\,. \tag{3.16}$$

The integrand is now free of the uncovered double poles, but requiring the absence of poles at infinity imposes further constraints on the numerator. If any of the parameters α, β, γ or δ grow large, the loop momentum ℓ_5 Eq. (3.12) also becomes large. Indeed, such a pole can be accessed by first taking the residue at $\delta = 0$, followed by taking the residues at $\alpha = 0$ and $\beta = 0$:

$$\operatorname*{Res}_{\substack{\delta=0\\ \alpha=\beta=0}}\left[\widetilde{\mathcal{I}}^{(\mathrm{NP})}\right] = \frac{\langle 3|Q|4]}{\gamma s^2\langle 13\rangle[14]}\,. \tag{3.17}$$

The resulting form $d\gamma/\gamma$ has a pole for $\gamma\to\infty$. Similarly, taking a residue at $\gamma = 0$, followed by residues at $\alpha = 0$ and $\beta = 0$ results in a single pole for $\delta\to\infty$. To prevent such poles at infinity from appearing requires $\langle 3|Q|4] = \langle 4|Q|3] = 0$, which in turn requires that $Q = \sigma_1 k_3 + \sigma_2 k_4$ with the σ_i arbitrary constants. This is enough to determine the numerator, up to two arbitrary coefficients.

As an exercise in the notation outlined in the beginning of the section, as well as to illustrate a second approach, we could also consider the cut sequence $\{B(\ell_6)\}$, following the notation defined at the end of Sect. 2.3. The resulting Jacobian is

$$J_6 = (\ell_5 - k_4)^2(\ell_5 - k_3)^2 - (\ell_5 + k_1 + k_2)^2\ell_5^2\,. \tag{3.18}$$

The two terms on the right already appear as propagators in the integrand, and so to avoid double poles, the $d\log$ numerator must scale as $N^{(\mathrm{NP})}\sim(\ell_5+k_1+k_2)^2\ell_5^2$ in the kinematic regions where $(\ell_5-k_4)^2(\ell_5-k_3)^2 = 0$. This constraint is sufficient to fix the ansatz Eq. (3.7) for $N^{(\mathrm{NP})}$.

In both approaches, the constraints of having only logarithmic singularities and no poles at infinity results in a numerator for the nonplanar double box of the form,

$$N^{(\mathrm{NP})} = a_1^{(\mathrm{NP})}(\ell_5-k_3)^2 + a_2^{(\mathrm{NP})}(\ell_5-k_4)^2\,, \tag{3.19}$$

where $a_1^{(\mathrm{NP})}$ and $a_2^{(\mathrm{NP})}$ are numerical coefficients. Finally, we impose that the numerator should respect the symmetries of the diagram. Because the nonplanar double box is symmetric under $k_3\leftrightarrow k_4$ this forces $a_2^{(\mathrm{NP})} = a_1^{(\mathrm{NP})}$, resulting in a unique numerator up to an overall constant

$$N_1^{(\mathrm{NP})} = (\ell_5-k_3)^2 + (\ell_5-k_4)^2\,. \tag{3.20}$$

3.2 Expansion of the amplitude

In the previous subsection we outlined a procedure to construct a basis of integrands where each element has only logarithmic singularities and no pole at infinity. The next step is to actually expand the amplitude in terms of this basis. As mentioned before, we primarily focus on the L-loop contribution to the $\mathcal{N}=4$ sYM theory, four-point amplitudes. Following the normalization conventions of Ref. [84]. these can be written in a diagrammatic representation

$$\mathcal{A}_4^{L-\text{loop}} = g^{2+2L}\frac{i^L\mathcal{K}}{(2\pi)^{DL}}\sum_{\mathcal{S}_4}\sum_x \frac{1}{S^{(x)}}c^{(x)}\int d\mathcal{I}^{(x)}(\ell_5,\ldots,\ell_{4+L})\,, \tag{3.21}$$

where $d\mathcal{I}^{(x)}$ is the integrand form defined in Eq. (3.2), and we have implicitly analytically continued the expression to D dimensions to be consistent with dimensional regularization. In Eq. (3.21) the sum labeled by x runs over the set of distinct, non-isomorphic diagrams with only cubic vertices, and the sum over $\mathcal{S}_4$ is over all 4! permutations of external legs. The symmetry factor $S^{(x)}$ then removes overcounting that arises from automorphisms of the diagrams. The color factor $c^{(x)}$ of diagram (x) is given by dressing every three-vertex with a group-theory structure constant, $\tilde{f}^{abc} = i\sqrt{2}f^{abc}$. In the sum over permutations in Eq. (3.21), any given $d\mathcal{I}^{(x')}$ is a momentum relabeling of $d\mathcal{I}^{(x)}$ in Eq. (3.2).

For the cases we consider, the prefactor is proportional to the color-ordered tree amplitude,

$$\mathcal{K} = stA_4^{\text{tree}}(1,2,3,4)\,. \tag{3.22}$$

Furthermore, $\mathcal{K}$ has a crossing symmetry so it can also be expressed in terms of the tree amplitude with different color orderings,

$$\mathcal{K} = suA_4^{\text{tree}}(1,2,4,3) = tuA_4^{\text{tree}}(1,3,2,4)\,. \tag{3.23}$$

The explicit values of the tree amplitudes are

$$A_4^{\text{tree}}(1,2,3,4) = i\frac{\delta^8(\mathcal{Q})}{\langle 12\rangle\langle 23\rangle\langle 34\rangle\langle 41\rangle}\,, \tag{3.24}$$

where the other two orderings are just relabelings of the first. The factor $\delta^8(\mathcal{Q})$ is the supermomentum conservation δ function, as described in e.g. Ref. [7]. The details of this factor are not important for our discussion. For external gluons with helicities $1^-, 2^-, 3^+, 4^+$ it is just $\langle 12\rangle^4$, up to Grassmann parameters.

A simple method for expanding the amplitude in terms of $d\log$ numerators is to use previously constructed representations of the amplitude as reference data, rather than

sew together lower-loop amplitudes directly. Especially at higher loops, this drastically simplifies the process of determining the coefficients $a_i^{(x)}$. To ensure that the constructed amplitude is complete and correct, we also check a complete set of unitarity cuts via the method of maximal cuts [97].

As an illustration of the procedure for determining the coefficients, consider the two-loop amplitude. A representation of the two-loop four-point amplitude is [77] Eqs. (3.21) and (3.3) with numerators

$$N_{\text{old}}^{(\text{P})} = s\,, \qquad\qquad N_{\text{old}}^{(\text{NP})} = s\,, \tag{3.25}$$

where we follow the normalization conventions of Ref. [84]. Following our strategy, we demand that the numerators are linear combinations of the basis elements constructed in Eqs. (3.6) and (3.19):

$$N^{(\text{P})} = a_1^{(\text{P})} s + a_2^{(\text{P})} t\,, \qquad\qquad N^{(\text{NP})} = a^{(\text{NP})}((\ell_5 - k_3)^2 + (\ell_5 - k_4)^2)\,, \tag{3.26}$$

where, for comparison to $N_{\text{old}}^{(\text{NP})}$, it is useful to rewrite the nonplanar numerator as

$$N^{(\text{NP})} = a^{(\text{NP})}(-s + (\ell_5 - k_3 - k_4)^2 + \ell_5^2)\,. \tag{3.27}$$

We can determine the coefficients by comparing the new and old expressions on the maximal cuts. By maximal cuts we mean replacing all propagators with on-shell conditions, $p_{\alpha_{(x)}}^2 = 0$, defined in Eq. (3.1). The planar double-box numerator is unchanged on the maximal cut, since it is independent of all loop momenta. Comparing the two expressions in Eqs. (3.25) and (3.26) gives

$$a_1^{(\text{P})} = 1\,, \qquad\qquad a_2^{(\text{P})} = 0\,. \tag{3.28}$$

For the nonplanar numerator we note that under the maximal cut conditions $\ell_5^2 = (\ell_5 - k_3 - k_4)^2 = 0$. Comparing the two forms of the nonplanar numerator in Eqs. (3.25) and (3.27) after imposing these conditions means

$$a_1^{(\text{NP})} = -1\,, \tag{3.29}$$

so that the final numerators are

$$N^{(\text{P})} = s\,, \qquad\qquad N^{(\text{NP})} = -((\ell_5 - k_3)^2 + (\ell_5 - k_4)^2)\,. \tag{3.30}$$

Although this fixes all coefficients in our basis, it does not prove that our construction gives the correct sYM amplitude. At two loops this was already proven in Ref. [76], where the difference between amplitudes in the old and the new representation was shown to vanish via the color Jacobi identity. More generally, we can appeal to the method of maximal cuts since it offers a systematic and complete means of ensuring that our constructed nonplanar amplitudes are correct.

3.3 Amplitudes and sums of $d\log$ forms

At any loop order, assuming the four-point $\mathcal{N}=4$ sYM amplitudes have only logarithmic singularities then we can write integrand forms as a sum of $d\log$ forms. At the relatively low loop orders that we are working, we can do this diagram by diagram, using the expansion of the diagrams given in Eq. (3.21). We then take each diagram form in Eq. (3.21) and expand it as a linear combination of $d\log$ forms,

$$d\mathcal{I}^{(x)} = \sum_{j=1}^{3} C_j \, d\mathcal{I}_j^{(x),d\log} \,, \tag{3.31}$$

where the $d\mathcal{I}_j^{(x),d\log}$ are (potentially sums of) $d\log$ $4L$ forms. As discussed in Ref. [71], for MHV amplitudes the coefficients C_j are Park-Taylor factors with different orderings. This follows from super-conformal symmetry of $\mathcal{N}=4$ sYM theory, which fixes the coefficients C_j to be holomorphic functions of spinor variables λ and normalizes $d\mathcal{I}^{(x)}$ to be a $d\log$ form. In the four-point nonplanar case this means that there are only three different coefficients we can get,

$$C_1 = A_4^{\text{tree}}(1,2,3,4)\,, \qquad C_2 = A_4^{\text{tree}}(1,2,4,3)\,, \qquad C_3 = A_4^{\text{tree}}(1,3,2,4)\,, \tag{3.32}$$

where the explicit form of the tree amplitudes are given in Eq. (3.24). The three coefficient are not independent, as they satisfy $C_1+C_2+C_3=0$. Suppose that the basis elements in Eq. (3.21) are chosen such that they have only logarithmic singularities. We will show, in Sect. 5, that we can indeed write the diagram as $d\log$ forms with coefficients given by the C_j.

4 Three-loop amplitude

In this section we follow the recipe of the previous section to find a basis of three-loop diagram integrands that have only logarithmic singularities and no poles at infinity. The three-loop four-point parent diagrams are shown in Fig. 4. These have been classified in Ref. [78, 83], where an unintegrated representation of the three-loop four-point amplitude of $\mathcal{N}=4$ sYM theory including nonplanar contributions was first obtained. As mentioned in Sect. 3.1, we restrict to parent diagrams where no bubble or triangle diagrams appear as subdiagrams; otherwise we would find a pole at infinity that cannot be removed. Diagrams with contact terms can be incorporated into a parent diagram by including inverse propagators in the numerator that cancel propagators.

Next we assign power counting of the numerator for each parent diagram. Applying the power-counting rules in Sect. 3.1, we find that the maximum powers of allowed loop

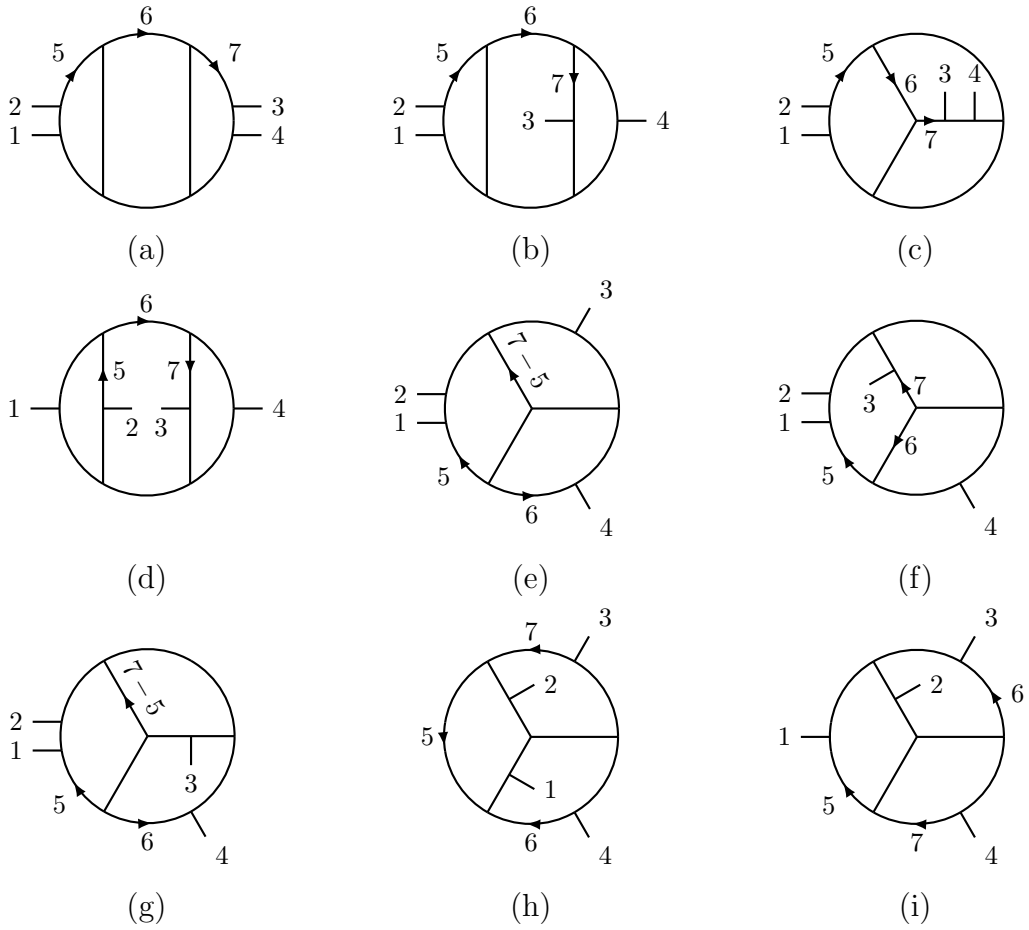

Figure 4. The distinct parent diagrams for three-loop four-point amplitudes. The remaining parent diagrams are obtained by relabeling external legs.

momenta for each parent diagram are

$$
\begin{aligned}
&N^{(\mathrm{a})} = \mathcal{O}(1)\,, \qquad N^{(\mathrm{b})} = \mathcal{O}(\ell_6^2)\,, \qquad N^{(\mathrm{c})} = \mathcal{O}(\ell_5^2\,, (\ell_5 \cdot \ell_7), \ell_7^2)\,,\\
&N^{(\mathrm{d})} = \mathcal{O}(\ell_6^4)\,, \qquad N^{(\mathrm{e})} = \mathcal{O}(\ell_5^2)\,, \qquad N^{(\mathrm{f})} = \mathcal{O}(\ell_5^4)\,, \qquad N^{(\mathrm{g})} = \mathcal{O}(\ell_5^2\ell_6^2)\,,\\
&N^{(\mathrm{h})} = \mathcal{O}(\ell_5^2\ell_6^2, \ell_5^2\ell_7^2,\ \ell_5^2(\ell_6 \cdot \ell_7))\,, \qquad N^{(\mathrm{i})} = \mathcal{O}(\ell_5^2\ell_6^2)\,,
\end{aligned}
\tag{4.1}
$$

where we use the labels in Fig. 4, since these give the most stringent power counts. For diagram (h) we need to combine restrictions from a variety of labelings to arrive at at this stringent power count. Ignoring the overall prefactor of $\mathcal{K}$, the overall dimension of each numerator is $\mathcal{O}(p^4)$, including external momenta.

4.1 Diagram numerators

The next step is to write down the most general diagram numerators that are consistent with the power count in Eq. (4.1), respect diagram symmetry, are built only from Lorentz dot products of the loop and external momenta, have only logarithmic singularities and have no poles at infinity. Although the construction is straightforward, the complete list of conditions is lengthy, so here we only present a few examples and then write down a table of numerators satisfying the constraints.

We start with diagram (a) in Fig. 4. The required numerators are simple to write down if we follow the same logic as in the two-loop example in Sect. 3.1. Since the numerator of diagram (a) is independent of all loop momenta as noted in Eq. (4.1), we can only write numerators that depend on the Mandelstam invariants s and t. There are three numerators that are consistent with the overall dimension,

$$N_1^{(\mathrm{a})} = s^2\,, \qquad N_2^{(\mathrm{a})} = st\,, \qquad N_3^{(\mathrm{a})} = t^2\,. \tag{4.2}$$

Following similar logic as at two loops, it is straightforward to check that there are no double poles or poles at infinity.

The numerator for diagram (b) is also easy to obtain, this time by following the logic of the two-loop nonplanar diagram. From Eq. (4.1), we see that the only momentum dependence of the numerator must be on ℓ_6. The two-loop subdiagram on the right side of diagram (b) in Fig. 4 containing ℓ_6 is just the two-loop nonplanar double box we already analyzed in Sect. 3.1. Repeating the earlier nonplanar box procedure for this subdiagram gives us the most general possible numerator for diagram (b),

$$N_1^{(\mathrm{b})} = s\big((\ell_6 - k_3)^2 + (\ell_6 - k_4)^2\big)\,. \tag{4.3}$$

This is just the two-loop nonplanar numerator with an extra factor of s. A factor of t instead of s is disallowed because it violates the $k_3 \leftrightarrow k_4$ symmetry of diagram (b).

As a somewhat more complicated example, consider diagram (e) in Fig. 4. Because this diagram is planar we could use dual conformal invariance to find the desired numerator. Instead, for illustrative purposes we choose to obtain it only from the requirements of having logarithmic singularities and no pole at infinity, without invoking dual conformal invariance. We discuss the relation to dual conformal symmetry further in Sect. 7.

From Eq. (4.1) we see that the numerator depends on the loop momentum ℓ_5 at most quadratically. Therefore we may start with the ansatz

$$N^{(\mathrm{e})} = (c_1 s + c_2 t)\big(\ell_5^2 + d_1(\ell_5 \cdot Q) + d_2 s + d_3 t\big)\,, \tag{4.4}$$

where Q is a vector independent of all loop momenta and the c_i and d_i are numerical constants. We have included an overall factor depending on s and t so that the numerator has the correct overall dimensions, but this factor does not play a role in canceling unwanted singularities of the integrand.

In order to extract conditions on the numerator ansatz Eq. (4.4), we need to find any hidden double poles or poles at infinity in the integrand. The starting integrand is

$$\begin{aligned}\mathcal{I}^{(\mathrm{e})} =& \frac{N^{(\mathrm{e})}}{\ell_6^2(\ell_6+\ell_5)^2(\ell_6+\ell_7)^2(\ell_6+k_4)^2(\ell_7-\ell_5)^2(\ell_7-k_1-k_2)^2(\ell_7+k_4)^2} \\ & \times \frac{1}{\ell_5^2(\ell_5-k_1)^2(\ell_5-k_1-k_2)^2}\,. \end{aligned} \tag{4.5}$$

Since our numerator ansatz (4.4) is a function of ℓ_5, we seek double poles only in the regions of momentum space that we can reach by choosing convenient on-shell values for ℓ_6 and ℓ_7. This leaves the numerator ansatz unaltered, making it straightforward to determine all coefficients.

To locate a double pole, consider the cut sequence

$$\text{cut} = \{B(\ell_6), B(\ell_7,\ell_7)\}\,, \tag{4.6}$$

where we follow the notation defined at the end of Sect. 2.3. Here $B(\ell_7,\ell_7)$ indicates that we cut the $1/\ell_7^2$ propagator produced by the $B(\ell_6)$ cut. This produces an overall Jacobian

$$J_{6,7} = s\left[(\ell_5+k_4)^2\right]^2\,. \tag{4.7}$$

After this sequence of cuts, the integrand of Eq. (4.5) becomes:

$$\operatorname*{Res}_{\substack{\ell_6\text{–cut}\\ \ell_7\text{–cut}}}\left[\mathcal{I}^{(\mathrm{e})}\right] = \frac{N^{(\mathrm{e})}}{\ell_5^2(\ell_5-k_1)^2(\ell_5-k_1-k_2)^2\left[(\ell_5+k_4)^2\right]^2 s}\,, \tag{4.8}$$

exposing a double pole at $(\ell_5+k_4)^2=0$.

To impose our desired constraints on the integrand, we need to cancel the double pole in the denominator with an appropriate numerator. We see that choosing the ansatz in Eq. (4.4) to have $Q=k_4$, $d_1=2$, $d_2=0$, $d_3=0$ gives us the final form of the allowed numerator,

$$N^{(\mathrm{e})} = (c_1 s + c_2 t)(\ell_5+k_4)^2\,, \tag{4.9}$$

so we have two basis numerators,

$$N_1^{(\mathrm{e})} = s(\ell_5+k_4)^2\,, \qquad\qquad N_2^{(\mathrm{e})} = t(\ell_5+k_4)^2\,. \tag{4.10}$$

We have also checked that this numerator passes all other double-pole constraints coming from different regions of momentum space. In addition, we have checked that

it has no poles at infinity. It is interesting that, up to a factor depending only on external momenta, these are precisely the numerators consistent with dual conformal symmetry. As we discuss in Sect. 7, this is no accident.

Next consider diagram (d) in Fig. 4. From the power counting arguments summarized in Eq. (4.1), we see that the numerator for this diagram is a quartic function of momentum ℓ_6, but that it depends on neither ℓ_5 nor ℓ_7. When constructing numerators algorithmically we begin with a general ansatz, but to more easily illustrate the role of contact terms we start from the natural guess that diagram (d) is closely related to a product of two two-loop nonplanar double boxes. Thus our initial guess is that the desired numerator is the product of numerators corresponding to the two-loop nonplanar subdiagrams:

$$\widetilde{N}^{(\mathrm{d})} = \left[(\ell_6 + k_1)^2 + (\ell_6 + k_2)^2\right] \left[(\ell_6 - k_3)^2 + (\ell_6 - k_4)^2\right] . \tag{4.11}$$

We label this numerator $\widetilde{N}^{(\mathrm{d})}$ because, as we see below, it is not quite the numerator $N^{(\mathrm{d})}$ that satisfies our pole constraints. As always, note that we have required the numerator to satisfy the symmetries of the diagram.

Although we do not do so here, one can show that this ansatz satisfies nearly all constraints on double poles and poles at infinity. The double pole not removed by the numerator is in the kinematic region:

$$\text{cut} = \{\ell_5^2, (\ell_5 + k_2)^2, \ell_7^2, (\ell_7 - k_3)^2, B(\ell_6)\} . \tag{4.12}$$

Before imposing the final box cut, we solve the first four cut conditions in terms of two parameters α and β:

$$\ell_5 = \alpha k_2 , \qquad \ell_7 = -\beta k_3 . \tag{4.13}$$

The final $B(\ell_6)$ represents a box-cut of four of the six remaining propagators that depend on α and β:

$$(\ell_6 - \alpha k_2)^2 = (\ell_6 - \alpha k_2 + k_1)^2 = (\ell_6 + \beta k_3)^2 = (\ell_6 + \beta k_3 - k_4)^2 = 0 . \tag{4.14}$$

Before cutting the $B(\ell_6)$ propagators, the integrand is

$$\operatorname*{Res}_{\substack{\ell_5\text{–cut} \\ \ell_7\text{–cut}}} \widetilde{\mathcal{I}}^{(\mathrm{d})} = \frac{\widetilde{N}^{(\mathrm{d})}}{\ell_6^2(\ell_6 + k_1 + k_2)^2(\ell_6 - \alpha k_2)^2(\ell_6 - \alpha k_2 + k_1)^2(\ell_6 + \beta k_3)^2(\ell_6 + \beta k_3 - k_4)^2} . \tag{4.15}$$

Localizing further to the $B(\ell_6)$ cuts produces a Jacobian

$$J_6 = su(\alpha - \beta)^2 , \tag{4.16}$$

while a solution to the box-cut conditions of Eq. (4.14)

$$\ell_6^* = \alpha\lambda_4\widetilde{\lambda}_2\frac{\langle 12\rangle}{\langle 14\rangle} - \beta\lambda_1\widetilde{\lambda}_3\frac{\langle 34\rangle}{\langle 14\rangle}\,, \tag{4.17}$$

turns the remaining uncut propagators of Eq. (4.15) into:

$$\ell_6^2 = s\alpha\beta\,, \qquad\qquad (\ell_6 + k_1 + k_2)^2 = s(1+\alpha)(1+\beta)\,. \tag{4.18}$$

The result of completely localizing all momenta in this way is:

$$\operatorname*{Res}_{\text{cuts}} \widetilde{\mathcal{I}}^{(\mathrm{d})} = -\frac{s^2(\alpha(1+\beta)+\beta(1+\alpha))^2}{s^3u\alpha\beta(1+\alpha)(1+\beta)(\alpha-\beta)^2}\,. \tag{4.19}$$

We see that there is a double pole located at $\alpha - \beta = 0$. To cancel this double pole, we are forced to add an extra term to the numerator. A natural choice is a term that collapses both propagators connecting the two two-loop nonplanar subdiagrams: $\ell_6^2(\ell_6+k_1+k_2)^2$. On the support of the cut solutions Eq. (4.17), this becomes $s^2\alpha\beta(\alpha+1)(\beta+1)$. We can cancel the double pole at $\alpha-\beta=0$ in Eq. (4.19) by choosing the linear combination

$$N_1^{(\mathrm{d})} = \left[(\ell_6+k_1)^2 + (\ell_6+k_2)^2\right]\left[(\ell_6-k_3)^2 + (\ell_6-k_4)^2\right] - 4\ell_6^2(\ell_6+k_1+k_2)^2\,. \tag{4.20}$$

Indeed, with this numerator the diagram lacks even a single pole at $\alpha-\beta=0$.

It is interesting to note that if we relax the condition that the numerator respects the diagram symmetry $k_1 \leftrightarrow k_2$ and $k_3 \leftrightarrow k_4$, there are four independent numerators with no double pole. For example,

$$\tilde{N}^{(\mathrm{d})} = (\ell_6+k_1)^2(\ell_6-k_3)^2 - \ell_6^2(\ell_6+k_1+k_2)^2\,, \tag{4.21}$$

is a *d*log numerator. When we require that $N^{(\mathrm{d})}$ respect diagram symmetry, we need the first four terms in Eq. (4.20), each with its own "correction" term $-\ell_6^2(\ell_6+k_1+k_2)^2$. This accounts for the factor of four on the last term in Eq. (4.20).

We have carried out detailed checks of all potentially dangerous regions of the integrand of diagram (d) showing that the numerator of Eq. (4.20) results in a diagram with only logarithmic singularities and no poles at infinity. In fact, the numerator (4.20) is the only one respecting the symmetries of diagram (d) with these properties. We showed this by starting with a general ansatz subject to the power counting constraint in Eq. (4.1) and showing that no other solution exists other than the one in Eq. (4.20).

We have gone through the diagrams in Fig. 4 in great detail, finding the numerators that respect diagram symmetry (including color signs), and that have only logarithmic

Diagram		Numerators
(a)	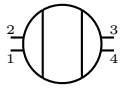	$N_1^{(\mathrm{a})} = s^2\,, \qquad N_2^{(\mathrm{a})} = st\,, \qquad N_3^{(\mathrm{a})} = t^2\,,$
(b)	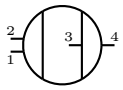	$N_1^{(\mathrm{b})} = s\left[(\ell_6 - k_3)^2 + (\ell_6 - k_4)^2\right]\,,$
(c)	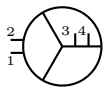	$N_1^{(\mathrm{c})} = s\left[(\ell_5 - \ell_7)^2 + (\ell_5 + \ell_7 + k_1 + k_2)^2\right]\,,$
(d)	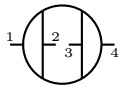	$N_1^{(\mathrm{d})} = \left[(\ell_6 + k_1)^2 + (\ell_6 + k_2)^2\right]^2 - 4\ell_6^2(\ell_6 + k_1 + k_2)^2\,,$
(e)	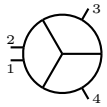	$N_1^{(\mathrm{e})} = s(\ell_5 + k_4)^2\,, \qquad N_2^{(\mathrm{e})} = t(\ell_5 + k_4)^2\,,$
(f)	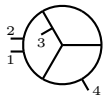	$N_1^{(\mathrm{f})} = (\ell_5 + k_4)^2\left[(\ell_5 + k_3)^2 + (\ell_5 + k_4)^2\right]\,,$
(g)	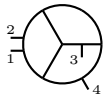	$N_1^{(\mathrm{g})} = s(\ell_5 + \ell_6 + k_3)^2\,, \qquad N_2^{(\mathrm{g})} = t(\ell_5 + \ell_6 + k_3)^2\,,$ $N_3^{(\mathrm{g})} = (\ell_5 + k_3)^2(\ell_6 + k_1 + k_2)^2\,, \qquad N_4^{(\mathrm{g})} = (\ell_5 + k_4)^2(\ell_6 + k_1 + k_2)^2\,,$
(h)	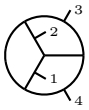	$N_1^{(\mathrm{h})} = (\ell_5 + k_2 + k_3)^2(\ell_6 + \ell_7)^2 - \ell_5^2(\ell_6 + \ell_7 - k_1 - k_2)^2\,,$ $N_2^{(\mathrm{h})} = \left[(\ell_6 + \ell_7 - k_1)^2 + (\ell_6 + \ell_7 - k_2)^2\right]\left[(\ell_5 - k_1)^2 + (\ell_5 - k_4)^2\right]$ $\quad - 4\,\ell_5^2(\ell_6 + \ell_7 - k_1 - k_2)^2\,,$
(i)	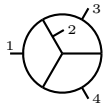	$N_1^{(\mathrm{i})} = (\ell_6 + k_4)^2\left[(\ell_5 - k_1 - k_2)^2 + (\ell_5 - k_1 - k_3)^2\right]$ $\quad - (\ell_5 + k_4)^2\left[(\ell_6 + k_1 + k_4)^2 + (\ell_6 + k_2 + k_4)^2\right]\,.$

Table 1. The numerator basis elements without canceled propagators, corresponding to the labels of the parent diagrams in Fig. 4. The basis elements respect the symmetries of the diagrams.

Diagram		Numerator
(c)	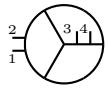	$N_2^{(\mathrm{c})} = (\ell_5)^2\,(\ell_7)^2 + (\ell_5+k_1+k_2)^2\,(\ell_7)^2 + (\ell_5)^2\,(\ell_7+k_1+k_2)^2 + (\ell_5+k_1+k_2)^2(\ell_7+k_1+k_2)^2\,,$
(f)	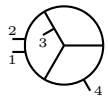	$N_2^{(\mathrm{f})} = \ell_5^2(\ell_5-k_1-k_2)^2\,,$
(g)	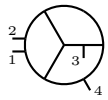	$N_5^{(\mathrm{g})} = (\ell_5-k_1-k_2)^2\left[(\ell_6+k_3)^2-\ell_6^2\right]\,,$ $N_6^{(\mathrm{g})} = (\ell_5-k_1-k_2)^2(\ell_6-k_4)^2\,,$ $N_7^{(\mathrm{g})} = \ell_5^2(\ell_6-k_4)^2\,,$
(h)	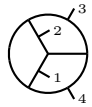	$N_3^{(\mathrm{h})} = (\ell_5-\ell_7)^2\left[(\ell_6+k_4+k_1)^2-(\ell_6+k_4)^2\right] - (\ell_6+k_4)^2\left[(\ell_5-\ell_7+k_1)^2-(\ell_5-\ell_7)^2\right] + (\ell_5+\ell_6)^2\left[(\ell_7+k_3+k_2)^2-(\ell_7+k_3)^2\right] + (\ell_7+k_3)^2\left[(\ell_5+\ell_6+k_2)^2-(\ell_5+\ell_6)^2\right] + (\ell_6)^2\left[(\ell_5-\ell_7+k_2+k_3)^2-(\ell_5-\ell_7+k_2)^2\right] - (\ell_5-\ell_7+k_2)^2\left[(\ell_6+k_3)^2-(\ell_6)^2\right] - (\ell_5+\ell_6-k_1)^2\left[(\ell_7+k_4)^2-(\ell_7)^2\right] - (\ell_7)^2\left[(\ell_5+\ell_6-k_1+k_4)^2-(\ell_5+\ell_6-k_1)^2\right]\,,$ $N_4^{(\mathrm{h})} = \ell_6^2(\ell_5-\ell_7)^2+\ell_7^2(\ell_5+\ell_6)^2+(\ell_6+k_4)^2(\ell_5-\ell_7+k_2)^2 + (\ell_5+\ell_6-k_1)^2(\ell_7+k_3)^2\,,$
(i)	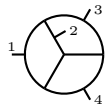	$N_2^{(\mathrm{i})} = \frac{1}{3}(\ell_5+\ell_6+k_4)^2\,[t-s]\,,$ $N_3^{(\mathrm{i})} = (\ell_6)^2\left[(\ell_5+k_2)^2-\ell_5^2\right]-(\ell_5)^2\left[(\ell_6+k_2)^2-\ell_6^2\right]\,,$ $N_4^{(\mathrm{i})} = (\ell_6)^2\,(\ell_5-k_1)^2-(\ell_5)^2\,(\ell_6-k_3)^2\,.$

Table 2. The parent diagram numerator basis elements where a numerator factor cancels a propagator. Each term in brackets does not cancel a propagator, while the remaining factors each cancel a propagator. Each basis numerator maintains the symmetries of the associated diagram, including color signs. The associated color factor can be read off from each diagram.

singularities and no poles at infinity. This gives us a set of basis $d$log numerators associated with each diagram. For the diagrams where numerator factors do not cancel any propagators, the set of numerators is collected in Table 1. In addition, there are also diagrams where numerators do cancel propagators. For the purpose of constructing amplitudes, it is convenient to absorb these contact contributions into the parent

Diagram		Numerator
(j)	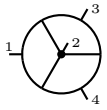	$N_1^{(\mathrm{j})} = s\,, \qquad N_2^{(\mathrm{j})} = t\,,$
(k)	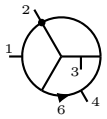	$N_1^{(\mathrm{k})} = (\ell_6 + k_3)^2 - \ell_6^2,$
(l)	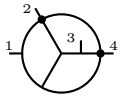	$N_1^{(\mathrm{l})} = 1\,.$

Table 3. The numerator basis elements corresponding to the contact term diagrams. Black dots indicate contact terms. Written this way, the numerators are simple, but the color factors cannot be read off from the diagrams.

diagrams of Fig. 4 to make color assignments manifest. This allows us to treat all contributions on an equal footing, such that we can read off the color factors directly from the associated parent diagram by dressing each three vertex with an $\tilde{f}^{abc}$. This distributes the contact term diagrams in Table 3 among the parent diagrams, listed in Table 2. When distributing the contact terms to the parent diagrams, we change the momentum labels to those of each parent diagram and then multiply and divide by the missing propagator(s). The reason the numerators in Table 2 appear more complicated than those in Table 3 is that a single term from Table 3 can appear with multiple momentum relabellings in order to enforce the symmetries of the parent diagrams on the numerators.

As an example of the correspondence between the numerators in Table 2 and Table 3, consider diagram (j) and the associated numerators, $N_1^{(\mathrm{j})}$ and $N_2^{(\mathrm{j})}$, in Table 3. To convert this into a contribution to diagram (i) in Table 2, we multiply and divide by the missing propagator $1/(\ell_5 + \ell_6 + k_4)^2$. Then we need to take the appropriate linear combination so that the diagram (i) antisymmetry (including the color sign) under $\{k_1 \leftrightarrow k_3, \ell_5 \leftrightarrow \ell_6, \ell_7 \leftrightarrow -\ell_7\}$ is satisfied. This gives,

$$N_2^{(\mathrm{i})} = \frac{1}{3}(\ell_5 + \ell_6 + k_4)^2\,[t - s]\,. \tag{4.22}$$

In fact, there are three alternative propagators that can be inserted instead of $1/(\ell_5 + \ell_6 + k_4)^2$ which are all equivalent to the three relabelings of external lines for diagram (i). We have absorbed a combinatorial factor of $\frac{1}{3}$ into the definition of the numerator

because of the differing symmetries between diagram (i) in Table 2 and diagram (j) in Table 3.

As a second example, consider diagram (k) in Table 3, corresponding to the basis element $N_1^{(\mathrm{k})}$. In this case, considering the three ways of multiplying and dividing by a missing propagator gives the numerators $N_5^{(\mathrm{g})}$, $N_3^{(\mathrm{i})}$ and $N_3^{(\mathrm{h})}$ in Table 2. The three different diagrams (g), (h) and (i) appear because they correspond to the three different ways of expanding the four-point contact vertex of diagram (k) in Table 3. Because we are requiring that the diagram numerators respect the symmetries of the diagrams, we get a single term for $N_4^{(\mathrm{g})}$, eight for diagram $N_3^{(\mathrm{h})}$ and two for $N_3^{(\mathrm{i})}$. For these numerators we have placed the factors corresponding to the relabelings of $N_1^{(\mathrm{k})}$ in Table 2 in brackets.

Similarly, if we put back the two missing propagators by multiplying and dividing by the appropriate inverse propagators, the contribution from diagram (l) in Table 3, corresponds to numerators $N_2^{(\mathrm{c})}$, $N_2^{(\mathrm{f})}$, $N_6^{(\mathrm{g})}$, $N_7^{(\mathrm{g})}$, $N_4^{(\mathrm{h})}$ and $N_4^{(\mathrm{i})}$ in Table 2.

In summary, the diagrams along with the numerators in Table 1 and 2 are a complete set with the desired power counting, have only logarithmic singularities and no poles at infinity. They are also constructed to satisfy diagram symmetries, including color signs.

4.2 Determining the coefficients

We now express the three-loop four-point $\mathcal{N} = 4$ sYM amplitude in terms of our constructed basis. We express the numerator in Eq. (3.21) directly in terms of our basis via Eq. (3.3). Because we have required each basis numerator to reflect diagram symmetry, we need only specify one numerator of each diagram topology and can obtain the remaining ones simple by relabeling of external legs.

The coefficients in front of all basis elements are straightforward to determine using simple unitarity cuts, together with previously determined representations of the three-loop amplitude. We start from the $\mathcal{N} = 4$ sYM numerators as originally determined in Ref. [78], since they happen to be in a particularly compact form. Rewriting these numerators using our choice of momentum labels gives

$$\begin{aligned}
N_{\mathrm{old}}^{(\mathrm{a})} &= N_{\mathrm{old}}^{(\mathrm{b})} = N_{\mathrm{old}}^{(\mathrm{c})} = N_{\mathrm{old}}^{(\mathrm{d})} = s^2\,, \\
N_{\mathrm{old}}^{(\mathrm{e})} &= N_{\mathrm{old}}^{(\mathrm{f})} = N_{\mathrm{old}}^{(\mathrm{g})} = s(\ell_5 + k_4)^2\,, \\
N_{\mathrm{old}}^{(\mathrm{h})} &= -st + 2s(k_2 + k_3)\cdot\ell_5 + 2t(\ell_6 + \ell_7)\cdot(k_1 + k_2)\,, \\
N_{\mathrm{old}}^{(\mathrm{i})} &= s(k_4 + \ell_5)^2 - t(k_4 + \ell_6)^2 - \frac{1}{3}(s - t)(k_4 + \ell_5 + \ell_6)^2\,.
\end{aligned} \tag{4.23}$$

To match to our basis we start by considering the maximal cuts, where all propagators of each diagram are placed on shell. The complete set of maximal cut solutions are

unique to each diagram, so we can match coefficients by considering only a single diagram at a time. We start with diagram (a) in Table 1. Here the numerator is a linear combination of three basis elements

$$N^{(\mathrm{a})} = a_1^{(\mathrm{a})} N_1^{(\mathrm{a})} + a_2^{(\mathrm{a})} N_2^{(\mathrm{a})} + a_3^{(\mathrm{a})} N_3^{(\mathrm{a})} \,, \tag{4.24}$$

corresponding to $N_j^{(\mathrm{a})}$ in Table 1. The $a_j^{(\mathrm{a})}$ are numerical parameters to be determined. This is to be compared to the old form of the numerator in Eq. (4.23). Here the maximal cuts have no effect because both the new and old numerators are independent of loop momentum. Matching the two numerators, the coefficients in front of the numerator basis are $a_1^{(\mathrm{a})} = 1$, $a_2^{(\mathrm{a})} = 0$ and $a_3^{(\mathrm{a})} = 0$.

Now consider diagram (b) in Fig. 4. Here the basis element is of a different form compared to the old version of the numerator in Eq. (4.23). The new form of the numerator is

$$N^{(\mathrm{b})} = a_1^{(\mathrm{b})} N_1^{(\mathrm{b})} = a_1^{(\mathrm{b})} s \left[(\ell_6 - k_3)^2 + (\ell_6 - k_4)^2\right] \,. \tag{4.25}$$

In order to make the comparison to the old version we impose the maximal cut conditions involving only ℓ_6:

$$\ell_6^2 = 0 \,, \qquad (\ell_6 - k_2 - k_3)^2 = 0 \,. \tag{4.26}$$

Applying these conditions:

$$\left[(\ell_6 - k_3)^2 + (\ell_6 - k_4)^2\right] \to -s \,. \tag{4.27}$$

Comparing to $N_{\mathrm{old}}^{(\mathrm{b})}$ in Eq. (4.23) gives us the coefficient $a_1^{(\mathrm{b})} = -1$.

As a more complicated example, consider diagram (i). In this case the numerators depend only on ℓ_5 and ℓ_6. The relevant cut conditions read off from Fig. 4(i) are

$$\ell_5^2 = \ell_6^2 = (\ell_5 - k_1)^2 = (\ell_6 - k_3)^2 = (\ell_5 + \ell_6 - k_3 - k_1)^2 = (\ell_5 + \ell_6 + k_4)^2 = 0 \,. \tag{4.28}$$

With these cut conditions, the old numerator in Eq. (4.23) becomes

$$N_{\mathrm{old}}^{(\mathrm{i})}\big|_{\mathrm{cut}} = 2s\,(k_4 \cdot \ell_5) - 2t\,(k_4 \cdot \ell_6) \,. \tag{4.29}$$

The full numerator for diagram (i) is a linear combination of the four basis elements for diagram (i) in Table 1 and 2,

$$N^{(\mathrm{i})} = a_1^{(\mathrm{i})} N_1^{(\mathrm{i})} + a_2^{(\mathrm{i})} N_2^{(\mathrm{i})} + a_3^{(\mathrm{i})} N_3^{(\mathrm{i})} + a_4^{(\mathrm{i})} N_4^{(\mathrm{i})} \,. \tag{4.30}$$

The maximal cut conditions immediately set to zero the last three of these numerators because they contain inverse propagators. Applying the cut conditions Eq. (4.28) to the nonvanishing term results in

$$N^{(\mathrm{i})}\big|_{\mathrm{cut}} = a_1^{(\mathrm{i})}[-2(\ell_6 \cdot k_4)t + 2(\ell_5 \cdot k_4)s] \,. \tag{4.31}$$

Comparing Eq. (4.29) to Eq. (4.31) fixes $a_1^{(\mathrm{i})} = 1$. The three other coefficients for diagram (i), $a_2^{(\mathrm{i})}$, $a_3^{(\mathrm{i})}$ and $a_4^{(\mathrm{i})}$, cannot be fixed from the maximal cuts.

In order to determine all coefficients and to prove that the answer is complete and correct, we need to evaluate next-to-maximal and next-to-next-to-maximal cuts. We need only evaluate the cuts through this level because of the especially good power counting of $\mathcal{N} = 4$ sYM. We do not describe this procedure in detail here. Details of how this is done may be found in Ref. [98]. Using these cuts we have the solution of the numerators in terms of the basis elements as

$$\begin{aligned}
N^{(\mathrm{a})} &= N_1^{(\mathrm{a})}\,, \\
N^{(\mathrm{b})} &= -N_1^{(\mathrm{b})}\,, \\
N^{(\mathrm{c})} &= -N_1^{(\mathrm{c})} + 2d_1 N_2^{(\mathrm{c})}\,, \\
N^{(\mathrm{d})} &= N_1^{(\mathrm{d})}\,, \\
N^{(\mathrm{e})} &= N_1^{(\mathrm{e})}\,, \\
N^{(\mathrm{f})} &= -N_1^{(\mathrm{f})} + 2d_2\, N_2^{(\mathrm{f})}\,, \\
N^{(\mathrm{g})} &= -N_1^{(\mathrm{g})} + N_3^{(\mathrm{g})} + N_4^{(\mathrm{g})} + (d_4+1)\, N_5^{(\mathrm{g})} + (d_1+d_3-1) N_6^{(\mathrm{g})} + (d_1-d_2) N_7^{(\mathrm{g})}\,, \\
N^{(\mathrm{h})} &= N_1^{(\mathrm{h})} - N_2^{(\mathrm{h})} + d_4\, N_3^{(\mathrm{h})} + 2d_3\, N_4^{(\mathrm{h})}\,, \\
N^{(\mathrm{i})} &= N_1^{(\mathrm{i})} + N_2^{(\mathrm{i})} + d_4\, N_3^{(\mathrm{i})} + (d_3-d_2) N_4^{(\mathrm{i})}\,,
\end{aligned} \tag{4.32}$$

where the four d_i are free parameters not fixed by any physical constraint.

The ambiguity represented by the four free parameters, d_i in Eq. (4.32), derives from color factors not being independent but instead related via the color Jacobi identity. This allows us to move contact terms between different diagrams without altering the amplitude. Consider, for example, the free parameter d_4. Different choices of this parameter move the contact contributions of the type represented by diagram (k) in Table 3 between parent diagrams (g), (h), (i). Similarly, the parameters d_1, d_2, d_3 correspond to three degrees of freedom from color Jacobi identities. These allow us to move contact contributions of diagram (l), where two propagators are collapsed, between different parent diagrams. The contact term in diagram (j) of Table 3 does not generate a fifth degree of freedom because the three resulting parent diagrams are all the same topology, corresponding to relabelings of the external legs of diagram (i). The potential freedom then cancels within a single diagram. We have explicitly checked that the d_i parameters in Eq. (4.32) drop out of the full amplitude after using appropriate color Jacobi identities. One choice of free parameters is to take them to all vanish

$$d_1 = 0\,, \qquad d_2 = 0\,, \qquad d_3 = 0\,, \qquad d_4 = 0\,. \tag{4.33}$$

In this case every nonvanishing numerical coefficient in front of a basis elements is ± 1. (Recall that $N_2^{(\mathrm{i})}$ absorbed the 1/3 combinatorial factor mismatch between diagram (i) and diagram (j).) Of course this is not some "best" choice of the d_i, given that the amplitude is unchanged for any other choice of d_i.

Once the coefficients in front of each basis numerator are determined, we are left with the question of whether the basis numerators properly capture all terms that are present in the amplitude. To answer this we turn to the method of maximal cuts [94]. This is a variation on the standard generalized unitarity method, but organized by starting with maximal cuts and systematically checking cuts with fewer and fewer propagators set on shell. This method has been described in considerable detail in Ref. [94], so we only mention a few points.

The overall power counting of the three-loop $\mathcal{N} = 4$ sYM amplitude is such that it can be written with at most two powers of loop momenta in the numerator [73, 78]. This means that in principle we can fully determine the amplitude using only next-to-maximal cuts. However, here we use a higher-power counting representation with up to four powers of loop momenta in the numerator corresponding to as many as two canceled propagators. This implies that to completely determine the amplitude using our representation we need to check cuts down to the next-to-next-to-maximal level. We have explicitly checked all next-to-next-to-maximal cuts, proving that the amplitudes obtained by inserting the numerators in Eq. (4.32) into Eqs. (3.21) and (3.3) gives the complete amplitude, and that it is entirely equivalent to earlier representations of the amplitude [73, 78, 83]. Because each numerator basis element is constructed such that each integrand has only logarithmic singularities and no poles at infinity, this proves that the full nonplanar three-loop four-point $\mathcal{N} = 4$ sYM amplitude has these properties, as conjectured in Ref. [76].

4.3 Relation to rung rule

Is it possible to determine the coefficients of the basis integrands as they appear in the $\mathcal{N} = 4$ sYM amplitude from simple heuristic rules? Such rules can be useful both because they offer a simple way to cross-check derived results, and because they can often point to deeper structures. Here we show that the rung rule of Ref. [77] gives at least some of the coefficients[4].

The rung rule was first introduced as a heuristic rule for generating contributions with correct iterated-two-particle cuts in $\mathcal{N} = 4$ sYM amplitudes [77]. It is also related to certain soft collinear cuts. Today the rung rule is understood as a means for gen-

[4]We thank Lance Dixon for pointing out to us that the rung rule is helpful for identifying nonplanar integrals with uniform transcendentality, suggesting a match to our construction as well.

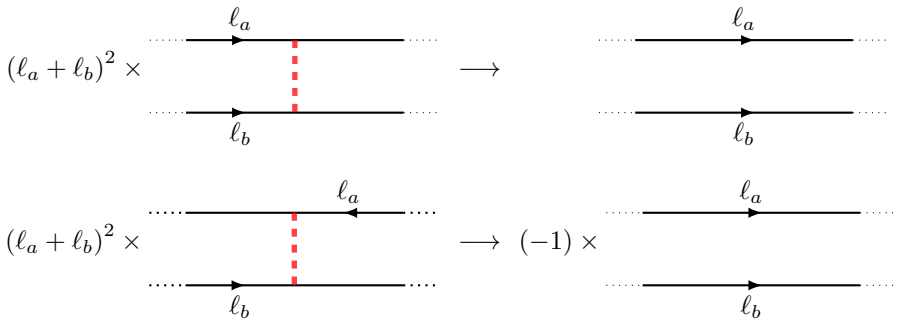

Figure 5. The rung rule gives the relative coefficient between an L-loop diagram and an $(L-1)$-loop diagram. The dotted shaded (red) line represents the propagator at L loops that is removed to obtain the $(L-1)$-loop diagram. As indicated on the second row, if one of the lines is twisted around, as can occur in nonplanar diagrams, there is an additional sign from the color antisymmetry.

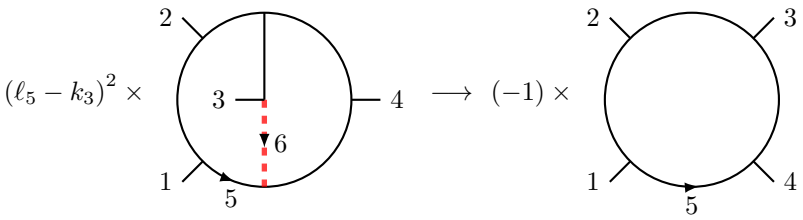

Figure 6. The rung rule determines the relative sign between the two-loop nonplanar contribution and the one-loop box to be negative.

erating contributions with simple properties under dual conformal invariance. In the planar case the rule applies even when the contributions cannot be obtained from iterated two-particle cuts [99]. However, the rung rule does not capture all contributions. It can also yield contributions that do not have the desired properties, but differ by contact terms from desired ones. For this reason, the rule is most useful once we have a basis of integrand and are interested in understanding the coefficients as they appear in amplitudes.

The rung rule was originally applied as a means for generating new L-loop contributions from $(L-1)$-loop ones. Here we use the rule in the opposite direction, going from an L-loop basis integrand to an $(L-1)$-loop contribution so as to determine the coefficient of the L-loop contribution to the amplitude. As illustrated in Fig. 5, if we

have a basis integrand containing a factor of $(\ell_a + \ell_b)^2$ and a propagator indicated by a dotted line, we can remove these to obtain a diagram with one fewer loop. According to the rung rule, the overall coefficient of the diagram obtained by removing a rung matches that of the lower-loop diagram in the amplitude. In the nonplanar case the diagrams can be twisted around, as displayed on the second line in Fig. 5, leading to relative signs. These relative signs can be thought of as coming from color factors.

Because we have already determined the three-loop $d$log numerators, we only need the rung rule to determine the sign of the numerator in the amplitude. This allows us to slightly generalize the rung rule beyond its original form. In the original version of the rung rule, the rung carries an independent loop momentum that becomes a new loop momentum in the diagram when the rung is added. The reverse of this means removing a rung from the diagram requires also removing an independent loop momentum. We will encounter cases where removing a rung and its loop momentum prevents the original version the rung rule from matching the desired $d$log numerators. We therefore slightly modify the rung rule by allowing the factors to be matched in any order of removing a given set of rungs or propagators. If we can match each factor in a numerator in at least one order of rung removal, then we just read off the overall sign as for other cases.

To illustrate how the rung rule determines a coefficient, consider the two-loop four-point amplitude. As discussed in Sect. 2, after removing the overall $\mathcal{K}$ from the amplitude, the only allowed numerator for the nonplanar double box in Fig. 3(b) with the desired properties is given in Eq. (3.30). The first step is to determine if a given numerator can be obtained from the rung rule. The first term, $(\ell_5 - k_3)^2$, in the nonplanar numerator $N^{(\text{NP})}$ (Eq. (3.30)) can be so determined. The rung corresponding to the $(\ell_5 - k_3)^2$ term is displayed as the dotted (red) line on the left side of Fig. 6. Removing this rung gives the one-loop box diagram on the right side of Fig. 6, which has coefficient $\mathcal{K}$. However, we need to flip over leg 3 to obtain the standard box from the diagram with the rung removed, resulting in a relative minus sign between color factors. This fixes $(\ell_5 - k_3)^2$ to enter the amplitude with a negative sign, because the box enters the amplitude with a positive sign. This precisely matches the sign in Eq. (3.29) obtained from the maximal cut.

At three loops the idea is the same. Consider, for example diagram (c). Examining the numerator basis element $N_1^{(\text{c})}$ from Table 1, we can identify the term $s(\ell_5 - \ell_7)^2$ as a rung-rule factor. In Fig. 7, the dotted (red) line in the top part of the diagram corresponds to the factor $(\ell_5 - \ell_7)^2$. After removing the top rung, the bottom rung is just a factor of $s = (k_1 + k_2)^2$. An overall sign comes from the fact that the first rung was twisted as in Fig. 5. This determines the coefficient to be -1, and symmetry then fixes the second rung rule numerator to have the same sign. This matches the sign of

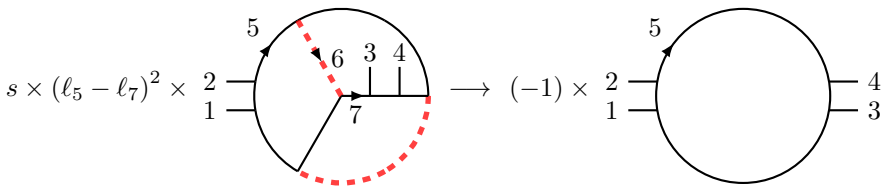

Figure 7. The rung rule determines that the basis element $N^{(\mathrm{c})}$ enters the amplitude with a relative minus sign.

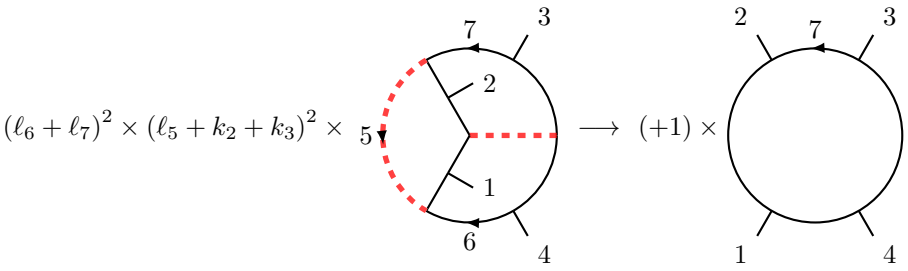

Figure 8. The rung rule determines that basis element $N_1^{(\mathrm{h})}$ enters the amplitude with a relative plus sign.

the numerator in Eq. (4.32) found via unitarity cuts.

Now consider the more complicated case of diagram (h). The coefficient of $N_1^{(\mathrm{h})}$ from Table 1 is more interesting, because the original rung rule does not match the coefficient. Nevertheless, using the slightly modified rung rule described above, we can still extract the desired coefficient in front of the basis element. Examining Fig. 8, notice that if we first remove the left rung, the rung rule gives one factor of $N_1^{(\mathrm{h})}$: $(\ell_6 + \ell_7)^2$, while if we first remove the right rung, the rung rule gives the other factor $(\ell_5 + k_2 + k_3)^2$. In both cases the rung rule sign is positive. Furthermore, flipping legs 1 and 2 to get the one-loop diagram on the right side of Fig. 8 does not change the sign. Thus the sign is positive, in agreement with Eq. (4.32).

The rung rule does not fix all coefficients of $d\log$ numerators in the amplitude. In particular, since the rule involves adding two propagators per rung, it can never generate terms proportional to propagators, such as those in Table 2 and 3. Nor is there any guarantee that basis integrands without canceled propagators can be identified as rung rule contributions. One might be able to find various extensions of the rung rule that handle more of these cases. Such an extension was discussed in Ref. [100], but for now

we do not pursue these ideas further.

5 Finding $d\log$ forms

In the previous section we performed detailed checks showing that the three-loop four-point $\mathcal{N}=4$ sYM amplitude has only logarithmic singularities and no poles at infinity. The first of these conditions is equivalent to being able to find $d\log$ forms, so if we can find such forms directly then we can bypass detailed analyses of the singularity structure of integrands. There is no general procedure for how to do this, so we have to rely on a case-by-case analysis. We build up technology at one and two loops, then apply that technology to a few examples at three loops, relegating a detailed discussion to the future. As expected, exactly the same Jacobians that lead to double or higher poles in our analysis of the singularity structure block us from finding $d\log$ forms, unless the Jacobians are appropriately canceled by numerator factors.

In this section, we use the terminology that an L-loop integrand form is a $d\log$ form if it can be written as a linear combination,

$$d\mathcal{I} = d^4\ell_5 \dots d^4\ell_{4+L} \frac{N^{(x)}(\ell_r, k_s)}{D^{(x)}(\ell_r, k_s)} = \sum_j c_j \; d\log f_1^{(j)} \wedge d\log f_2^{(j)} \wedge \cdots \wedge d\log f_{4L}^{(j)} \,, \tag{5.1}$$

where $N^{(x)}(\ell_r, k_s)$ is a diagram numerator, the denominator $D^{(x)}(\ell_r, k_s)$ is the usual product of propagators, $f_i^{(j)} = f_i^{(j)}(\ell_r, k_s)$ is a function of loop and external momenta. The coefficients c_j are the leading singularities of $d\mathcal{I}$ on a $4L$ cut, where we take $f_1^{(j)} = f_2^{(j)} = \cdots = f_{4L}^{(j)} = 0$. It is still an open question whether the smallest irreducible $d\log$ forms may be expressed as a single form with unit leading singularity,

$$d\mathcal{I} \stackrel{?}{=} d\log f_1 \wedge d\log f_2 \wedge \cdots \wedge d\log f_{4L} \,. \tag{5.2}$$

We can determine on a case by case basis if the change of variables (5.2) exists by checking if the integrand form has: (i) only logarithmic singularities and (ii) only unit leading singularities. An integrand form has unit leading singularities if the $4L$-cut of the integrand form is

$$\operatorname*{Res}_{\ell_r = \ell_r^*} d\mathcal{I} = \pm 1, 0 \,, \tag{5.3}$$

where ℓ_r^* are positions for quadruple cuts for all loop variables. In the $d\log$ form it is a simple matter to extract the residues via

$$\operatorname*{Res}_{f_1=0} d\mathcal{I} = d\log f_2 \wedge \cdots \wedge d\log f_{4L} \,, \tag{5.4}$$

and the residues at the other $f_j = 0$ may be obtained analogously. In doing so there are signs from the wedge products which we do not track. Clearly, it is better to find single-term $d\log$ forms as in Eq. (5.2), which we do in many examples. However the multiterm $d\log$ form (5.1) is sufficient for our purposes because it makes manifest that the integrand form has only logarithmic singularities.

In the previous sections, we normalized the forms such that a factor $\mathcal{K}$, defined in Eq. (3.22), was factored out. In this section, we restore this factor as

$$\mathcal{K} = stC_1 \,, \tag{5.5}$$

using the definitions from Eqs. (3.22) and (3.32). In some cases it is best to use the symmetry (3.23) to write instead,

$$\mathcal{K} = suC_2 \,, \qquad\qquad \mathcal{K} = tuC_3 \,. \tag{5.6}$$

As noted in Sect. 3.3, in general, we write the integrand forms as linear combinations of $d\log$ forms using the C_i as prefactors, as we find below.

5.1 One loop

At higher loops, a good starting point for finding $d\log$ forms is to express one-loop subdiagrams in $d\log$ forms. Following standard integral decomposition methods, any one loop integrand form with no poles at infinity can be decomposed in terms of box and pentagon forms:

$$d\mathcal{I} = \sum_j a_j^{(5)}\, d\mathcal{I}_5^{(j)} + \sum_k b_k^{(4)}\, d\mathcal{I}_4^{(k)} \,. \tag{5.7}$$

Triangle or bubble integrand forms do not appear in this decomposition because they would introduce poles at infinity.

The decomposition in Eq. (5.7) is valid beyond the usual one-loop integrals. We can consider any integrand form with m generalized propagators which are at most quadratic in the momenta:

$$d\mathcal{I} = \frac{d^4\ell\; N_m}{F_1 F_2 \dots F_m} \,, \qquad \text{where} \qquad F_j = \alpha_j \ell^2 + (\ell \cdot Q_j) + P_j \,. \tag{5.8}$$

We can then use the same expansion (5.7) for these objects and express it in terms of *generalized boxes* and *generalized pentagons* which are integrals with four or five generalized propagators, F_j. Unlike in the case of regular one-loop integrals, there is no simple power-counting constraint on the numerator such that $d\mathcal{I}$ is guaranteed not to have any poles at infinity. Instead one needs to check for poles at infinity case by case.

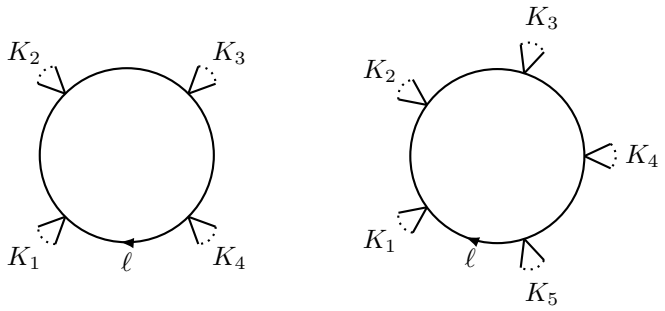

Figure 9. One-loop box and pentagon diagrams.

At one loop, Eq. (5.7) tells us that we need only consider boxes and pentagons, since the higher-point cases can be reduced to these. First consider the standard box form with (off-shell) external momenta K_1, K_2, K_3, K_4 shown in Fig. 9(a):

$$d\mathcal{I}_4 \left[\begin{matrix} \ell^2 & (\ell - K_1 - K_2)^2 \\ (\ell - K_1)^2 & (\ell + K_4)^2 \end{matrix} \right] \equiv d^4\ell \, \frac{N_4}{\ell^2 (\ell - K_1)^2 (\ell - K_1 - K_2)^2 (\ell + K_4)^2} \,. \tag{5.9}$$

Here on the left hand side we introduce a compact notation for the $d\log$ form that will be useful at higher loops. The actual positions of the arguments do not matter, since swapping the locations of arguments will only alter the overall sign of the form due to the wedge products; in amplitudes such signs are fixed using unitarity. The numerator N_4 is just the Jacobian J_ℓ given in Eq. (2.20), using the labels of the box in Fig. 9(a). With this numerator $d\mathcal{I}_4$ has unit leading singularities, and we can write it as a single-term $d\log$ form,

$$\begin{aligned} &d\mathcal{I}_4 \left[\begin{matrix} \ell^2 & (\ell - K_1 - K_2)^2 \\ (\ell - K_1)^2 & (\ell + K_4)^2 \end{matrix} \right] \\ &\quad = d\log \frac{\ell^2}{(\ell - \ell^*)^2} \wedge d\log \frac{(\ell - K_1)^2}{(\ell - \ell^*)^2} \wedge d\log \frac{(\ell - K_1 - K_2)^2}{(\ell - \ell^*)^2} \wedge d\log \frac{(\ell + K_4)^2}{(\ell - \ell^*)^2} \,, \end{aligned} \tag{5.10}$$

as already noted in Sect. 2.3. Here the $d\log$ form depends on ℓ^*, which is a solution for ℓ on the quadruple cut

$$\ell^2 = (\ell - K_1)^2 = (\ell - K_1 - K_2)^2 = (\ell + K_4)^2 = 0 \,. \tag{5.11}$$

There are two independent ℓ^* that satisfy these equations, and we are free to choose either of them. Both give the same results when substituted into the $d\log$ form.

An important nontrivial property of a $d\log$ form is that the residue located at $(\ell - \ell^*)^2 = 0$ cancels. If it were not to cancel, then there would be an unphysical singularity

which could feed into our higher-loop discussion. We illustrate the cancellation for the massless box where $K_i = k_i$ with $k_i^2 = 0$ for all $i = 1, \ldots, 4$. In this case $\ell^* = -\frac{[12]}{[24]}\lambda_1\widetilde{\lambda}_4$ and the residue of $d\mathcal{I}_4$ in (5.10) on $(\ell - \ell^*)^2 = 0$ is

$$\begin{aligned}\text{Res}\, d\mathcal{I}_4 = & \, d\log(\ell^2) \wedge d\log(\ell - k_1)^2 \wedge d\log(\ell - k_1 - k_2)^2 \\ & - d\log(\ell^2) \wedge d\log(\ell - k_1)^2 \wedge d\log(\ell + k_4)^2 \\ & + d\log(\ell^2) \wedge d\log(\ell - k_1 - k_2)^2 \wedge d\log(\ell + k_4)^2 \\ & - d\log(\ell - k_1)^2 \wedge d\log(\ell - k_1 - k_2)^2 \wedge d\log(\ell + k_4)^2 \,. \end{aligned} \tag{5.12}$$

The simplest way to see the cancellation is that on the solution of $(\ell - \ell^*)^2 = 0$, the following identity is satisfied

$$\ell^2(\ell - k_1 - k_2)^2 = (\ell - k_1)^2(\ell + k_4)^2 \,. \tag{5.13}$$

Using this we can express, say, ℓ^2 in terms of other propagators and substitute into Eq. (5.12). All terms in Eq. (5.12) then cancel pairwise because of the antisymmetry property of the wedge product. A similar derivation can be carried out for the generic four-mass case, but we refrain from doing so here.

The *generalized box*, in terms of which Eq. (5.8) can be expanded, is:

$$d\mathcal{I}_4 \begin{bmatrix} F_1 & F_2 \\ F_3 & F_4 \end{bmatrix} = \frac{d^4\ell \; N}{F_1 F_2 F_3 F_4} = d\log\frac{F_1}{F^*} \wedge d\log\frac{F_2}{F^*} \wedge d\log\frac{F_3}{F^*} \wedge d\log\frac{F_4}{F^*} \,, \tag{5.14}$$

where the numerator N is again a Jacobian (2.20) of the solution to the system of equations $P_i = 0$ for $P = \{F_1, F_2, F_3, F_4\}$ and $F^* = (\ell - \ell^*)^2$. Here ℓ^* is the solution for ℓ at $F_i = 0$ for $i = 1, 2, 3, 4$. It is not automatic that $d\mathcal{I}_4$ can be put into a $d\log$ form for any set of F_i's. This depends on whether $d\mathcal{I}_4$ has only logarithmic singularities. If it has other types of singularities, then no change of variables will give a $d\log$ representation for $d\mathcal{I}_4$. As a simple example of a form that cannot be rewritten in $d\log$ form consider the generalized box

$$d^4\ell \, \frac{N_4}{\ell^2(\ell + k_1)^2(\ell + k_2)^2(\ell + k_4)^2} \,, \tag{5.15}$$

where the numerator is independent of loop momentum ℓ. Using a parametrization of the type of Eq. (2.10), we find that on the collinear cut $\ell^2 = (\ell + k_1)^2 = 0$ where $\ell = \alpha_1 k_1$, there is a double pole $d\alpha_1/\alpha_1^2$. Therefore no $d\log$ form exists. In any case, at higher loops we will find the notion of a generalized box very useful for finding $d\log$ forms.

Next we consider a generic one-loop pentagon form,

$$d\mathcal{I}_5 = \frac{d^4\ell \, N_5}{\ell^2(\ell - K_1)^2(\ell - K_1 - K_2)^2(\ell - K_1 - K_2 - K_3)^2(\ell + K_5)^2} \,, \tag{5.16}$$

with off-shell momenta K_j. The numerator N_5 is not fixed by the normalization whereas it was in the case of the box. Also unlike in the case of the box, there are multiple numerators N_5 that give unit leading singularities. The constraint of no poles at infinity constrains N_5 to be quadratic: $N_5 = g_1\ell^2 + g_2(\ell\cdot Q) + g_3$, where the g_k are some constants and Q is a constant vector. The simplest way to decompose the pentagon form (5.16) is to start with a reference pentagon form,

$$d\widetilde{\mathcal{I}}_5 \equiv d\log\frac{(\ell-K_1)^2}{\ell^2}\wedge d\log\frac{(\ell-K_1-K_2)^2}{\ell^2}\wedge d\log\frac{(\ell+K_4+K_5)^2}{\ell^2}\wedge d\log\frac{(\ell+K_5)^2}{\ell^2}\,, \tag{5.17}$$

in terms of which we express all other pentagons. This reference $d\log$ form corresponds to a parity-odd integrand form and gives zero when integrating over Minkowski space. In Eq. (5.17) we single out ℓ^2, but one can show that all five choices of singling out one of the inverse propagators are equivalent. We then can decompose the generic pentagon form (5.16) into the reference pentagon form (5.17) $d\widetilde{\mathcal{I}}_5$ plus box forms,

$$d\mathcal{I}_5 = c_0 d\widetilde{\mathcal{I}}_5 + \sum_{j=1}^{5} c_j d\mathcal{I}_4^{(j)}\,, \tag{5.18}$$

where c_j are coefficients most easily determined by imposing cut conditions on both sides of Eq. (5.18) and matching. While we can express Eq. (5.17) as a loop-integrand, its numerator $\widetilde{N}_5$ is complicated, and it is better to use directly the $d\log$ form (5.17) for obtaining cuts.

The expansion (5.18) is always valid for up to two powers of loop momentum in the numerator N_5, but in higher-loop calculations it is often more convenient to use alternative decompositions. It is also possible to define generalized pentagons with propagators other than the standard ones. These will be useful in subsequent discussion.

5.2 Two loops

At two loops there are only two distinct integrand forms to consider: the planar and nonplanar double boxes displayed in Figs. 3 and 10. As shown in Ref. [76], we can choose the numerators such that all integrals individually have only logarithmic singularities and no poles at infinity. As already noted, in previous sections we suppressed a factor of $\mathcal{K}$ (defined in Eq. (3.22)), that we now restore to make the connection to $d\log$ forms and the leading singularity coefficients more straightforward.

We start with the planar double box of Fig. 3. It appears in the amplitude as

$$d\mathcal{I}^{(\mathrm{P})} = \frac{d^4\ell_5\, d^4\ell_6\; s^2 t C_1}{\ell_5^2(\ell_5+k_1)^2(\ell_5-k_2)^2(\ell_5+\ell_6-k_2-k_3)^2\ell_6^2(\ell_6-k_3)^2(\ell_6+k_4)^2}\,, \tag{5.19}$$

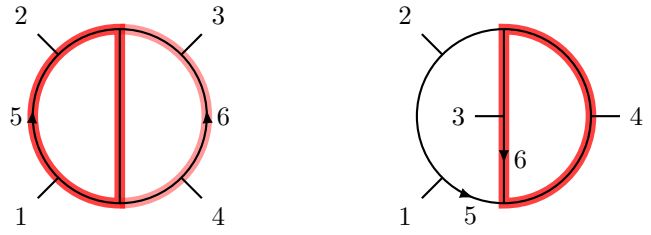

Figure 10. The (a) planar and (b) nonplanar two-loop four-point parent diagrams. In each case one-loop box subdiagrams are shaded (red). In the planar diagram, the Jacobian from the one-loop box subdiagram combines with the remaining three lightly shaded (light red) propagators to form a second box.

where C_1 is defined in Eq. (3.32). It is straightforward to put this integrand form into a *d*log form by iterating the one-loop single-box case in Eq. (3.32). We immediately obtain a product of two one-loop box integrand forms,

$$\begin{aligned} d\mathcal{I}^{(\mathrm{P})} &= C_1 \left[\frac{d^4\ell_5 \; s(\ell_6 - k_2 - k_3)^2}{\ell_5^2(\ell_5 + k_1)^2(\ell_5 - k_2)^2(\ell_5 + \ell_6 - k_2 - k_3)^2} \right] \\ &\quad \times \left[\frac{d^4\ell_6 \; st}{\ell_6^2(\ell_6 - k_3)^2(\ell_6 + k_4)^2(\ell_6 - k_2 - k_3)^2} \right] \\ &= C_1 \, d\mathcal{I}_4 \begin{bmatrix} \ell_5^2 & (\ell_5 + k_1)^2 \\ (\ell_5 - k_2)^2 & (\ell_5 + \ell_6 - k_2 - k_3)^2 \end{bmatrix} \wedge d\mathcal{I}_4 \begin{bmatrix} \ell_6^2 & (\ell_6 - k_3)^2 \\ (\ell_6 + k_4)^2 & (\ell_6 - k_2 - k_3)^2 \end{bmatrix}. \end{aligned} \tag{5.20}$$

Thus, $d\mathcal{I}^{(P)}$ is a *d*log eight-form given by the wedge product of two $d\mathcal{I}_4$ box four-forms, multiplied by the coefficient C_1. By symmetry, we can also reverse the order of iterating the one-loop box forms to obtain instead

$$d\mathcal{I}^{(\mathrm{P})} = C_1 \, d\mathcal{I}_4 \begin{bmatrix} \ell_5^2 & (\ell_5 + k_1)^2 \\ (\ell_5 - k_2)^2 & (\ell_5 - k_2 - k_3)^2 \end{bmatrix} \wedge d\mathcal{I}_4 \begin{bmatrix} \ell_6^2 & (\ell_6 - k_3)^2 \\ (\ell_6 + k_4)^2 & (\ell_5 + \ell_6 - k_2 - k_3)^2 \end{bmatrix}. \tag{5.21}$$

Despite the fact that the two *d*log forms in Eqs. (5.20) and (5.21) look different, they are equal. This is another illustration that *d*log forms are not unique, and there are many different ways to write them.

The nonplanar double box in Fig. 3 is more complicated, since it contains both box and pentagon subdiagrams. It is given by

$$d\mathcal{I}^{(\mathrm{NP})} = \frac{d^4\ell_5 \, d^4\ell_6 \;\; C_1 st[(\ell_5 - k_4)^2 + (\ell_5 - k_3)^2]}{\ell_5^2(\ell_5 + k_1)^2(\ell_5 + k_1 + k_2)^2\ell_6^2(\ell_6 + k_3)^2(\ell_6 + \ell_5)^2(\ell_6 + \ell_5 - k_4)^2}. \tag{5.22}$$

We start by writing the ℓ_6 box subdiagram highlighted in Fig. 10 as a $d\log$ form, so that

$$d\mathcal{I}^{(\mathrm{NP})} = d\mathcal{I}_{\ell_6} \wedge d\mathcal{I}_{\ell_5}\,, \tag{5.23}$$

where

$$d\mathcal{I}_{\ell_6} = \frac{d^4\ell_6\ (\ell_5\cdot q)(\ell_5\cdot\overline{q})}{\ell_6^2(\ell_6+k_3)^2(\ell_6+\ell_5)^2(\ell_6+\ell_5-k_4)^2} = d\mathcal{I}_4\begin{bmatrix}\ell_6^2 & (\ell_6+\ell_5)^2\\ (\ell_6+k_3)^2 & (\ell_6+\ell_5-k_4)^2\end{bmatrix}. \tag{5.24}$$

The $d\mathcal{I}_{\ell_6}$ form is normalized with the Jacobian numerator $(\ell_5\cdot q)(\ell_5\cdot\overline{q})$, where $q=\lambda_3\widetilde{\lambda}_4$ and $\overline{q}=\lambda_4\widetilde{\lambda}_3$. This is just a relabeling of the two-mass-easy normalization given in Eq. (2.22). The remaining integral can then be divided into two parts,

$$d\mathcal{I}_{\ell_5} = C_1\, d\mathcal{I}_5^{\chi_1} + C_2\, d\mathcal{I}_5^{\chi_2}\,, \tag{5.25}$$

where we have used $tC_1 = uC_2$ and

$$\begin{aligned} d\mathcal{I}_5^{\chi_1} &\equiv \frac{d^4\ell_5\ st(\ell_5-k_4)^2}{\ell_5^2(\ell_5+k_1)^2(\ell_5+k_1+k_2)^2(\ell_5\cdot q)(\ell_5\cdot\overline{q})}\,,\\ d\mathcal{I}_5^{\chi_2} &\equiv d\mathcal{I}_5^{\chi_1}\Big|_{k_3\leftrightarrow k_4}. \end{aligned} \tag{5.26}$$

These are exactly generalized pentagons, of the type we discussed in the previous subsection. It is straightforward to check that there are only logarithmic singularities and no poles at infinity. Because of the two propagators linear in ℓ_5, these two forms are not canonical one-loop integrand forms. Nevertheless, we can find a change of variables for $d\mathcal{I}_5^{\chi_1}$ and $d\mathcal{I}_5^{\chi_2}$ so that each is a single $d\log$ form,

$$d\mathcal{I}_5^{\chi_1} = d\log\frac{\ell_5^2}{(\ell_5\cdot\overline{q})}\wedge d\log\frac{(\ell_5+k_1)^2}{(\ell_5\cdot\overline{q})}\wedge d\log\frac{(\ell_5+k_1+k_2)^2}{(\ell_5\cdot q)}\wedge d\log\frac{(\ell_5-\ell_5^*)^2}{(\ell_5\cdot q)}\,, \tag{5.27}$$

where $\ell_5^* = \frac{\langle 34\rangle}{\langle 31\rangle}\lambda_1\widetilde{\lambda}_4$ is the solution of cut conditions $\ell_5^2=(\ell_5+k_1)^2=(\ell_5+k_1+k_2)^2=(\ell_5\cdot q)=0$. A similar result is obtained for $d\mathcal{I}_{\ell_5}^{\chi_2}$ by swapping k_3 and k_4. The final result for the $d\log$ form of the nonplanar double box is

$$d\mathcal{I}^{(\mathrm{NP})} = C_1\, d\mathcal{I}_{\ell_6}\wedge d\mathcal{I}_{\ell_5}^{\chi_1} + C_2\, d\mathcal{I}_{\ell_6}\wedge d\mathcal{I}_{\ell_5}^{\chi_2}\,. \tag{5.28}$$

Since each term carries a different normalization, this expression cannot be uniformly normalized to have unit leading singularities on all cuts. We choose a normalization such that C_1 or C_2 are the leading singularities of the integrand form, depending on which residue we take. This construction is useful at three loops, as we see below.

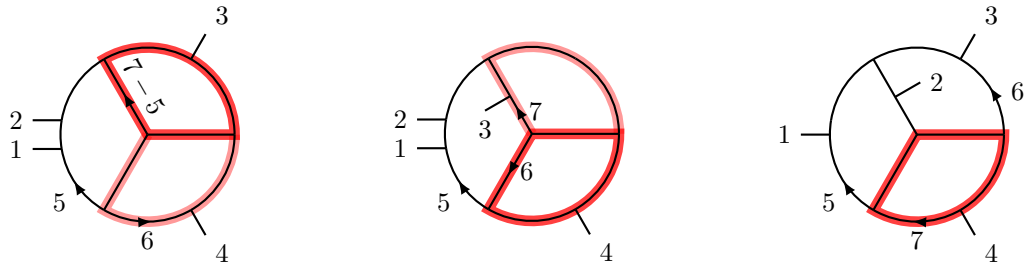

(e) (f) (i)

Figure 11. The three-loop diagrams with highlighted one-loop box subdiagrams used in the construction of *d*log forms. In diagram (e) we start with the top (red) box whose Jacobian generates the missing fourth propagator for the bottom (light red) box. In diagram (f) we start with the bottom (red) box whose Jacobian generates the missing fourth propagator for the top (light red) box. In diagram (i), there is only one box on the bottom (red).

5.3 Three loops

We now turn to the main subject: constructing the three-loop four-point nonplanar *d*log forms. Unfortunately, at present there is no general procedure to rewrite high-loop order integrand forms into *d*log forms. Nevertheless, we can proceed with our general strategy: whenever there is a box subdiagram, we rewrite it in a *d*log form and then deal with the remaining forms by again looking at subdiagrams. This tactic works well at three loops: We have worked out *d*log forms for all diagrams that have box subdiagrams. This consists of all diagrams except for diagram (h), which is the most complicated case because it has only pentagon subdiagrams. Diagrams (a) and (b) are simple because they are directly related to the one- and two-loop cases. In this subsection we show explicit examples of diagrams (e), (f) and (i), which are less trivial. Each example shows how to overcome some new obstacle to constructing a *d*log form.

We start with diagram (e) in Figs. 4 and 11. The numerator is $\mathcal{K}N^{(\mathrm{e})} = C_1 s^2 t(\ell_5 + k_4)^2$. This gives us the integrand form,

$$d\mathcal{I}^{(\mathrm{e})} = \frac{d^4\ell_5\, d^4\ell_6\, d^4\ell_7\; C_1 s^2 t(\ell_5 + k_4)^2}{\ell_5^2(\ell_5 - k_1)^2(\ell_5 - k_1 - k_2)^2(\ell_5 + \ell_6)^2\ell_6^2(\ell_6 - k_4)^2} \times \frac{1}{(\ell_7 - \ell_5)^2(\ell_7 + \ell_6)^2(\ell_7 + k_4)^2(\ell_7 - k_1 - k_2)^2}\,, \tag{5.29}$$

where C_1 is defined in Eq. (3.32). There are two box subdiagrams in this case, both of which are highlighted in Fig. 11(e). We start with the top (red) box in Fig. 11, which

carries loop momentum ℓ_7. The $d\log$ form for this box subdiagram is

$$d\mathcal{I}_{\ell_7} = d\mathcal{I}_4 \begin{bmatrix} (\ell_7 - \ell_5)^2 & (\ell_7 + k_4)^2 \\ (\ell_7 + \ell_6)^2 & (\ell_7 - k_1 - k_2)^2 \end{bmatrix}. \tag{5.30}$$

Using Eq. (2.21) and relabeling, we find that this box carries a normalization factor

$$J_7 = (\ell_5 + k_4)^2(\ell_6 - k_3 - k_4)^2 - (\ell_5 - k_1 - k_2)^2(\ell_6 - k_4)^2\,, \tag{5.31}$$

which then goes into the denominator of the remaining ℓ_5, ℓ_6 forms. The ℓ_6 integrand form is a generalized box formed from the three bottom (light red) propagators in Fig. 11 and a generalized propagator J_7 . We can then rewrite the ℓ_6 integrand form as a $d\log$ form,

$$d\mathcal{I}_{\ell_6} = d\mathcal{I}_4 \begin{bmatrix} \ell_6^2 & (\ell_6 + \ell_5)^2 \\ (\ell_6 - k_4)^2 & [(\ell_5 + k_4)^2(\ell_6 - k_3 - k_4)^2 - (\ell_5 - k_1 - k_2)^2(\ell_6 - k_4)^2] \end{bmatrix}. \tag{5.32}$$

The normalization required by this generalized box can be computed from the generic Jacobian formula (2.20) and gives

$$J_6 = s[(\ell_5 + k_4)^2]^2\,, \tag{5.33}$$

exactly matching Eq. (4.7) which was obtained by searching for double poles. This confirms that a factor $(\ell_5 + k_4)^2$ is needed in the numerator of Eq. (5.29): it cancels the double pole in the remaining ℓ_5 form. After canceling the double propagator against the numerator factor, we then have the last box form,

$$d\mathcal{I}_{\ell_5} = d\mathcal{I}_4 \begin{bmatrix} \ell_5^2 & (\ell_5 + k_4)^2 \\ (\ell_5 - k_1)^2 & (\ell_5 - k_1 - k_2)^2 \end{bmatrix}. \tag{5.34}$$

The final result for the integrand form of Eq. (5.29) is thus

$$d\mathcal{I}^{(\mathrm{e})} = C_1\, d\mathcal{I}_{\ell_5} \wedge d\mathcal{I}_{\ell_6} \wedge d\mathcal{I}_{\ell_7}\,. \tag{5.35}$$

The derivation of a $d\log$ form for this case is relatively straightforward, because at each step we encounter only generalized box forms.

As a less straightforward example, consider the nonplanar diagram (f) in Figs. 4 and 11, using the numerator $\mathcal{K}N_1^{(\mathrm{f})}$ in Table 1. This integrand form is

$$\begin{aligned} d\mathcal{I}^{(\mathrm{f})} = \frac{d^4\ell_5\, d^4\ell_6\, d^4\ell_7 \;\; C_1 st(\ell_5 + k_4)^2\,[(\ell_5 + k_3)^2 + (\ell_5 + k_4)^2]}{\ell_5^2\,(\ell_5 - k_1)^2(\ell_5 - k_1 - k_2)^2\ell_7^2(\ell_7 - k_3)^2(\ell_5 + \ell_7 + k_4)^2} \\ \times \frac{1}{\ell_6^2(\ell_6 - \ell_5)^2(\ell_6 - \ell_5 - k_4)^2(\ell_6 + \ell_7)^2}\,, \end{aligned} \tag{5.36}$$

where we include numerator $N_1^{(\mathrm{f})}$ from Table 1. As indicated in Fig. 11 for diagram (f), there are two box subdiagrams that can be put into $d\log$ form. We write the ℓ_6 and ℓ_7 forms as box-forms straight away:

$$d\mathcal{I}_{\ell_6} = d\mathcal{I}_4 \begin{bmatrix} \ell_6^2 & (\ell_6-\ell_5-k_4)^2 \\ (\ell_6+\ell_7)^2 & (\ell_6-\ell_5)^2 \end{bmatrix},$$
$$d\mathcal{I}_{\ell_7} = d\mathcal{I}_4 \begin{bmatrix} \ell_7^2 & (\ell_7+\ell_5+k_4)^2 \\ (\ell_7-k_3)^2 & [(\ell_5+k_4)^2(\ell_5+\ell_7)^2 - \ell_5^2(\ell_5+\ell_7+k_4)^2] \end{bmatrix}. \tag{5.37}$$

The ℓ_6 box introduced a Jacobian which is then used in the ℓ_7 box as a new generalized propagator. The remaining ℓ_5 form, including also the Jacobian from the ℓ_7 generalized box, is then a generalized pentagon form,

$$d\mathcal{I}_{\ell_5} = \frac{d^4\ell_5\, C_1\, st\, [(\ell_5+k_3)^2+(\ell_5+k_4)^2]}{\ell_5^2(\ell_5-k_1)^2(\ell_5-k_1-k_2)^2(\ell_5\cdot q)(\ell_5\cdot\overline{q})}, \tag{5.38}$$

where $q = \lambda_3\widetilde{\lambda}_4$, $\overline{q} = \lambda_4\widetilde{\lambda}_3$. This generalized pentagon form is a relabeling of the one we encountered for the two loop nonplanar double box so we can write,

$$d\mathcal{I}_{\ell_5} = C_1\, d\mathcal{I}_5^{\chi_1} + C_2\, d\mathcal{I}_5^{\chi_2}, \tag{5.39}$$

where the forms $d\mathcal{I}_5^{\chi_1}$ and $d\mathcal{I}_5^{\chi_2}$ are defined in Eq. (5.26). The final result for $d\mathcal{I}^{(\mathrm{f})}$ in Eq. (5.36) is then

$$d\mathcal{I}^{(\mathrm{f})} = C_1\, d\mathcal{I}_{\ell_6}\wedge d\mathcal{I}_{\ell_7}\wedge d\mathcal{I}_5^{\chi_1} + C_2\, d\mathcal{I}_{\ell_6}\wedge d\mathcal{I}_{\ell_7}\wedge d\mathcal{I}_5^{\chi_2}. \tag{5.40}$$

An even more complicated example is diagram (i) in Figs. 4 and 11. Consider the first term in numerator $N_1^{(\mathrm{i})}$ in Table 1 given by $(\ell_6+k_4)^2(\ell_5-k_1-k_2)^2$. The three other terms in numerator $N_1^{(\mathrm{i})}$ are related to this one by symmetry, so it is sufficient to consider this one term in order to find a $d\log$ form for all four terms. Putting back the overall normalization $C_1 st$, we have the integrand form

$$d\mathcal{I}_1^{(\mathrm{i})} = \frac{d^4\ell_5\, d^4\ell_6\, d^4\ell_7\;\; C_1 st(\ell_6+k_4)^2(\ell_5-k_1-k_2)^2}{\ell_5^2(\ell_5-k_1)^2\ell_6^2(\ell_6-k_3)^2(\ell_6+\ell_5-k_1-k_3)^2(\ell_6+\ell_5+k_4)^2} \times \frac{1}{\ell_7^2(\ell_7+k_4)^2(\ell_7-\ell_5)^2(\ell_7+\ell_6+k_4)^2}. \tag{5.41}$$

As in all other cases we start with a box subintegral. Here there is only a single choice, as highlighted in Fig. 11(i):

$$d\mathcal{I}_{\ell_7} = \frac{d^4\ell_7\;\; [(\ell_5+k_4)^2(\ell_6+k_4)^2-\ell_5^2\ell_6^2]}{\ell_7^2(\ell_7+k_4)^2(\ell_7-\ell_5)^2(\ell_7+\ell_6+k_4)^2} = d\mathcal{I}_4 \begin{bmatrix} \ell_7^2 & (\ell_7-\ell_5)^2 \\ (\ell_7+k_4)^2 & (\ell_7+\ell_6+k_4)^2 \end{bmatrix}. \tag{5.42}$$

The ℓ_6 integrand form is then a generalized pentagon,

$$d\mathcal{I}_{\ell_6} = \frac{d^4\ell_6\ st(\ell_6+k_4)^2}{\ell_6^2(\ell_6-k_3)^2(\ell_6+\ell_5-k_1-k_3)^2(\ell_6+\ell_5+k_4)^2\left[(\ell_5+k_4)^2(\ell_6+k_4)^2-\ell_5^2\ell_6^2\right]}\,. \tag{5.43}$$

In principle we could follow a general pentagon decomposition procedure, but there is a simpler way to obtain the result. We can rewrite the numerator as

$$(\ell_6+k_4)^2 = \frac{1}{(\ell_5+k_4)^2}\left[(\ell_5+k_4)^2(\ell_6+k_4)^2-\ell_5^2\ell_6^2\right] + \frac{\ell_5^2}{(\ell_5+k_4)^2}\,\ell_6^2\,. \tag{5.44}$$

After canceling factors in each term against denominator factors, we get two generalized box integrand forms. The decomposition is

$$d\mathcal{I}_1^{(\mathrm{i})} = C_1\, d\mathcal{I}_{\ell_7}\wedge d\mathcal{I}_{\ell_6}^{(1)}\wedge d\mathcal{I}_{\ell_5}^{(1)} + C_3\, d\mathcal{I}_{\ell_7}\wedge d\mathcal{I}_{\ell_6}^{(2)}\wedge d\mathcal{I}_{\ell_5}^{(2)}\,, \tag{5.45}$$

where the ℓ_6 integrand forms can be put directly into $d\log$ forms:

$$\begin{aligned}
d\mathcal{I}_{\ell_6}^{(1)} &= \frac{d^4\ell_6\ \left[(\ell_5-k_1-k_2)^2(\ell_5-k_1-k_3)^2-(\ell_5+k_4)^2(\ell_5-k_1)^2\right]}{\ell_6^2(\ell_6-k_3)^2(\ell_6+\ell_5-k_1-k_3)^2(\ell_6+\ell_5+k_4)^2} \\
&= d\mathcal{I}_4\begin{bmatrix}\ell_6^2 & (\ell_6+\ell_5+k_4)^2\\ (\ell_6-k_3)^2 & (\ell_6+\ell_5-k_1-k_3)^2\end{bmatrix}, \\
d\mathcal{I}_{\ell_6}^{(2)} &= \frac{d^4\ell_6\ (\ell_5\cdot q)(\ell_5\cdot\bar{q})(\ell_5-k_1-k_2)^2}{(\ell_6-k_3)^2(\ell_6+\ell_5-k_1-k_3)^2(\ell_6+\ell_5+k_4)^2\left[(\ell_5+k_4)^2(\ell_6+k_4)^2-\ell_5^2\ell_6^2\right]} \\
&= d\mathcal{I}_4\begin{bmatrix}(\ell_6-k_3)^2 & (\ell_6+\ell_5-k_1-k_3)^2\\ (\ell_6+\ell_5+k_4)^2 & (\ell_5+k_4)^2(\ell_6+k_4)^2-\ell_5^2\ell_6^2)\end{bmatrix},
\end{aligned} \tag{5.46}$$

with $q=\lambda_2\widetilde{\lambda}_4$ and $\bar{q}=\lambda_4\widetilde{\lambda}_2$. Here we have normalized both integrand forms properly to have unit leading singularities so that they are $d\log$ forms. As indicated in Eq. (5.45), the remaining ℓ_5 integrand forms are different for $d\mathcal{I}_{\ell_6}^{(1)}$ and $d\mathcal{I}_{\ell_6}^{(2)}$.

Writing the integrand form for ℓ_5 following from $d\mathcal{I}_{\ell_6}^{(1)}$,

$$\begin{aligned}
d\mathcal{I}_{\ell_5}^{(1)} &= \frac{d^4\ell_5\ st(\ell_5-k_1-k_2)^2}{\ell_5^2(\ell_5-k_1)^2(\ell_5+k_4)^2[(\ell_5-k_1-k_2)^2(\ell_5-k_1-k_3)^2-(\ell_5+k_4)^2(\ell_5-k_1)^2]} \\
&= \frac{d^4\ell_5\ st(\ell_5-k_1-k_2)^2}{\ell_5^2(\ell_5-k_1)^2(\ell_5+k_4)^2((\ell_5-k_1)\cdot q)((\ell_5-k_1)\cdot\bar{q})},
\end{aligned} \tag{5.47}$$

where $q=\lambda_2\widetilde{\lambda}_3$ and $\bar{q}=\lambda_3\widetilde{\lambda}_2$. In the last expression we used the fact that the quartic expression was a two-mass-easy Jacobian of the ℓ_6 integrand, which factorizes into a product. Up to relabeling, this is the same integrand as the first nonplanar pentagon

form in Eq. (5.26), and we can write it as the $d\log$ form

$$d\mathcal{I}^{(1)}_{\ell_5} = d\log\frac{(\ell_5-k_1)^2}{((\ell_5-k_1)\cdot\overline{q})}\; d\log\frac{\ell_5^2}{((\ell_5-k_1)\cdot\overline{q})}\; d\log\frac{(\ell_5+k_4)^2}{((\ell_5-k_1)\cdot q)}\; d\log\frac{(\ell_5-\ell_5^*)^2}{((\ell_5-k_1)\cdot q)}, \tag{5.48}$$

where $q = \lambda_3\widetilde{\lambda}_2$, $\overline{q} = \lambda_2\widetilde{\lambda}_3$ and $\ell_5^* = \frac{\langle 32\rangle}{\langle 31\rangle}\lambda_1\widetilde{\lambda}_2$. For the second integrand form in Eq. (5.46), the remaining ℓ_5 integral is (for $q = \lambda_2\widetilde{\lambda}_4$ and $\overline{q} = \lambda_4\widetilde{\lambda}_2$) just a generalized box and can be directly written as the $d\log$ form,

$$d\mathcal{I}^{(2)}_{\ell_5} = \frac{d^4\ell_5\; ut}{(\ell_5-k_1)^2(\ell_5+k_4)^2(\ell_5\cdot q)(\ell_5\cdot\overline{q})} = d\mathcal{I}_4\begin{bmatrix}(\ell_5-k_1)^2 & (\ell_5\cdot q)\\ (\ell_5+k_4)^2 & (\ell_5\cdot\overline{q})\end{bmatrix}. \tag{5.49}$$

To obtain this, we used the relation $sC_1 = uC_3$ to write C_3 as the overall factor of the second term in the assembled result given in Eq. (5.45).

We have carried out similar procedures on all contributions to the three-loop four-point amplitude, except for the relatively complicated case of diagram (h). In all these cases we find explicit $d\log$ forms. These checks directly confirm that there are only logarithmic singularities in the integrand, as we found in Sect. 4. At relatively low loop orders, detailed analysis of the cut structure, as carried out in Sect. 4, provides a straightforward proof of this property. At higher loop orders, the space of all possible singularities grows rapidly and finding dlog forms, as we did in the present section, becomes a more practical way of showing that there are only logarithmic singularities. Even so, one cannot completely avoid detailed checks of the singularity structure because, in general, $d\log$ forms do not necessarily make manifest that there are no poles at infinity.

6 Logarithmic singularities at higher loops

Complete amplitudes for unintegrated four-point $\mathcal{N} = 4$ sYM amplitudes, including their nonplanar parts, have been obtained at four and five loops in Refs. [84, 97, 101]. In principle, we could repeat the same procedure we did for three loops at higher loops to construct $d\log$ numerators. However, the number of parent diagrams grows: at four loops there are 85 diagrams and by five loops there are 410 diagrams. Many of the diagrams are simple generalizations of the already analyzed three-loop diagrams, so their analysis is straightforward. Some, however, are new topologies, for which an exhaustive search for double or higher poles and poles at infinity would be nontrivial. Such an analysis would require either a more powerful means of identifying numerators with the desired properties, or computer automation to sweep through all dangerous kinematic regions of the integrands while looking for unwanted singularities. This of course is an interesting problem for the future.

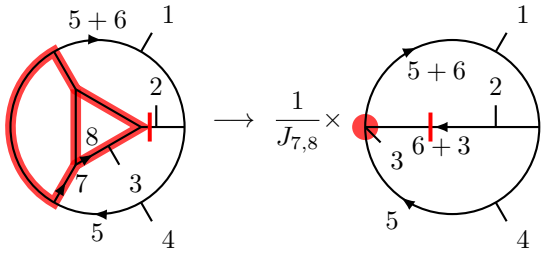

Figure 12. The left diagram contributes to the four-loop four-point $\mathcal{N} = 4$ sYM amplitude [101]. The shaded (red) lines indicate propagators that are replaced by on-shell conditions as given in Eq. (6.1). These propagators are removed from the diagram and leave behind an inverse Jacobian, given in Eq. (6.2). The resulting simplified diagram is given on the right. The vertical shaded (red) line crossing the propagator carrying momentum $\ell_6 + k_3$ indicates that it too is replaced with an on-shell condition at the start of this process.

Here we take initial steps at higher loops, investigating sample four- and five-loop cases to provide supporting evidence that only logarithmic singularities are present in the nonplanar sector. We do so by showing compatibility between $d\log$ numerators and known expressions for the amplitudes [97, 101] on maximal cuts.

As a first example, consider the nonplanar four-loop diagram on the left in Fig. 12. We wish to show that the maximal cuts are compatible with a numerator that ensures only logarithmic singularities and no poles at infinity. Since this diagram has a hexagon subdiagram carrying loop momentum ℓ_6 and a pentagon subdiagram carrying loop momentum ℓ_5, the overall dimensionality and asymptotic scaling constraints of Sect. 3 require $N^{4\text{-loop}} \sim \mathcal{O}((\ell_6)^4\,, (\ell_5)^2)$.

In order to derive the desired numerator for this diagram, we use the cut sequence

$$\text{cuts} = \{(\ell_6 + k_3)^2, B(\ell_8), B(\ell_7, \ell_7 - k_3)\}\,, \tag{6.1}$$

where the notation is defined in Sect. 2.3. The first cut setting $(\ell_6+k_3)^2 = 0$ is indicated in Fig. 12 by the vertical shaded (red) line crossing the corresponding propagator. The remaining cuts leave behind Jacobians; the propagators placed on-shell by these cuts are indicated by the shaded (red) thick lines. The resulting Jacobian is

$$J_{7,8} = (\ell_5 - k_3)^2 \left[\ell_6^2\right]^2\,. \tag{6.2}$$

Since the Jacobian appears in the denominator, this gives us an unwanted double pole in the integrand when $\ell_6^2 = 0$. Thus, to remove it on the cuts (6.1) we require the numerator be proportional to ℓ_6^2:

$$N^{4\text{-loop}}(\ell_5, \ell_6)\big|_{\text{cut}} = \ell_6^2 \widetilde{N}^{4\text{-loop}}(\ell_5, \ell_6)\big|_{\text{cut}}\,. \tag{6.3}$$

After canceling one factor of ℓ_6^2 from the Jacobian in Eq. (6.2) against a factor in the numerator, we can use the remaining ℓ_6^2 or $(\ell_5 - k_3)^2$ from the Jacobian together with the remaining uncut propagators on the right of Fig. 12 to give two distinct relabelings of the two-loop nonplanar diagram in Fig. 3(b), if we also cancel the other propagator factor coming from the Jacobian. We then relabel the $d\log$ numerators for the two-loop nonplanar diagram in Eq. (3.30) to match the labels of the simplified four-loop diagram on the right in Fig. 12. Including factors to cancel the double pole and unwanted Jacobian factor, we have two different $d\log$ numerators for the four-loop diagram of Fig. 12:

$$\begin{aligned} N_1^{\text{4-loop}}(\ell_5,\ell_6)\big|_{\text{cut}} =& \ell_6^2(\ell_5 - k_3)^2 \left[(\ell_6 - k_4)^2 + (\ell_6 - k_1)^2\right]\big|_{\text{cut}}\,, \\ N_2^{\text{4-loop}}(\ell_5,\ell_6)\big|_{\text{cut}} =& [\ell_6^2]^2 \left[(\ell_5 - k_2 - k_3)^2 + (\ell_5 - k_1 - k_3)^2\right]\big|_{\text{cut}}\,. \end{aligned} \tag{6.4}$$

The integrands with these numerators then have only logarithmic singularities and no poles at infinity in the kinematic region of the cut, as inherited from the two-loop nonplanar double box.

Are these $d\log$ numerators compatible with the known four-loop amplitude? Relabeling the numerator of the corresponding diagram 32 in Fig. 23 of Ref. [101] to match our labels, we see that a valid numerator that matches the maximal cuts is

$$N_{\text{old}}^{\text{4-loop}} = \ell_6^2(s\ell_6^2 - t(\ell_5 - k_3)^2 - s(\ell_6 + \ell_5)^2)\,. \tag{6.5}$$

To check compatibility with our $d\log$ numerators we take the maximal cut, replacing all propagators with on-shell conditions. This selects out a piece unique to this diagram.[5] On the maximal cut, Eq. (6.5) simplifies to

$$N_{\text{old}}^{\text{4-loop}}\Big|_{\substack{\text{max}\\ \text{cut}}} = \ell_6^2(s\ell_6^2 + t(2\ell_5 \cdot k_3)) = \left(N_1^{\text{4-loop}} - N_2^{\text{4-loop}}\right)\Big|_{\substack{\text{max}\\ \text{cut}}}\,. \tag{6.6}$$

This shows that the maximal cut of diagram 32 with the old numerator is a linear combination of the maximal cut of diagram 32 with the two $d\log$ numerators in Eq. (6.4). We note that by following through the modified rung rule of Sect. 4.3, we obtain the same coefficients as those determined from the maximal cuts.

Next consider a five-loop example: the nonplanar five-loop diagram on the left of Fig. 13. As in the four-loop case, we identify potential double poles by choosing a sequence of cuts that uncovers a lower-loop embedding for which a $d\log$ numerator is already known. Our order of taking cuts is

$$\text{cuts} = \{B(\ell_7), B(\ell_9, \ell_9 + k_1)\}\,, \tag{6.7}$$

[5] Other diagrams do not mix with the one under consideration if we use all solutions to the maximal cut.

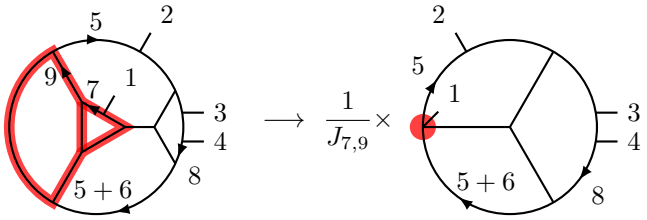

Figure 13. The left diagram contributes to the five-loop four-point $\mathcal{N} = 4$ sYM amplitude [97]. The shaded (red) lines indicate propagators that are replaced by on-shell conditions as given in Eq. (6.1). These propagators are removed from the diagram and leave behind an inverse Jacobian, given in Eq. (6.8). The resulting simplified diagram is given on the right. The factor ℓ_6^2 in the Jacobian can be used to expand the shaded (red) region, resulting in a graph isomorphic to the three-loop diagram Fig. 4(g).

resulting in the Jacobian

$$J_{7,9} = \ell_6^2 \left[\ell_6^2(\ell_5 + k_1)^2 - \ell_5^2(\ell_6 - k_1)^2\right]. \tag{6.8}$$

Collecting the ℓ_6^2-factor of this Jacobian with the remaining uncut propagators reproduces a relabeling of three-loop diagram (g), with numerator given in Eq. (4.32). To ensure this five-loop nonplanar integrand has a $d\log$ numerator, we require the numerator to cancel the Jacobian, as well as to contain a factor of the three-loop numerator,

$$N^{(\mathrm{g})} = -s(\ell_8 - \ell_5)^2 + (\ell_5 + k_1)^2 \left[(\ell_8 - k_1)^2 + (\ell_8 - k_2)^2\right], \tag{6.9}$$

obtained from Eq. (4.32) and relabeled to match Fig. 13. We have not included the last three terms in the numerator given in Eq. (4.32), because they vanish on maximal cuts, which we impose below in our compatibility test. Here we are not trying to find all $d\log$ numerators, but just those that we can use for testing compatibility with the known results. Combining the Jacobian (6.8) with the relabeled numerator $N^{(\mathrm{g})}$ gives a valid $d\log$ numerator,

$$N^{\text{5-loop}}\big|_{\text{cut}} = \left[\ell_6^2(\ell_5 + k_1)^2 - \ell_5^2(\ell_6 - k_1)^2\right] N^{(\mathrm{g})}\big|_{\text{cut}}. \tag{6.10}$$

A straightforward exercise then shows that on the maximal cut of the five-loop diagram in Fig. 13, $N^{\text{5-loop}}$ matches the numerator from Ref. [97]:

$$N^{\text{5-loop}}\big|_{\substack{\text{max}\\\text{cut}}} = N_{\text{old}}^{\text{5-loop}}\Big|_{\substack{\text{max}\\\text{cut}}} = -\frac{1}{2} s(\ell_8 \cdot k_1)(\ell_6 \cdot k_1)(\ell_5 \cdot k_1). \tag{6.11}$$

Here we have compared to diagram 70 of the ancillary file of Ref. [97] and shifted momentum labels to match ours. Again the modified rung rule matches the $\ell_6^2(\ell_5 + k_1)^2$ term, which is the only non-vanishing contribution to $N^{\text{5-loop}}$ on the maximal cut.

We have also checked a variety of other four- and five-loop examples. These provide higher-loop evidence that we should find only logarithmic singularities and no poles at infinity. We build on this theme in the next section by considering the consequences of *d*log numerators at high loop-order in the planar sector.

7 Back to the planar integrand

How powerful is the requirement that an expression has only logarithmic singularities and no poles at infinity? To answer this we re-examine the planar sector of $\mathcal{N} = 4$ sYM theory and argue that these requirements on the singularity structure are even more restrictive than dual conformal invariance. Specifically we make the following conjecture:

- Logarithmic singularities and absence of poles at infinity imply dual conformal invariance of local integrand forms to all loop orders in the planar sector.

To give supporting evidence for this conjecture, as well as to show that the constraints on the singularities are even stronger than implied by dual conformal symmetry, we work out a variety of nontrivial examples. In particular, we show in detail that at three- and four-loops the singularity conditions exactly select the dual conformal invariant integrand forms that appear in the amplitudes. We also look at a variety of other examples through seven loops. This conjecture means that by focusing on the singularity structure we can effectively carry over the key implications of dual conformal symmetry to the nonplanar sector even if we do not know how to carry over the symmetry itself. This suggests that there may be some kind of generalized version of dual conformal symmetry for the complete four-point amplitudes in $\mathcal{N} = 4$ sYM theory, including the nonplanar sector. We put off further speculation on this point until future work.

We also show that the conditions of no double poles are even more constraining than dual conformal symmetry. In fact, we demonstrate that the singularity constraints explain why certain dual conformal numerators cannot appear in the $\mathcal{N} = 4$ sYM integrand. We describe simple rules for finding non-logarithmic poles in momentum twistor space. These rules follow the spirit of Ref. [102] and allow us to restrict the set of dual conformal numerators to a smaller subset of potential *d*log numerators. While these rules do not fully eliminate all dual conformal numerators that lead to unwanted double poles, they offer a good starting point for finding a basis of *d*log numerators.

Furthermore, we give explicit examples at five and six loops where the pole constraints not only identify contributions with zero coefficient but also explain nonvanishing relative coefficients between various dual conformally invariant contributions.

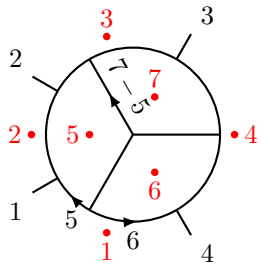

(e)

Figure 14. The planar three-loop diagram (e), including shaded (red) dots and labels to indicate the face or dual variables.

From this perspective, requiring only logarithmic singularities is a stronger constraint than requiring dual conformal symmetry.

In our study we use the four-loop results from Ref. [99] and results through seven-loops from Ref. [103]. Equivalent results at five and six loops can be found in Refs. [98, 104, 105].

7.1 Brief review of dual conformal invariance

Dual conformal symmetry [19–21] has been extensively studied for planar $\mathcal{N} = 4$ sYM amplitudes. For a detailed review, see Ref. [7, 8]. Here we only require the part useful for multiloop four point amplitudes, which we briefly review. Dual or region variables are the natural variables to make dual conformal symmetry manifest. To indicate the dual variables, we draw graphs in momentum space with the corresponding dual faces marked with a shaded (red) dot and labeled with a shaded (red) number. This is illustrated in Fig. 14.

We define the relation between external momenta k_i and external dual variables (region momenta) x_i as

$$k_i = x_{i+1} - x_i \,, \quad i = 1, 2, 3, 4 \,, \quad x_5 \equiv x_1 \,. \tag{7.1}$$

In term of dual variables, the Mandelstam invariants are

$$s = (k_1 + k_2)^2 \equiv x_{13}^2 \,, \qquad t = (k_2 + k_3)^2 \equiv x_{24}^2 \,. \tag{7.2}$$

The internal faces are parametrized by additional x_j, with $j = 5, 6, \ldots, 4 + L$ corresponding to loop momenta. In terms of the dual coordinates, loop momenta are defined from the diagrams as:

$$\ell = x_{\text{right}} - x_{\text{left}} \,, \tag{7.3}$$

where x_{right} is the dual coordinate to the right of ℓ when traveling in the direction of ℓ, and x_{left} is the dual coordinate to the left of ℓ when traveling in the direction of ℓ.

The key symmetry property of the integrand forms is invariance under inversion, $x_i^\mu \to x_i^\mu / x_i^2$ so that

$$x_{ij}^2 \to \frac{x_{ij}^2}{x_i^2 x_j^2}\,, \qquad\qquad d^4 x_i \to \frac{d^4 x_i}{x_i^2}\,. \tag{7.4}$$

We say that a four-point planar integrand form is dual conformally invariant if $d\mathcal{I} \to d\mathcal{I}$ under this transformation.

7.2 Dual conformal invariance at three and four loops

First consider three loops. There are two planar diagrams, diagrams (a) and (e) in Fig. 4. Diagram (a) is a bit trivial because the numerator does not contain any loop momenta, so we do not discuss it in any detail. Diagram (e), together with its face variables, is shown in Fig. 14. The only allowed $d$log numerator for this diagram is given in Eq. (4.32) and Table 1. Written in dual coordinates, it is

$$N^{(\text{e})} = s(\ell_5 + k_4)^2 = x_{13}^2 x_{45}^2\,. \tag{7.5}$$

This numerator exactly matches the known result [13, 77] for the three-loop planar amplitude consistent with dual conformal symmetry [19], giving (somewhat trivial) evidence for our conjecture. When counting the dual conformal weights via Eq. (7.4), we need to account for the factor of $st = x_{13}^2 x_{24}^2$ in the prefactor $\mathcal{K}$ defined in Eq. (3.22). We note that the conditions of logarithmic singularities do not fix the overall prefactor of s, but such loop momentum independent factors are easily determined from maximal cut or leading singularity constraints when expanding the amplitude.

A more interesting test of our conjecture starts at four loops. We construct a basis of $d$log-integrands for the planar amplitude following the same techniques we used at three loops. We then compare these to known results for the amplitude that manifest dual conformal invariance [99]. Following the algorithm of Sect. 3, we define trivalent parent diagrams. These are given in Fig. 15.

We have constructed all $d$log numerators for the four-loop four-point planar amplitude. To illustrate this construction, consider first diagram (4c) of Fig. 15. This is a particularly simple case, because it follows from taking diagram (e) at three loops in Fig. 14 and forming an additional box by inserting an extra propagator between two external lines. The extra box introduces only a factor of s to the three-loop numerator $N^{(\text{e})}$. This then gives us the four loop numerator

$$N^{(\text{4c})} = s\, N^{(\text{e})}\big|_{\ell_5 \to \ell_6} = (x_{13}^2)^2 x_{46}^2\,, \tag{7.6}$$

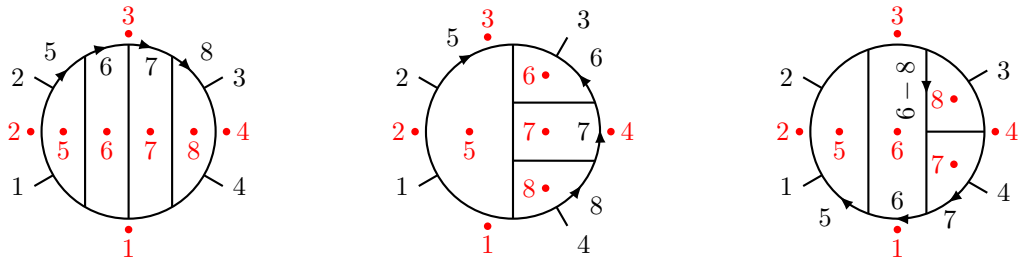

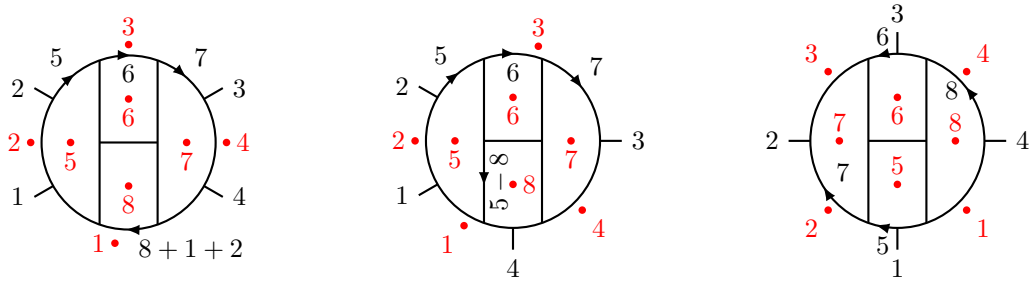

Figure 15. Parent diagrams contributing to the four-loop planar amplitude. The shaded (red) dots indicate the face or dual labels of the planar graph.

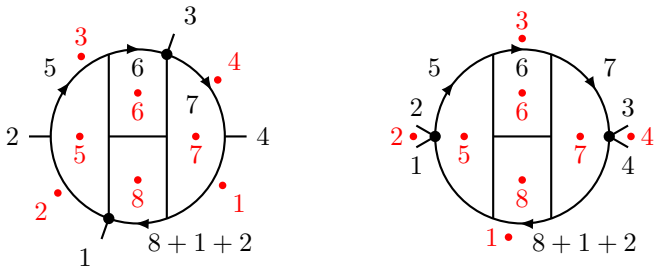

Figure 16. Diagram (4d$_2$) contributes to the planar amplitude at four-loops. Diagram (4d′) does not. Shaded (red) dots represent dual coordinates. Black dots represent contact terms.

where the relabeling $\ell_5 \to \ell_6$ changes from the three-loop diagram (e) labels of Fig. 4 to the four-loop labels of diagram (4c).

As a more complicated example, consider diagram (4d) of Fig. 15. This contains

two pentagon subdiagrams parametrized by ℓ_5 and ℓ_7 and so has a numerator scaling as $N^{(4f)} \sim \mathcal{O}(\ell_5^2, \ell_7^2)$. We skip the details here, and just list the two[6] independent numerators that result from applying all $d$log-conditions:

$$N_1^{(4d)} = s^2(\ell_5 - \ell_7)^2 = (x_{13}^2)^2 x_{57}^2 \,, \tag{7.7}$$

$$N_2^{(4d)} = s\ell_7^2(\ell_5 + k_1 + k_2)^2 = x_{13}^2 x_{37}^2 x_{15}^2 \longrightarrow N^{(4d_2)} = x_{13}^2 \,. \tag{7.8}$$

In Eq. (7.8), we have indicated that the numerator $N_2^{(4d)}$ cancels two propagators to produce exactly Fig. 16 ($4d_2$), with numerator $N^{(4d_2)}$. The numerator $N_1^{(4d)}$ is one of the known dual conformal numerators, and the lower-propagator diagram Fig. 16($4d_2$) is also a well-known dual conformal diagram.

Interestingly, dual conformal invariance allows two additional numerators

$$N_3^{(4d)} = x_{13}^2 x_{27}^2 x_{45}^2 \,, \tag{7.9}$$

$$N_4^{(4d)} = x_{13}^2 x_{25}^2 x_{47}^2 \longrightarrow N^{(4d')} = x_{13}^2 \,, \tag{7.10}$$

where again $N_4^{(4d)}$ reduces to diagram ($4d'$) in Fig. 16 upon canceling propagators. These two numerators do not meet the no double poles and no poles at infinity constraints. This is not a coincidence and fits nicely with the fact that these two numerators have zero coefficient in the amplitude [99, 102].

The other diagrams are similar, and we find that for all cases the $d$log-requirement selects out the dual conformal planar integrands that actually contribute to the amplitude and rejects those that do not. Our analysis also proves that, at least for this amplitude, each dual conformally invariant term in the amplitudes, as given in Ref. [99], is free of non-logarithmic singularities and poles at infinity.

7.3 Simple rules for eliminating double poles

In the previous subsection, we highlighted the relationship between dual conformal invariance and the singularity structure of integrands. Here we go further and demonstrate that the requirement of having no other singularities than logarithmic ones puts tighter constraints on the integrand than dual conformal symmetry.

We start from the observation of Drummond, Korchemsky and Sokatchev (DKS) [102] that certain integrands upon integration are not well defined in the infrared, even with external off-shell legs. They found that if any set of four loop variables $\{x_{i_1}, x_{i_2}, x_{i_3}, x_{i_4}\}$ approach the same external point x_j such that $\rho^2 = x_{i_1 j}^2 + x_{i_2 j}^2 + x_{i_3 j}^2 + x_{i_4 j}^2 \to 0$ and

[6] There is a third numerator $s\ell_7^2(\ell_5 + k_1 + k_2)^2$ that is a relabeling of $N_2^{(4d)}$ under automorphisms of diagram (4d). Here and below we omit such relabelings.

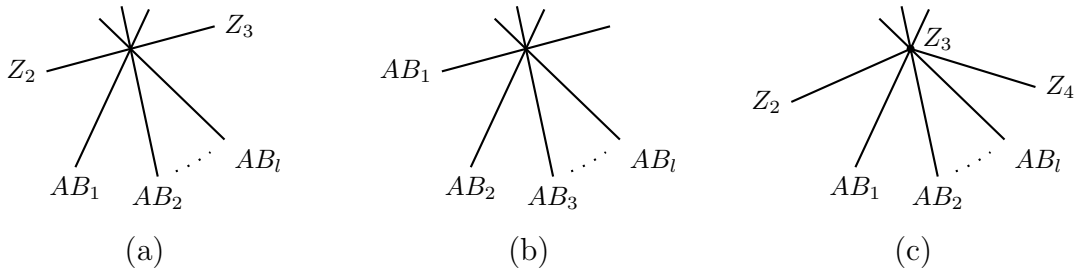

Figure 17. Cut configurations in momentum twistor geometry. Our type I conditions correspond to (b), type II to (a) and type III to (c).

the integrand scales as

$$d\mathcal{I} = \frac{d^4x_{i_1}\cdots d^4x_{i_4}\ N(x_i)}{D(x_i)} \sim \frac{d\rho}{\rho}\,. \tag{7.11}$$

The singularity $\rho \to 0$ corresponds to an integrand double pole in our language, as we shall see below. The singularity (7.11) occurs in the region of integration and results in an infrared divergent integral even for off-shell external momenta. It is therefore not a sensible dual conformal integral. Such ill-defined integrals should not contribute, as DKS confirmed in various examples, leading to their all loop order conjecture [102]. A trivial generalization is to group l loop variables at a time, $\rho^2 = x_{i_1 j}^2 + x_{i_2 j}^2 + \cdots + x_{i_l j}^2 \to 0$. Again the requirement is that the integral not be divergent with off-shell external momenta. Of course, this rule was not meant to explain all vanishings of coefficients nor to explain why terms appear in certain linear combinations.

Here we wish to extend this line of reasoning using our new insight into the singularity structure of amplitudes. For this exercise it is convenient to switch to momentum twistor coordinates, for which the problem of approaching certain dangerous on-shell kinematic regions becomes purely geometric; see Ref. [22, 106] for a discussion of momentum twistor geometry. To facilitate comparisons to existing statements in the literature, we translate the results back to dual coordinates (region momenta) at the end.

First we rewrite the DKS observation in momentum twistor variables. To be concrete, we can take $x_j = x_3$ to be the designated external point, but in fact there is nothing special about that choice. Consider the case of l loop variables. The l loop variables $\{x_{i_1}, \ldots, x_{i_l}\}$ correspond to l lines $(AB)_1, \ldots, (AB)_l$ in momentum twistor space. In our notation, the point x_3 in dual coordinates corresponds to the line $Z_2 Z_3$ in momentum twistor space. Geometrically, the condition $\rho^2 \to 0$ corresponds to a configuration in momentum twistor space for which all l lines intersect the line $Z_2 Z_3$ at the same point, as in Fig. 17(a).

If we parametrize

$$A_i = Z_2 + \rho_i Z_3 + \sigma_i Z_4 \,, \tag{7.12}$$

where ρ_i, σ_i are free parameters, then setting $\rho_i = \rho^*$ and $\sigma_i = 0$ results in the desired configuration, where ρ^* is arbitrary but the same for all i. We use a collective coordinate:

$$\rho_1 = \rho^*, \qquad \rho_j = \rho^* + t\widetilde{\rho}_j \qquad \sigma_i = \widetilde{\sigma}_i t \,, \tag{7.13}$$

for $j = 2, \ldots, l$ and $i = 1, \ldots, l$, which sets all parameters to the desired configuration in the limit $t \to 0$. In this limit, the measure scales as

$$\prod_{i=1,j=2}^{l} d\rho_j \, d\sigma_i \sim t^{2l-2} dt \,, \tag{7.14}$$

and all propagators of the form $\langle (AB)_i \, (AB)_j \rangle$ and $\langle (AB)_i \, Z_2 Z_3 \rangle$ scale like t. The result is that the integrand behaves as

$$d\mathcal{I} = \prod_{i=1,j=2}^{l} d\rho_j \, d\sigma_i \frac{N(\rho_j, \sigma_i)}{D(\rho_j, \sigma_i)} \sim dt \; t^{2l-2} \cdot \frac{t^N}{t^P} = \frac{dt}{t^{P-N-2l+2}} \,, \tag{7.15}$$

where $N(t) \sim t^N$ is the behavior of the numerator in this limit and $D(t) \sim t^P$ is the behavior of the denominator, meaning that P is the number of propagators that go to zero as $t \to 0$. To avoid unwanted double or higher poles, we demand that $P < N + 2l$. Note the shift by one in the counting rules with respect to Eq. (7.11). That equation counts overall scaling in the integration, while we study singularities in the integrand in an inherently on-shell manner. Either way we arrive at the same conclusion.

As an example consider diagram (4d). One of the numerators is $N_1^{(4\text{d})} = (x_{13})^2 x_{57}^2$ and so has $N = 1$, while there are $l = 4$ loops, and there are a total of $P = 8$ propagators of the form $\langle (AB)_i \, (AB)_j \rangle$ and $\langle (AB)_i \, Z_2 Z_3 \rangle$. In this case

$$P = 8 < 9 = 1 + 2 \cdot 4 = N + 2l \,, \tag{7.16}$$

and so the numerator is allowed by this double pole constraint. In fact, both numerators $N_1^{(4\text{d})}$ and $N_2^{(4\text{d})}$ from Eqs. (7.7) and (7.8) have the same values of P, l, and N, and so each passes this double pole test and has only single poles. In contrast, the numerators $N_3^{(4\text{d})}$ and $N_4^{(4\text{d})}$ from Eqs. (7.9) and (7.10) have $N = 0$ and fail the inequality, so they have double poles and do not contribute to the amplitude.

Now we can generalize this and consider two similar cases: all lines $(AB)_i$ intersect at a generic point as in Fig. 17(b), or all lines intersect at a given external point as in Fig. 17(c). The crux of the argument is the same as the first: if the integrand has a

double pole we reject it. The resulting inequalities to avoid these singularities follow analogously; the only difference with the first case is the geometric issue of how many of the l lines are made to intersect. We summarize the results in terms of N, the number of numerator factors that vanish, P, the number of vanishing propagators, and the subset of l loop dual coordinates $\{x\}_L \equiv \{x_{i_1}, \ldots, x_{i_l}\}$. Corresponding to each of the diagrams in Fig. 17, we obtain three types of conditions:

- Type I (Fig. 17(b)):
$$P < N + 2l - 2\,, \tag{7.17}$$
in the limit that loop dual coordinates are light-like separated from each other: $x_{ij}^2 = 0$ for all $x_i, x_j \in \{x\}_L$.

- Type II (Fig. 17(a)):
$$P < N + 2l\,, \tag{7.18}$$
in the limit that loop dual coordinates are light-like separated from each other and from one external point: $x_{ij}^2 = x_{ki}^2 = 0$ for all $x_i, x_j \in \{x\}_L$, $k = 1, 2, 3, 4$

- Type III (Fig. 17(c)):
$$P < N + 2l + 1\,, \tag{7.19}$$
in the limit that loop dual coordinates are light-like separated from each other and from two external points: $x_{ij}^2 = x_{ki}^2 = x_{k'i}^2 = 0$, for all $x_i, x_j \in \{x\}_L$, $k, k' = 1, 2, 3, 4$.[7]

These rules prevent certain classes of non-logarithmic singularities from appearing. In the four-loop case, these rules are sufficient to reconstruct all dual conformal numerators, automatically precluding those that do not contribute to the amplitude. Up to seven loops, we used a computer code to systematically check that all contributions to the amplitude pass the above rules. Furthermore, we were able to explain all coefficient zero diagrams up to five loops and many coefficient zero diagrams up to seven loops using these rules and the available data provided in Ref. [103]. In the next subsection we give examples illustrating the above three conditions in action, as well as examples of non-logarithmic singularities not detected by these tests. Not surprisingly, as the number of loops increases there are additional types of nonlogarithmic singularities. Indeed, at sufficiently high loop order we expect that cancellations of unwanted singularities can involve multiple diagrams.

[7] The equations $x_{ki}^2 = x_{k'i}^2 = 0$ have two solutions so we have to choose the same solution for all x_i.

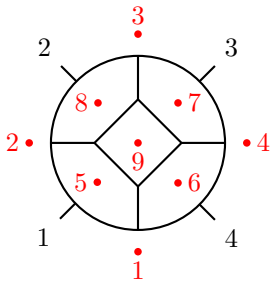

(5a)

Figure 18. A sample five-loop planar diagram. Shaded (red) dots and labels represent dual coordinates.

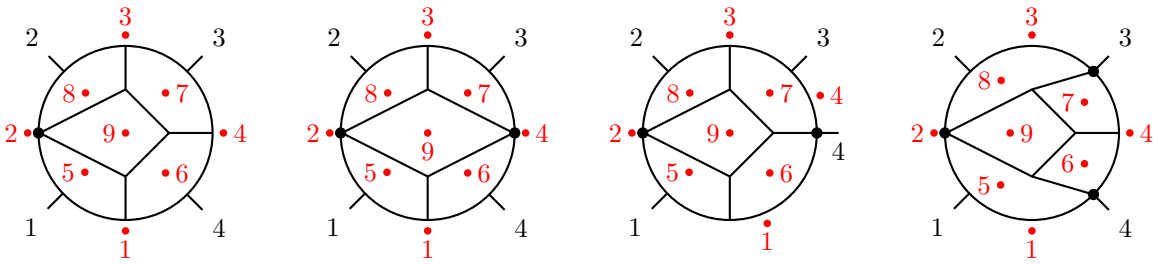

(5b) (5c) (5d) (5e)

Figure 19. Descendants of the five-loop planar diagram of Fig. 18 with numerator coefficients determined to be *non-zero* by testing for non-logarithmic singularities.

7.4 Applications of three types of rules

We now consider three examples to illustrate the rules. First we examine a five-loop example where the rules forbid certain dual conformal numerators from contributing to the amplitude. We will see in that example that double poles beyond the scope of the above three rules determine relative coefficients between integrands consistent with the reference data [98, 103]. We then consider two different six-loop diagrams that have zero coefficient in the expansion of the amplitude. In the first example, the three rules are sufficient to determine that the numerator has zero coefficient in the amplitude, while the integrand in the second example has hidden double poles not accounted for by the rules.

We first consider the diagram of Fig. 18. We take a slightly different approach here than in previous subsections. First we list the set of all dual conformal numerators allowed by power counting, then eliminate numerators that do not pass the three rules

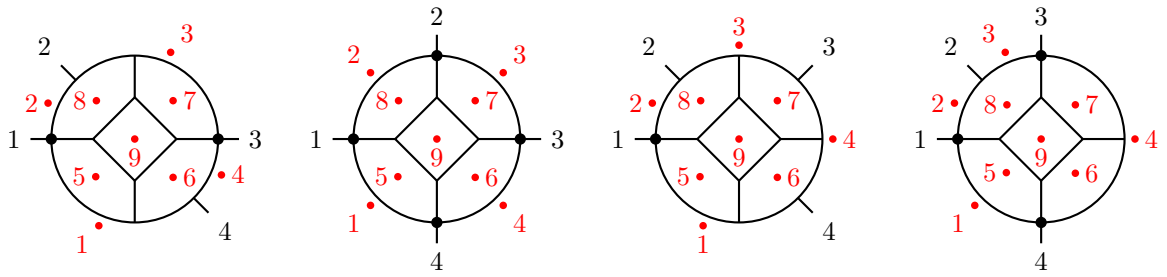

Figure 20. Descendants of the five-loop planar diagram of Fig. 18 with numerator coefficients determined to be *zero* by testing positive for non-logarithmic singularities.

of the previous subsection.

The dual conformal numerators that do not collapse any propagators in Fig. 18 are

$$N_1^{(5a)} = x_{24}^2 x_{35}^2 x_{17}^2 x_{68}^2 \,, \qquad N_2^{(5a)} = -x_{13}^2 x_{24}^2 x_{57}^2 x_{68}^2 \,,$$
$$N_3^{(5a)} = x_{18}^2 x_{27}^2 x_{36}^2 x_{45}^2 \,, \tag{7.20}$$

where we omit any dual conformal numerators that are relabelings of these numerators under automorphisms of the diagram. These three numerators correspond to diagrams 21, 22 and 35, respectively, of Ref. [98]. However, notice that in the notation used here an overall factor of $st = x_{13}^2 x_{24}^2$ has been stripped off. For the three kinematic conditions of the rules, this diagram has three different values of P:

$$P_{\rm I} = 8 \,, \quad P_{\rm II} = 10 \,, \quad \text{and} \quad P_{\rm III} = 12 \,, \tag{7.21}$$

where the subscript denotes the kinematic case we consider. The type I kinematics is most constraining in this example, and for $l = 5$ requires $N > 0$. Converting this back to a statement about the numerator, we conclude that all $d$log numerators for this diagram must have at least one factor of the form $x_{l_1 l_2}$, for x_{l_1} and x_{l_2} in the set of loop face variables. Only $N_1^{(5a)}$ and $N_2^{(5a)}$ have this correct loop dependence. So we conclude that both $N_1^{(5a)}$ and $N_2^{(5a)}$ can appear in the amplitude, while $N_3^{(5a)}$ yields an integrand with non-logarithmic poles, and so has coefficient zero in the amplitude.

In addition to the numerators in Eq. (7.20), there are other dual conformal numerators that cancel propagators of the parent diagram, resulting in contact-term diagrams depicted in Figs. 19 and 20. If we consider only the contact terms that can be obtained from the diagram in Fig. 18, the numerators that pass the three types of checks are

$$N^{(5b)} = -x_{24}^2 x_{17}^2 x_{36}^2 \,, \qquad N^{(5c)} = x_{13}^2 x_{24}^2 \,,$$

$$N^{(5d)} = -x_{13}^2 x_{27}^2\,, \qquad\qquad N^{(5e)} = x_{24}^2\,, \tag{7.22}$$

where the four numerators respectively correspond to diagrams 31, 32, 33, and 34 in Ref. [98]. Besides $N_3^{(5a)}$, there are four more numerators that display dual conformal invariance at the integrand level, but are invalid by applying the type II rules, which is equivalent to the DKS observation that they are ill defined:

$$\begin{aligned} N^{(5f)} &= x_{18}^2 x_{36}^2\,, & N^{(5g)} &= 1\,, \\ N^{(5h)} &= x_{17}^2 x_{36}^2 x_{48}^2\,, & N^{(5i)} &= x_{35}^2\,. \end{aligned} \tag{7.23}$$

These correspond to diagrams 36, 37, 38 and 39, respectively, of Ref. [98]. The numerators listed in Eq. (7.22) are numerators for the lower-propagator topologies in Fig. 19, and the numerators listed in Eq. (7.23) are numerators for the lower-propagator topologies in Fig. 20. We again omit the other dual conformal numerators that are relabelings of these numerators under automorphism of the diagram.

With this analysis, we have not proved that $N_{1,2}^{(5a)}$ through $N^{(5e)}$ ensure a $d\log$ form; we have only argued that the corresponding integrands do not contain the types of non-logarithmic singularities detected by our three rules. It is still possible for those integrands to have non-logarithmic poles buried in certain kinematic regimes deeper in the cut structure. Indeed, under more careful scrutiny we find additional constraints from the requirements of no double poles. In particular, we find that only the following combinations of integrands corresponding to Figs. 18 and 19 are free of double poles:

$$\mathcal{I}^{(A)} = \mathcal{I}_1^{(5a)} + \mathcal{I}^{(5b)} + \mathcal{I}^{(5e)}\,, \qquad \mathcal{I}^{(B)} = \mathcal{I}_2^{(5a)} + \mathcal{I}^{(5c)}\,, \qquad \mathcal{I}^{(D)} = \mathcal{I}^{(5d)}\,. \tag{7.24}$$

The notation is, for example, that the integrand $\mathcal{I}_1^{(5a)}$ has the propagators of diagram (5a) and the numerator $N_1^{(5a)}$ in Eq. (7.20). Similarly, the corresponding numerators for the integrands of diagrams (5b)–(5e) are given in Eq. (7.22). The integrand for diagram (5a) with numerator $N_3^{(5a)}$ is not present, because no contact terms can remove all double poles of $\mathcal{I}_3^{(5a)}$. In this case, all cancellations of double poles are between the parent and descendant diagrams. However, at higher loops the situation can very well be more complicated: unwanted singularities can cancel between different parent diagrams as well.

We now illustrate how pole constraints can explain why some six-loop diagrams enter the planar amplitude with zero coefficient. We choose two examples that both fall outside the type II classification of the effective rules of the previous subsection. This means both numerators escape detection by the original DKS rule, and so far could not be easily identified as coefficient-zero terms. The two examples are the six-loop "bowtie" in Fig. 21(6a) and another six-loop diagram with two contact terms in

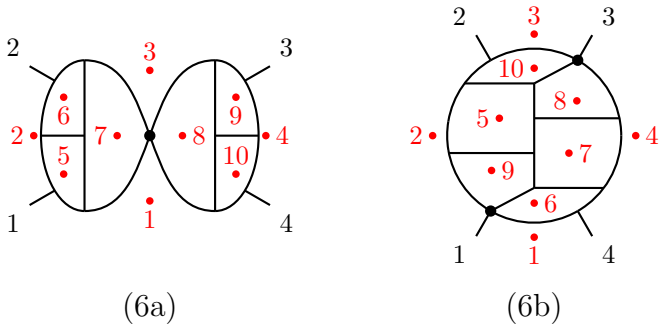

Figure 21. Two six-loop diagrams that have coefficient zero in the amplitude because they have non-logarithmic singularities. Diagram (6a) has non-logarithmic poles detected by our rules. Diagram (6b) requires explicit checks to locate double poles.

Fig. 21(6b). The dual conformal numerators of these diagrams are [103][8]

$$N^{(6a)} = x_{13}^3 x_{24}\,, \qquad\qquad N^{(6b)} = x_{24}^2 x_{27}^2 x_{45}^2\,. \tag{7.25}$$

There are other dual conformal numerators for (6b), but they belong to lower-propagator diagrams, so we ignore them in this discussion.

We first consider diagram (6a). This integrand suffers from poles of type III. We see this by cutting

$$x_{25}^2 = x_{26}^2 = x_{36}^2 = x_{37}^2 = x_{56}^2 = x_{57}^2 = x_{67}^2 = 0\,. \tag{7.26}$$

We are then looking at the $l = 3$, $N = 0$, $P = 7$ case and the corresponding inequality $P < N + 2l + 1$ is violated, indicating a non-logarithmic pole. This means the non-logarithmic rules immediately offer a reason why this diagram contributes to the amplitude with coefficient zero. This agrees with Ref. [103].

The six-loop example (6b) in Fig. 21 is more subtle, since it is not ruled out by the three rules. However, it does have a double pole. We know from Ref. [103] that this diagram with numerator $N^{(6b)}$ does not enter the expansion of the amplitude but has coefficient zero. Presumably, the double pole cannot cancel against other diagrams.

We also conducted a variety of checks at seven loops using the integrand given in Ref. [103]. We applied the three rules to all 2329 potential contributions and found that all 456 contributions that failed the tests did not appear in the amplitude, as expected. We also checked dozens of examples that have vanishing coefficients and we were able

[8]These diagrams and numerators can be found in the associated files of Ref. [103] in the list of six loop integrands that do not contribute to the amplitude. In our notation, we have again stripped off a factor of $st = x_{13}^2 x_{24}^2$.

to identify problematic singularities. More generally, as we saw at five loops, the double poles can cancel nontrivially between different contributions. We leave a detailed study of the restrictions that logarithmic singularities and poles at infinity place on higher-loop planar amplitudes to future work. In any case, the key implication is that we should be able to carry over the key consequences of dual conformal symmetry to the nonplanar sector, even though we do not know how to define the symmetry in this sector.

8 From gauge theory to gravity

Ref. [76] noted that the two-loop four-point amplitude of $\mathcal{N} = 8$ supergravity has only logarithmic singularities and no poles at infinity. Does this remain true at higher loops? In this section we use BCJ duality to analyze this question. Indeed, we make the following conjecture:

- At finite locations, the four-point momentum-space integrand forms of $\mathcal{N} = 8$ supergravity have only logarithmic singularities.

However, we will prove that in $\mathcal{N} = 8$ supergravity there are poles at infinity whose degree grows with the loop order, as one might have guessed from power counting. This conjecture relies on two other conjectures: the duality between color and kinematics [73], and the conjecture that nonplanar $\mathcal{N} = 4$ sYM amplitudes have only logarithmic singularities and are free of poles at infinity [76]. Explicit local expressions for numerators that satisfy the duality between color and kinematics are known at four points through four loops [84]. At higher loops the duality is a conjecture and it may require nonlocal numerators for it to hold, resulting in poles at finite points in momentum space for supergravity amplitudes. Our conjecture proposes that if this were to happen it would introduce no worse than logarithmic singularities. With modifications it should be possible to extend our conjecture beyond four points, but for $\mathrm{N}^k\mathrm{MHV}$ amplitudes with $k \geq 3$, the second sYM conjecture that we rely on holds only in the Grassmannian space and not momentum space, as noted earlier. Given that all our explicit studies are at four points, we leave our conjecture at this level for now.

We note that our conjecture effectively states that one of the key properties linked to dual conformal symmetry not only transfers to the nonplanar sector of $\mathcal{N} = 4$ sYM theory, but transfers to $\mathcal{N} = 8$ supergravity as well. Because there are poles at infinity, dual conformal symmetry is not quite present in supergravity. However, a strong echo remains in $\mathcal{N} = 8$ supergravity.

To gather evidence for our conjecture, we construct the complete three-loop four-point amplitude of $\mathcal{N} = 8$ supergravity, and do so in a form that makes it obvious that

the conjecture is true for this case. To demonstrate that there are poles at infinity, we analyze a certain easy-to-construct cut of the four-point amplitude to all loop orders. Using the duality between color and kinematics [72, 73], it is easy to obtain the complete three-loop four-point amplitude of $\mathcal{N} = 8$ supergravity in a format that makes the singularity structure manifest. Here, we simply quote a main result of the duality, and refer to Ref. [107] for a recent review. According to the duality conjecture, $\mathcal{N} = 8$ supergravity numerators may be constructed by replacing the color factors of each diagram of an $\mathcal{N} = 4$ sYM amplitude by kinematic numerators of a second copy, constrained to the same algebraic relations as the color factors. Although the general existence of numerators with the required property is unproven, here we only need the three-loop case, for which such numerators are explicitly known. Whenever duality satisfying numerators are available we immediately have the $\mathcal{N} = 8$ diagram numerators in terms of gauge-theory ones:

$$N^{(x)}_{\mathcal{N}=8} = N^{(x)}\, N^{(x)}_{\text{BCJ}}\,, \tag{8.1}$$

where (x) labels the diagram. The gauge-theory numerator $N^{(x)}$ is exactly one of the numerators in Eq. (4.32), while $N^{(x)}_{\text{BCJ}}$ is one of the $\mathcal{N} = 4$ sYM BCJ numerators from Ref. [73].

To be concrete, we construct the $\mathcal{N} = 8$ supergravity numerator for diagram (f) in Fig. 4. Multiplying the sYM $d$log numerator $N^{(\text{f})}$ in Eq. (4.32) by the corresponding BCJ numerator gives the $\mathcal{N} = 8$ supergravity numerator:

$$\begin{aligned} N^{(\text{f})}_{\mathcal{N}=8} = &-\Big[(\ell_5 + k_4)^2((\ell_5 + k_3)^2 + (\ell_5 + k_4)^2)\Big] \\ &\times \Big[(s(-\tau_{35} + \tau_{45} + t) - t(\tau_{25} + \tau_{45}) + u(\tau_{25} - \tau_{35}) - s^2)/3\Big]\,, \end{aligned} \tag{8.2}$$

where $\tau_{ij} = 2k_i{\cdot}\ell_j$. As for the gauge-theory case, we remove overall factors of $\mathcal{K}$ (defined in Eq. (3.22)). The construction of the complete three-loop supergravity amplitude is then trivial using Eq. (8.1), Eq. (4.32) and Table 1 of Ref. [73]. This construction is designed to give correct $\mathcal{N} = 8$ supergravity unitarity cuts.

Based on the BCJ construction, we immediately learn some nontrivial properties about $\mathcal{N} = 8$ supergravity. Since the supergravity and sYM diagrams have identical propagators, and each numerator has a factor of $N^{(x)}$, all unwanted double poles located at finite values are canceled. However, in general the factor $N^{(x)}_{\text{BCJ}}$ in Eq. (8.1) carries additional powers of loop momenta. These extra powers of loop momentum in the numerator compared to the $\mathcal{N} = 4$ sYM case generically lead to poles at infinity, as we prove below. However, because the three-loop BCJ numerators are at most linear in

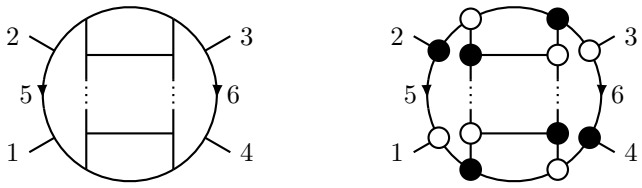

Figure 22. At $L > 3$ loops, diagram (a) contains a pole at infinity that cannot cancel against other diagrams. By cutting all propagators in diagram (a) we obtain the corresponding on-shell diagram (b), which gives a residue of the amplitude on one of the solutions of the L-loop maximal cut. This is the only contribution.

loop momentum, only single poles, or equivalently logarithmic singularities, can develop at infinity. At higher loops, the BCJ numerators contribute ever larger powers of loop momenta. These additional loop momenta generate non-logarithmic singularities as the orders of the poles at infinity grow.

To analyze the poles at infinity, we turn to a particular set of cuts chosen so that we can study poles at infinity at any loop order. While we do not yet know the four-point $\mathcal{N} = 8$ supergravity amplitude at five or higher loops, we do have partial information about the structure of the amplitude to all loop orders. In particular, we know the value of the maximal cut of the diagram in Fig. 22(a) that is displayed in Fig. 22(b). One could evaluate the cut directly in terms of amplitudes, using superspace machinery [108, 109]. However, it is much simpler to use the rung rule [77], which is equivalent to evaluating iterated two-particle cuts. This gives the value for the numerator

$$N = \left[(\ell_5 + \ell_6 + k_2 + k_3)^2\right]^{\delta(L-3)} , \tag{8.3}$$

up to terms that vanish on the maximal cut. Here $\delta = 1$ for $\mathcal{N} = 4$ sYM theory and $\delta = 2$ for $\mathcal{N} = 8$ supergravity. As usual factors of $\mathcal{K}$ have been removed.

We carefully[9] choose a set of maximal cuts as encoded in Fig. 22(b) so that only a single diagram is selected. On this solution, the two loop momenta labeled in Fig. 22 have solutions

$$\ell_5 = \alpha\lambda_1\widetilde{\lambda}_2 , \qquad \ell_6 = \beta\lambda_3\widetilde{\lambda}_4 . \tag{8.4}$$

The Jacobian for this cut is

$$J = s^2\alpha\beta[(\ell_5 + \ell_6 + k_2 + k_3)^2]^{L-2}F(\sigma_1, \ldots \sigma_{L-3}) , \tag{8.5}$$

[9]To avoid mixing in any additional solutions, we must first take a next-to-maximal cut, then make a final cut to hone in on the single solution in Eq. (8.4).

where the function F depends on the remaining $L-3$ parameters, σ_i, of the cut solution, and not on α or β. On the cut, the parametrization Eq. (8.4) implies that

$$(\ell_5 + \ell_6 + k_2 + k_3)^2\big|_{\text{cut}} = (\alpha\langle 13\rangle + \langle 23\rangle)(\beta[24] + [23])\,. \tag{8.6}$$

Then the residue in the sYM case is

$$\operatorname*{Res}_{\text{cut}} d\mathcal{I}_{\text{YM}} \sim \frac{d\alpha}{\alpha(\alpha-\alpha_0)} \wedge \frac{d\beta}{\beta(\beta-\beta_0)} \wedge \frac{d\sigma_1 \ldots d\sigma_{L-3}}{F(\sigma_1,\ldots,\sigma_{L-3})}\,, \tag{8.7}$$

with $\alpha_0 = -\langle 23\rangle/\langle 13\rangle$, $\beta_0 = -[23]/[24]$. So the sYM integrand has only logarithmic singularities and no pole at infinity in α or β. On the other hand, in the supergravity case the residue is

$$\operatorname*{Res}_{\text{cut}} d\mathcal{I}_{\text{GR}} \sim \frac{d\alpha}{\alpha(\alpha-\alpha_0)^{4-L}} \wedge \frac{d\beta}{\beta(\beta-\beta_0)^{4-L}} \wedge \frac{d\sigma_1 \ldots d\sigma_{L-3}}{F(\sigma_1,\ldots,\sigma_{L-3})}\,. \tag{8.8}$$

We see that these forms have the same structure as sYM for $L = 3$, but for $L > 3$ they differ. In the latter case, the sYM expression in Eq. (8.7) stays logarithmic with no poles at $\alpha, \beta \to \infty$, while the supergravity residue Eq. (8.8) loses the poles at α_0 and β_0 for $L = 4$ and develops a logarithmic pole at infinity. However, for $L \geq 5$ the poles at infinity become non-logarithmic, and the degree grows linearly with L. Since the cut was carefully chosen so that no other diagrams can mix with Fig. 22(a), the poles at infinity identified in Eq. (8.8) for $L \geq 4$ cannot cancel against other diagrams, and so the $\mathcal{N} = 8$ supergravity amplitudes indeed have poles at infinity. This can also be verified by the direct evaluation of the on-shell diagram in Fig. 22(b). In fact, at three loops there is another contribution (different from Fig. 22) that leads to a pole at infinity as well. As it does not offer qualitatively new insights, we will not show this example here.

We conclude that in contrast to $\mathcal{N} = 4$ sYM theory, $\mathcal{N} = 8$ supergravity has poles at infinity with a degree that grows linearly with the loop order. An interesting question is what this might imply about the ultraviolet properties of $\mathcal{N} = 8$ supergravity. While it is true that a lack of poles at infinity implies an amplitude is ultraviolet finite, the converse argument that poles at infinity imply divergences is not necessarily true. There are a number of reasons to believe that this converse fails in supergravity. First, at three and four loops the four-point $\mathcal{N} = 8$ supergravity amplitudes have exactly the same degree of divergence as the corresponding $\mathcal{N} = 4$ sYM amplitudes [78, 83, 84], even though the supergravity amplitudes have poles at infinity. Indeed, when calculating supergravity divergences in critical dimensions where the divergences first appear, they are proportional to divergences in subleading-color parts of gauge-theory amplitudes [84]. In addition, recent work in $\mathcal{N} = 4$ and $\mathcal{N} = 5$ supergravity shows that nontrivial cancellations, beyond those that have been understood by standard-symmetry

considerations, occur between the diagrams of any covariant formulation [110, 111]. Furthermore, suppose that under the rescaling $\ell_i \to t\ell_i$ with $t \to \infty$ the supergravity integrand scales as $1/t^m$. If $m \leq 4L$ where L is the number of loops, we can interpret this behavior as a pole at infinity. However, as we have demonstrated in this paper, after applying cuts this pole can still be present or disappear, and other poles at infinity can appear. Thus, the relation between ultraviolet properties of integrated results and the presence of poles at infinity is nontrivial. It will be fascinating to study this relation.

9 Conclusion

In this paper, we have studied in some detail the singularity structure of integrands of $\mathcal{N} = 4$ sYM theory, including nonplanar contributions. These contributions were recently conjectured to have only logarithmic singularities and no poles at infinity [76], just as for the planar case [28]. In this paper, besides providing nontrivial evidence in favor of this conjecture, we made two additional conjectures. First, we conjectured that in the planar sector of $\mathcal{N} = 4$ sYM theory, constraints on the amplitudes that follow from dual conformal symmetry can instead be obtained from requirements on singularities. The significance of this conjecture is that it implies that consequences of dual conformal symmetry on the analytic structure of amplitudes carry over to the nonplanar sector. We described evidence in favor of this conjecture through seven loops. Our second conjecture involves $\mathcal{N} = 8$ supergravity. While we proved that the amplitudes of this theory have poles at infinity, we conjectured that at finite locations, at least the four-point amplitude should have only logarithmic singularities, matching the $\mathcal{N} = 4$ sYM behavior.

To carry out our checks we developed a procedure for analyzing the singularity structure, which we then applied to the three-loop four-point amplitude of $\mathcal{N} = 4$ sYM theory. Using this approach we found an explicit representation of this amplitude, where the desired properties hold term by term. We also partially analyzed the singularity structure of four-point amplitudes through seven loops. We illustrated at three loops how to make the logarithmic singularity property manifest by finding $d\log$ forms.

Our strategy for studying the nonplanar singularity structure required subdividing the integrand into diagrams and assuming that we could impose the desired properties on individual diagram integrands. Unitarity constraints then allowed us to find the appropriate linear combinations of integrands to build an integrand valid for the full amplitude. Interestingly, many coefficients of the basis integrands follow a simple pattern dictated by the rung rule [77].

More generally, the study of planar $\mathcal{N} = 4$ sYM amplitudes has benefited greatly by identifying hidden symmetries. Dual conformal symmetry, in particular, imposes an extremely powerful constraint on planar $\mathcal{N} = 4$ sYM amplitudes. When combined with superconformal symmetry, it forms a Yangian symmetry which is tied to the presumed integrability of the planar theory. However, at present we do not know how to extend this symmetry to the nonplanar sector. Nevertheless, as we argued in this paper, the key analytic restrictions on the amplitude do, in fact, carry over straightforwardly to the nonplanar sector. This bodes well for future studies of full amplitudes in $\mathcal{N} = 4$ sYM theory.

Our basis integrands are closely related to the integrals used by Henn et al. [80, 81] to find a simplified basis of master integrals determined from integration-by-parts identities [112, 113]. In this simplified basis, all master integrals have uniform transcendental weight, which then leads to simple differential equations for the integrals. This basis overlaps with our construction, except that we include only cases where the integrands do not have poles at infinity, since those are the ones relevant for $\mathcal{N} = 4$ sYM theory. The $d$log forms we described are in some sense partway between the integrand and the integrated expressions.

An interesting avenue of further exploration is to apply these ideas to $\mathcal{N} = 8$ supergravity. Using BCJ duality [72, 73], we converted the four-point three-loop $\mathcal{N} = 4$ sYM integrand forms with into ones for $\mathcal{N} = 8$ supergravity. We proved that the three-loop four-point integrand form of $\mathcal{N} = 8$ supergravity has only logarithmic singularities. However, there are singularities at infinity. Indeed, we proved that, to all loop orders, there are poles at infinity whose degree grows with the loop order. A deeper understanding of these poles might shed new light on the surprisingly tame ultraviolet properties of supergravity amplitudes, and in particular on recently uncovered [111] "enhanced ultraviolet cancellations", which are nontrivial cancellations that occur between diagrams.

In summary, by directly placing constraints on the singularity structure of integrands in $\mathcal{N} = 4$ sYM theory, we have a means for carrying over the key consequences of dual conformal symmetry and more to the nonplanar sector. A key conclusion of our study is that the nonplanar sector of $\mathcal{N} = 4$ sYM theory is more similar to the planar sector than arguments based on symmetry considerations suggest. Of course, one would like to do better by finding a formulation that makes manifest the singularity structure. The explicit results presented in this paper should aid that goal.

Acknowledgments

We thank Nima Arkani-Hamed, Jacob Bourjaily, Scott Davies, Lance Dixon and Josh Nohle for helpful discussions. We especially thank Johannes Henn for discussions and

detailed comparisons to unpublished results for various nonplanar master integrals. This work was supported in part by the US Department of Energy under Award Numbers DE-SC0009937 and DE-SC0011632. J. T. is supported in part by the David and Ellen Lee Postdoctoral Scholarship. E. H. is supported in part by a Dominic Orr Graduate Fellowship.

References

[1] L. Brink, J. H. Schwarz, and J. Scherk, *Supersymmetric Yang-Mills Theories*, *Nucl.Phys.* **B121** (1977) 77.

[2] F. Gliozzi, J. Scherk, and D. I. Olive, *Supersymmetry, Supergravity Theories and the Dual Spinor Model*, *Nucl.Phys.* **B122** (1977) 253–290.

[3] Z. Bern, L. J. Dixon, and D. A. Kosower, *Progress in one loop QCD computations*, *Ann.Rev.Nucl.Part.Sci.* **46** (1996) 109–148, [hep-ph/9602280].

[4] F. Cachazo and P. Svrcek, *Lectures on twistor strings and perturbative Yang-Mills theory*, *PoS* **RTN2005** (2005) 004, [hep-th/0504194].

[5] N. Beisert, C. Ahn, L. F. Alday, Z. Bajnok, J. M. Drummond, et al., *Review of AdS/CFT Integrability: An Overview*, *Lett.Math.Phys.* **99** (2012) 3–32, [arXiv:1012.3982].

[6] J. Drummond, *Tree-level amplitudes and dual superconformal symmetry*, *J.Phys.* **A44** (2011) 454010, [arXiv:1107.4544].

[7] H. Elvang and Y.-t. Huang, *Scattering Amplitudes*, arXiv:1308.1697.

[8] J. M. Henn and J. C. Plefka, *Scattering Amplitudes in Gauge Theories*, *Lect.Notes Phys.* **883** (2014) 1–195.

[9] L. J. Dixon, J. M. Drummond, and J. M. Henn, *Analytic result for the two-loop six-point NMHV amplitude in N=4 super Yang-Mills theory*, *JHEP* **1201** (2012) 024, [arXiv:1111.1704].

[10] L. J. Dixon, J. M. Drummond, C. Duhr, M. von Hippel, and J. Pennington, *Bootstrapping six-gluon scattering in planar N=4 super-Yang-Mills theory*, *PoS* **LL2014** (2014) 077, [arXiv:1407.4724].

[11] L. J. Dixon, J. M. Drummond, C. Duhr, and J. Pennington, *The four-loop remainder function and multi-Regge behavior at NNLLA in planar $N = 4$ super-Yang-Mills theory*, *JHEP* **1406** (2014) 116, [arXiv:1402.3300].

[12] L. J. Dixon and M. von Hippel, *Bootstrapping an NMHV amplitude through three loops*, arXiv:1408.1505.

[13] Z. Bern, L. J. Dixon, and V. A. Smirnov, *Iteration of planar amplitudes in maximally supersymmetric Yang-Mills theory at three loops and beyond*, *Phys.Rev.* **D72** (2005) 085001, [hep-th/0505205].

[14] E. Witten, *Perturbative gauge theory as a string theory in twistor space*, *Commun.Math.Phys.* **252** (2004) 189–258, [hep-th/0312171].

[15] R. Roiban, M. Spradlin, and A. Volovich, *A Googly amplitude from the B model in twistor space*, *JHEP* **0404** (2004) 012, [hep-th/0402016].

[16] R. Britto, F. Cachazo, and B. Feng, *New recursion relations for tree amplitudes of gluons*, *Nucl.Phys.* **B715** (2005) 499–522, [hep-th/0412308].

[17] R. Britto, F. Cachazo, B. Feng, and E. Witten, *Direct proof of tree-level recursion relation in Yang-Mills theory*, *Phys.Rev.Lett.* **94** (2005) 181602, [hep-th/0501052].

[18] N. Arkani-Hamed, J. L. Bourjaily, F. Cachazo, S. Caron-Huot, and J. Trnka, *The All-Loop Integrand For Scattering Amplitudes in Planar N=4 SYM*, *JHEP* **1101** (2011) 041, [arXiv:1008.2958].

[19] J. Drummond, J. Henn, V. Smirnov, and E. Sokatchev, *Magic identities for conformal four-point integrals*, *JHEP* **0701** (2007) 064, [hep-th/0607160].

[20] L. F. Alday and J. M. Maldacena, *Gluon scattering amplitudes at strong coupling*, *JHEP* **0706** (2007) 064, [arXiv:0705.0303].

[21] J. Drummond, J. Henn, G. Korchemsky, and E. Sokatchev, *Dual superconformal symmetry of scattering amplitudes in N=4 super-Yang-Mills theory*, *Nucl.Phys.* **B828** (2010) 317–374, [arXiv:0807.1095].

[22] A. Hodges, *Eliminating spurious poles from gauge-theoretic amplitudes*, *JHEP* **1305** (2013) 135, [arXiv:0905.1473].

[23] L. Mason and D. Skinner, *The Complete Planar S-matrix of N=4 SYM as a Wilson Loop in Twistor Space*, *JHEP* **1012** (2010) 018, [arXiv:1009.2225].

[24] S. Caron-Huot, *Notes on the scattering amplitude / Wilson loop duality*, *JHEP* **1107** (2011) 058, [arXiv:1010.1167].

[25] L. F. Alday, B. Eden, G. P. Korchemsky, J. Maldacena, and E. Sokatchev, *From correlation functions to Wilson loops*, *JHEP* **1109** (2011) 123, [arXiv:1007.3243].

[26] B. Eden, G. P. Korchemsky, and E. Sokatchev, *From correlation functions to scattering amplitudes*, *JHEP* **1112** (2011) 002, [arXiv:1007.3246].

[27] B. Eden, G. P. Korchemsky, and E. Sokatchev, *More on the duality correlators/amplitudes*, *Phys.Lett.* **B709** (2012) 247–253, [arXiv:1009.2488].

[28] N. Arkani-Hamed, J. L. Bourjaily, F. Cachazo, A. B. Goncharov, A. Postnikov, and J. Trnka, *Scattering Amplitudes and the Positive Grassmannian*, arXiv:1212.5605.

[29] N. Arkani-Hamed, F. Cachazo, C. Cheung, and J. Kaplan, *A Duality For The S Matrix*, *JHEP* **1003** (2010) 020, [arXiv:0907.5418].

[30] N. Arkani-Hamed, F. Cachazo, and C. Cheung, *The Grassmannian Origin Of Dual Superconformal Invariance*, *JHEP* **1003** (2010) 036, [arXiv:0909.0483].

[31] L. Mason and D. Skinner, *Dual Superconformal Invariance, Momentum Twistors and Grassmannians*, *JHEP* **0911** (2009) 045, [arXiv:0909.0250].

[32] N. Arkani-Hamed, J. Bourjaily, F. Cachazo, and J. Trnka, *Unification of Residues and Grassmannian Dualities*, *JHEP* **1101** (2011) 049, [arXiv:0912.4912].

[33] N. Arkani-Hamed, J. Bourjaily, F. Cachazo, and J. Trnka, *Local Spacetime Physics from the Grassmannian*, *JHEP* **1101** (2011) 108, [arXiv:0912.3249].

[34] Y.-T. Huang and C. Wen, *ABJM amplitudes and the positive orthogonal grassmannian*, *JHEP* **1402** (2014) 104, [arXiv:1309.3252].

[35] Y.-t. Huang, C. Wen, and D. Xie, *The Positive orthogonal Grassmannian and loop amplitudes of ABJM*, arXiv:1402.1479.

[36] J. Kim and S. Lee, *Positroid Stratification of Orthogonal Grassmannian and ABJM Amplitudes*, *JHEP* **1409** (2014) 085, [arXiv:1402.1119].

[37] H. Elvang, Y.-t. Huang, C. Keeler, T. Lam, T. M. Olson, et al., *Grassmannians for scattering amplitudes in 4d $\mathcal{N} = 4$ SYM and 3d ABJM*, arXiv:1410.0621.

[38] B. Chen, G. Chen, Y.-K. E. Cheung, Y. Li, R. Xie, et al., *Nonplanar On-shell Diagrams and Leading Singularities of Scattering Amplitudes*, arXiv:1411.3889.

[39] N. Arkani-Hamed and J. Trnka, *The Amplituhedron*, arXiv:1312.2007.

[40] N. Arkani-Hamed and J. Trnka, *Into the Amplituhedron*, arXiv:1312.7878.

[41] S. Franco, D. Galloni, A. Mariotti, and J. Trnka, *Anatomy of the Amplituhedron*, arXiv:1408.3410.

[42] T. Lam, *Amplituhedron cells and Stanley symmetric functions*, arXiv:1408.5531.

[43] Y. Bai and S. He, *The Amplituhedron from Momentum Twistor Diagrams*, arXiv:1408.2459.

[44] G. Lusztig, *Total positivity in partial flag manifolds*, *Represent. Theory* **2** (1998) 70–78.

[45] A. Postnikov, *Total positivity, Grassmannians, and networks*, *ArXiv Mathematics e-prints* (Sept., 2006) [math/0609764].

[46] A. Postnikov, D. Speyer, and L. Williams, *Matching polytopes, toric geometry, and the non-negative part of the Grassmannian*, *ArXiv e-prints* (June, 2007) [arXiv:0706.2501].

[47] L. K. Williams, *Enumeration of totally positive Grassmann cells*, *ArXiv Mathematics e-prints* (July, 2003) [math/0307271].

[48] A. B. Goncharov and R. Kenyon, *Dimers and cluster integrable systems*, *ArXiv e-prints* (July, 2011) [arXiv:1107.5588].

[49] A. Knutson, T. Lam, and D. Speyer, *Positroid Varieties: Juggling and Geometry*, *ArXiv e-prints* (Nov., 2011) [arXiv:1111.3660].

[50] J. M. Drummond, J. M. Henn, and J. Plefka, *Yangian symmetry of scattering amplitudes in N=4 super Yang-Mills theory*, *JHEP* **0905** (2009) 046, [arXiv:0902.2987].

[51] A. Kotikov and L. Lipatov, *On the highest transcendentality in N=4 SUSY*, *Nucl.Phys.* **B769** (2007) 217–255, [hep-th/0611204].

[52] B. Eden and M. Staudacher, *Integrability and transcendentality*, *J.Stat.Mech.* **0611** (2006) P11014, [hep-th/0603157].

[53] N. Beisert, B. Eden, and M. Staudacher, *Transcendentality and Crossing*, *J.Stat.Mech.* **0701** (2007) P01021, [hep-th/0610251].

[54] A. E. Lipstein and L. Mason, *From d logs to dilogs the super Yang-Mills MHV amplitude revisited*, *JHEP* **1401** (2014) 169, [arXiv:1307.1443].

[55] A. B. Goncharov, M. Spradlin, C. Vergu, and A. Volovich, *Classical Polylogarithms for Amplitudes and Wilson Loops*, *Phys.Rev.Lett.* **105** (2010) 151605, [arXiv:1006.5703].

[56] J. Golden, A. B. Goncharov, M. Spradlin, C. Vergu, and A. Volovich, *Motivic Amplitudes and Cluster Coordinates*, *JHEP* **1401** (2014) 091, [arXiv:1305.1617].

[57] J. Golden, M. F. Paulos, M. Spradlin, and A. Volovich, *Cluster Polylogarithms for Scattering Amplitudes*, arXiv:1401.6446.

[58] J. Golden and M. Spradlin, *A Cluster Bootstrap for Two-Loop MHV Amplitudes*, arXiv:1411.3289.

[59] N. Beisert and M. Staudacher, *The N=4 SYM integrable super spin chain*, *Nucl.Phys.* **B670** (2003) 439–463, [hep-th/0307042].

[60] B. Basso, A. Sever, and P. Vieira, *Spacetime and Flux Tube S-Matrices at Finite Coupling for N=4 Supersymmetric Yang-Mills Theory*, *Phys.Rev.Lett.* **111** (2013), no. 9 091602, [arXiv:1303.1396].

[61] B. Basso, A. Sever, and P. Vieira, *Space-time S-matrix and Flux tube S-matrix II. Extracting and Matching Data*, *JHEP* **1401** (2014) 008, [arXiv:1306.2058].

[62] B. Basso, A. Sever, and P. Vieira, *Space-time S-matrix and Flux-tube S-matrix III. The two-particle contributions*, *JHEP* **1408** (2014) 085, [arXiv:1402.3307].

[63] B. Basso, A. Sever, and P. Vieira, *On the collinear limit of scattering amplitudes at strong coupling*, arXiv:1405.6350.

[64] B. Basso, A. Sever, and P. Vieira, *Space-time S-matrix and Flux-tube S-matrix IV. Gluons and Fusion*, *JHEP* **1409** (2014) 149, [arXiv:1407.1736].

[65] L. Ferro, T. Lukowski, C. Meneghelli, J. Plefka, and M. Staudacher, *Harmonic R-matrices for Scattering Amplitudes and Spectral Regularization*, *Phys.Rev.Lett.* **110** (2013), no. 12 121602, [arXiv:1212.0850].

[66] L. Ferro, T. Lukowski, C. Meneghelli, J. Plefka, and M. Staudacher, *Spectral Parameters for Scattering Amplitudes in N=4 Super Yang-Mills Theory*, *JHEP* **1401** (2014) 094, [arXiv:1308.3494].

[67] N. Beisert, J. Broedel, and M. Rosso, *On Yangian-invariant regularization of deformed on-shell diagrams in $\mathcal{N} = 4$ super-Yang-Mills theory*, *J.Phys.* **A47** (2014) 365402, [arXiv:1401.7274].

[68] J. Broedel, M. de Leeuw, and M. Rosso, *Deformed one-loop amplitudes in $N = 4$ super-Yang-Mills theory*, arXiv:1406.4024.

[69] L. Ferro, T. Lukowski, and M. Staudacher, *N=4 Scattering Amplitudes and the Deformed Grassmannian*, arXiv:1407.6736.

[70] T. Bargheer, Y.-t. Huang, F. Loebbert, and M. Yamazaki, *Integrable Amplitude Deformations for N=4 Super Yang–Mills and ABJM Theory*, arXiv:1407.4449.

[71] N. Arkani-Hamed, J. L. Bourjaily, F. Cachazo, A. Postnikov, and J. Trnka, *On-Shell Structures of MHV Amplitudes Beyond the Planar Limit*, to appear.

[72] Z. Bern, J. Carrasco, and H. Johansson, *New Relations for Gauge-Theory Amplitudes*, *Phys.Rev.* **D78** (2008) 085011, [arXiv:0805.3993].

[73] Z. Bern, J. J. M. Carrasco, and H. Johansson, *Perturbative Quantum Gravity as a Double Copy of Gauge Theory*, *Phys.Rev.Lett.* **105** (2010) 061602, [arXiv:1004.0476].

[74] S. G. Naculich, H. Nastase, and H. J. Schnitzer, *Two-loop graviton scattering relation and IR behavior in N=8 supergravity*, *Nucl.Phys.* **B805** (2008) 40–58, [arXiv:0805.2347].

[75] A. Brandhuber, P. Heslop, A. Nasti, B. Spence, and G. Travaglini, *Four-point Amplitudes in N=8 Supergravity and Wilson Loops*, *Nucl.Phys.* **B807** (2009) 290–314, [arXiv:0805.2763].

[76] N. Arkani-Hamed, J. L. Bourjaily, F. Cachazo, and J. Trnka, *On the Singularity Structure of Maximally Supersymmetric Scattering Amplitudes*, arXiv:1410.0354.

[77] Z. Bern, J. Rozowsky, and B. Yan, *Two loop four gluon amplitudes in N=4 superYang-Mills*, *Phys.Lett.* **B401** (1997) 273–282, [hep-ph/9702424].

[78] Z. Bern, J. Carrasco, L. J. Dixon, H. Johansson, D. Kosower, and R. Roiban, *Three-Loop Superfiniteness of N=8 Supergravity*, *Phys.Rev.Lett.* **98** (2007) 161303, [hep-th/0702112].

[79] J. M. Henn, *Multiloop integrals in dimensional regularization made simple*, *Phys.Rev.Lett.* **110** (2013), no. 25 251601, [arXiv:1304.1806].

[80] J. M. Henn, A. V. Smirnov, and V. A. Smirnov, *Analytic results for planar three-loop*

four-point integrals from a Knizhnik-Zamolodchikov equation, *JHEP* **1307** (2013) 128, [arXiv:1306.2799].

[81] J. M. Henn, A. V. Smirnov, and V. A. Smirnov, *Evaluating single-scale and/or non-planar diagrams by differential equations*, *JHEP* **1403** (2014) 088, [arXiv:1312.2588].

[82] Z. Bern, L. J. Dixon, D. Dunbar, M. Perelstein, and J. Rozowsky, *On the relationship between Yang-Mills theory and gravity and its implication for ultraviolet divergences*, *Nucl.Phys.* **B530** (1998) 401–456, [hep-th/9802162].

[83] Z. Bern, J. Carrasco, L. J. Dixon, H. Johansson, and R. Roiban, *Manifest Ultraviolet Behavior for the Three-Loop Four-Point Amplitude of N=8 Supergravity*, *Phys.Rev.* **D78** (2008) 105019, [arXiv:0808.4112].

[84] Z. Bern, J. Carrasco, L. Dixon, H. Johansson, and R. Roiban, *Simplifying Multiloop Integrands and Ultraviolet Divergences of Gauge Theory and Gravity Amplitudes*, *Phys.Rev.* **D85** (2012) 105014, [arXiv:1201.5366].

[85] G. Passarino and M. Veltman, *One Loop Corrections for e^+e^- Annihilation Into $\mu^+\mu^-$ in the Weinberg Model*, *Nucl.Phys.* **B160** (1979) 151.

[86] Z. Bern, L. J. Dixon, and D. A. Kosower, *Dimensionally regulated pentagon integrals*, *Nucl.Phys.* **B412** (1994) 751–816, [hep-ph/9306240].

[87] Z. Bern, J. J. Carrasco, T. Dennen, Y.-t. Huang, and H. Ita, *Generalized Unitarity and Six-Dimensional Helicity*, *Phys.Rev.* **D83** (2011) 085022, [arXiv:1010.0494].

[88] F. Cachazo, *Sharpening The Leading Singularity*, arXiv:0803.1988.

[89] Z. Bern, L. J. Dixon, and D. A. Kosower, *Dimensionally regulated pentagon integrals*, *Nucl.Phys.* **B412** (1994) 751–816, [hep-ph/9306240].

[90] G. 't Hooft and M. Veltman, *Regularization and Renormalization of Gauge Fields*, *Nucl.Phys.* **B44** (1972) 189–213.

[91] Z. Bern, L. J. Dixon, and D. A. Kosower, *Dimensionally regulated pentagon integrals*, *Nucl.Phys.* **B412** (1994) 751–816, [hep-ph/9306240].

[92] Z. Bern and G. Chalmers, *Factorization in one loop gauge theory*, *Nucl.Phys.* **B447** (1995) 465–518, [hep-ph/9503236].

[93] C. Anastasiou, Z. Bern, L. J. Dixon, and D. Kosower, *Planar amplitudes in maximally supersymmetric Yang-Mills theory*, *Phys.Rev.Lett.* **91** (2003) 251602, [hep-th/0309040].

[94] Z. Bern, J. Carrasco, H. Johansson, and D. Kosower, *Maximally supersymmetric planar Yang-Mills amplitudes at five loops*, *Phys.Rev.* **D76** (2007) 125020, [arXiv:0705.1864].

[95] N. Bjerrum-Bohr and P. Vanhove, *Absence of Triangles in Maximal Supergravity Amplitudes*, *JHEP* **0810** (2008) 006, [arXiv:0805.3682].

[96] N. Arkani-Hamed, F. Cachazo, and J. Kaplan, *What is the Simplest Quantum Field Theory?*, *JHEP* **1009** (2010) 016, [arXiv:0808.1446].

[97] Z. Bern, J. Carrasco, H. Johansson, and R. Roiban, *The Five-Loop Four-Point Amplitude of N=4 super-Yang-Mills Theory*, *Phys.Rev.Lett.* **109** (2012) 241602, [arXiv:1207.6666].

[98] Z. Bern, J. Carrasco, H. Johansson, and D. Kosower, *Maximally supersymmetric planar Yang-Mills amplitudes at five loops*, *Phys.Rev.* **D76** (2007) 125020, [arXiv:0705.1864].

[99] Z. Bern, M. Czakon, L. J. Dixon, D. A. Kosower, and V. A. Smirnov, *The Four-Loop Planar Amplitude and Cusp Anomalous Dimension in Maximally Supersymmetric Yang-Mills Theory*, *Phys.Rev.* **D75** (2007) 085010, [hep-th/0610248].

[100] F. Cachazo and D. Skinner, *On the structure of scattering amplitudes in N=4 super Yang-Mills and N=8 supergravity*, arXiv:0801.4574.

[101] Z. Bern, J. Carrasco, L. J. Dixon, H. Johansson, and R. Roiban, *The Complete Four-Loop Four-Point Amplitude in N=4 Super-Yang-Mills Theory*, *Phys.Rev.* **D82** (2010) 125040, [arXiv:1008.3327].

[102] J. Drummond, G. Korchemsky, and E. Sokatchev, *Conformal properties of four-gluon planar amplitudes and Wilson loops*, *Nucl.Phys.* **B795** (2008) 385–408, [arXiv:0707.0243].

[103] J. L. Bourjaily, A. DiRe, A. Shaikh, M. Spradlin, and A. Volovich, *The Soft-Collinear Bootstrap: N=4 Yang-Mills Amplitudes at Six and Seven Loops*, *JHEP* **1203** (2012) 032, [arXiv:1112.6432].

[104] B. Eden, P. Heslop, G. P. Korchemsky, and E. Sokatchev, *Constructing the correlation function of four stress-tensor multiplets and the four-particle amplitude in N=4 SYM*, *Nucl.Phys.* **B862** (2012) 450–503, [arXiv:1201.5329].

[105] Z. Bern, J. J. Carrasco, L. J. Dixon, M. R. Douglas, M. von Hippel, et al., *$D = 5$ maximally supersymmetric Yang-Mills theory diverges at six loops*, *Phys.Rev.* **D87** (2013) 025018, [arXiv:1210.7709].

[106] N. Arkani-Hamed, J. L. Bourjaily, F. Cachazo, and J. Trnka, *Local Integrals for Planar Scattering Amplitudes*, *JHEP* **1206** (2012) 125, [arXiv:1012.6032].

[107] J. J. M. Carrasco and H. Johansson, *Generic multiloop methods and application to N=4 super-Yang-Mills*, *J.Phys.* **A44** (2011) 454004, [arXiv:1103.3298].

[108] H. Elvang, D. Z. Freedman, and M. Kiermaier, *Recursion Relations, Generating*

Functions, and Unitarity Sums in N=4 SYM Theory, *JHEP* **0904** (2009) 009, [arXiv:0808.1720].

[109] Z. Bern, J. Carrasco, H. Ita, H. Johansson, and R. Roiban, *On the Structure of Supersymmetric Sums in Multi-Loop Unitarity Cuts*, *Phys.Rev.* **D80** (2009) 065029, [arXiv:0903.5348].

[110] Z. Bern, S. Davies, T. Dennen, and Y.-t. Huang, *Absence of Three-Loop Four-Point Divergences in $N = 4$ Supergravity*, *Phys.Rev.Lett.* **108** (2012) 201301, [arXiv:1202.3423].

[111] Z. Bern, S. Davies, and T. Dennen, *Enhanced Ultraviolet Cancellations in $N = 5$ Supergravity at Four Loop*, arXiv:1409.3089.

[112] F. Tkachov, *A Theorem on Analytical Calculability of Four Loop Renormalization Group Functions*, *Phys.Lett.* **B100** (1981) 65–68.

[113] K. Chetyrkin and F. Tkachov, *Integration by Parts: The Algorithm to Calculate Beta Functions in 4 Loops*, *Nucl.Phys.* **B192** (1981) 159–204.